GEM Technical Report 2010-4

“Best Practices” for Using Macroseismic Intensity and Ground Motion Intensity Conversion Equations for Hazard and Loss Models in GEM1

G. Cua, D. J. Wald, T. I. Allen, D. Garcia, C. B. Worden, M. Gerstenberger, K. Lin, K. Marano

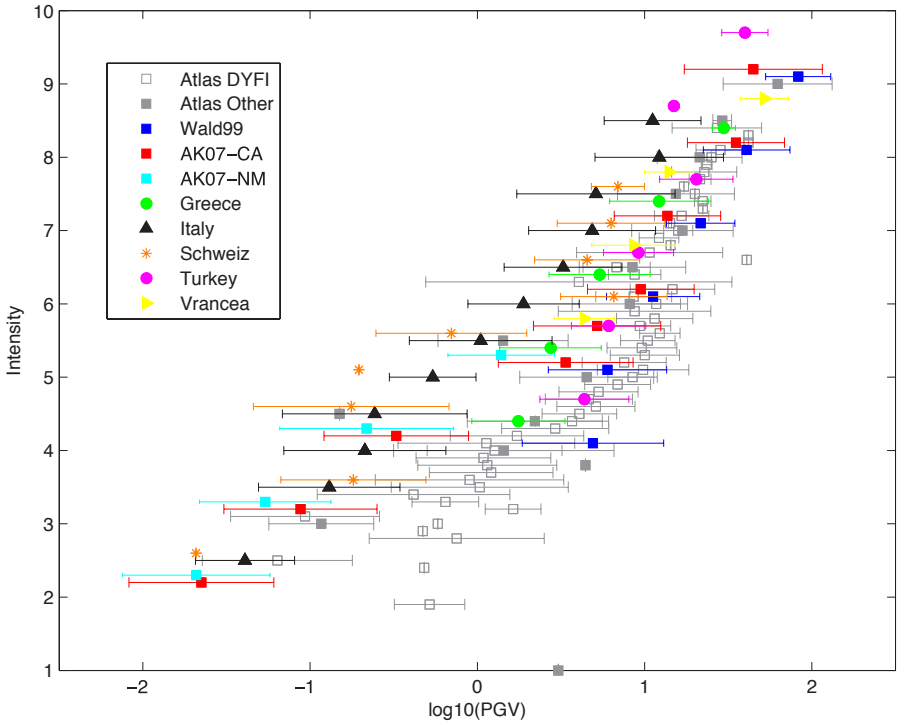

“Best Practices” for Using Macroseismic Intensity and Ground Motion Intensity Conversion Equations for Hazard and Loss Models in GEM1

By G. Cua[1], **D.J. Wald**[2], **T.I Allen**[3], **D. Garcia**.[2], **C.B. Worden**[4], **M. Gerstenberger**[5], **K. Lin**[2], **K Marano**[2]

October 2010

1. *Swiss Seismological Service, ETH Zurich, Zurich, Switzerland*
2. *National Earthquake Information Center, US Geological Survey, Golden, Colorado, USA*
3. *Risk and Impact Analysis & Earth Monitoring Groups, Geospatial and Earth Monitoring Division, Geoscience Australia, Canberra ACT, Australia*
4. *Synergetics, Inc., Fort Collins, Colorado, USA*
5. *GNS Science, Lower Hutt, New Zealand*

Citation: Cua G., Wald D. J., Allen T. I., Garcia D., Worden C.B, Gerstenberger M., Lin K., and Marano K. (2010) “Best Practices” for Using Macroseismic Intensity and Ground Motion-Intensity Conversion Equations for Hazard and Loss Models in GEM1, GEM Technical Report 2010-4, GEM Foundation, Pavia, Italy.

www.globalquakemodel.org

ABSTRACT

Macroseismic shaking intensity is a fundamental parameter for the development, calibration, and use in a variety of hazard maps as well as in empirical (direct) and semi-empirical (indirect) earthquake shaking loss methodologies. Macroseismic data also quantify damage from past and present events and facilitate communicating ground motion levels in terms of human experiences and incurred losses. The aim of this report is to summarize and recommend “best practices” for the use of macroseismic intensity in conjunction with hazard maps (particularly ShakeMaps) and as input to associated loss models. The continued reliance on macroseismic intensity data dictates that ground motion prediction equations (GMPEs) alone are not always sufficient for estimating or constraining shaking hazards. Relations that allow direct estimation of intensity given an earthquake magnitude and distance, and those that convert ground motions to intensity (and vice versa) are required. Forward estimation of macroseismic intensities take two primary forms: 1) direct intensity prediction equations (IPEs), and 2) ground-motion-to-intensity conversion equations (GMICE). In addition, one can potentially better constrain historical ground motions at particular sites by employing intensity-to-ground-motion conversion equations (IGMCEs), though such equations are rare. Both the Global Earthquake Model (GEM) and Global ShakeMap (GSM) require advice and optimization in the state-of-the-art use of ground motion and intensity data. We provide background on the issues relating ground motions to intensities, directly predicting intensities, and offer insight into their uses. In the end, we recommend initial default IPE and GMICE selections for use in the immediate short term while additional research on these fronts continues and develops. A brief summary of highly related, current studies that help inform this report is also provided. Based on these ongoing analyses, and this report’s summary, we provide recommendations for further refinements in the form of continued research and development efforts.

Keywords: Macroseismic intensity, strong ground motions, ground motion prediction equations, intensity conversion equations, intensity prediction equations.

ACRONYMS

ACR.	Active Crustal Region.
DYFI?	Did You Feel It?
EMS-98.	European Macroseismic Scale (1998 update).
GM.	Geometric mean, in the context of defining peak ground motion as the geometric mean of the maximum amplitudes on two orthogonal horizontal channels.
GMPE.	Ground Motion Prediction Equation; also referred to as “attenuation relation”.
GMICE.	Ground Motion to Intensity Conversion Equation.
GSM.	Global ShakeMap.
IPE.	Intensity Prediction Equation; also referred to as “intensity attenuation relation”
IGMCE.	Intensity to Ground Motion Conversion Equation.
maxEnv.	Maximum envelope, in the context of defining peak ground motion as the larger of the maximums of two orthogonal horizontal channels.
MMI.	Modified Mercalli Intensity scale.
NGA.	Next Generation Attenuation.
PAGER.	Prompt Assessment of Global Earthquakes for Response
PGA.	Peak Ground Acceleration
PGM.	Peak Ground Motion
PGV.	Peak Ground Velocity
SCR.	Stable Continental Region
SZ.	Subduction Zone.

TABLE OF CONTENTS

Page

ABSTRACT ii
ACRONYMS ii
TABLE OF CONTENTS iii
LIST OF FIGURES v
LIST OF TABLES vi
1 Introduction 1
2 Shakemap Related Issues 3
2.1 Shakemap's new approach for incorporating peak motions and macroseismic data 3
2.2 Shakemap Atlas 5
2.3 Dependency between GMPEs and Conversion Equations 8
3 Intensity Prediction Equations (IPEs) 10
3.1 Macroseismic Intensity Data 11
3.2 IPE Candidate Models 12
3.2.1 Tectonically Active Regions 17
3.2.2 Stable Continental Regions 20
3.2.3 Subduction zones 22
4 Ground Motion to Intensity Conversion Equations (GMICEs) 25
4.1 GMICE Functional Forms and Datasets 26
4.1.1 Active Crustal Regions 29
4.1.2 Stable Continental Regions 33
4.1.3 Stable Continental Regions 33
4.1.4 Subduction Zones 33
5 Intensity to Ground Motion Conversion Equations (IGMCEs) 36
6 Summary and recommendations 38
REFERENCES 40
APPENDIX A Active Crustal Macroseismic Data I
APPENDIX B Stable Continental Region Macroseismic Data V
APPENDIX C Subduction Zone Macroseismic Data VII
APPENDIX D Magnitude Dependence of Selected Active Crustal IPEs IX
APPENDIX E Magnitude Dependence of Selected Stable Continental IPEs XII

LIST OF FIGURES

Page

Figure 2.1 Mean PGV error for events with at least ten predictions, sorted by increasing mean error of ShakeMap predictions. From Worden et al. (2010). 4

Figure 2.2 Logic tree currently in use for Global ShakeMap defining default tectonic environment from earthquake location and magnitude (from Allen et al., 2008)..... 5

Figure 2.3 Flowchart of the earthquake/GMPE determination scheme for Active Crustal Regions (ACRs). Similarly complex logic is required to assign GMPEs for SCR and SZ regimes. From Garcia et al. (2010). 7

Figure 2.4 ShakeMaps produced using the National Earthquake Information Center (NEIC) preliminary location of the Padang (Indonesia) earthquake of September 30, 2009 (moment magnitude M_W 7.6; depth H = 50 km) using the subduction-zone GMPE by Youngs et al. (1997) for: (a) interface earthquakes; and (b) intraslab earthquakes. (c) Location map showing the focal mechanism obtained at NEIC from W-phase inversion 19 minutes after the origin time. In (a) and (b) population exposure at MMI VI and above, estimated from the PAGER system, is indicated (in millions of persons). Refined locations in the following days set the depth at 81 km, revealing the event was an intraslab earthquake (from Garcia et al., 2010). 8

Figure 2.5 Residuals for the peak ground-motion-to-intensity conversions for global active crustal regions using the Wald et al. (1999c) GMICE relations. (a) Indicates the median intensity residuals using the Chiou and Youngs (2008) GMPE as the predictor of peak ground motions. (b) Indicates the median intensity residuals using the Boore et al. (1997) GMPE as the predictor of peak ground motions. Predicted instrumental ground motions are calculated using the aforementioned GMPEs and converted to intensity. The intensity residual is subsequently calculated. Residuals are binned in 10-kilometer windows and the median residual is plotted. The standard deviation of the residuals is indicated and vertical dashed lines indicate the maximum distance of usage of the GMPEs. 9

Figure 3.1 Residuals for macroseismic intensity prediction equations (IPEs) against global active crust intensity data. Residuals are binned in 10-kilometer windows and the median residual is plotted. The standard deviation of the residuals is indicated. Vertical dashed lines indicate the maximum distance of usage as recommended by each of the authors..... 18

Figure 3.2 Comparison of several common intensity prediction methods for shallow active crustal regions (ACRs) assuming a uniform site condition with V_{S30} of 425 m/s at magnitudes of M_W 5.5, 6.5 and 7.5. Four of the techniques apply direct IPEs: Dowrick and Rhoades (2005); Atkinson and Wald (2007); Sørensen et al. (2009b); and Allen and Wald (2010). The other two models use GMPE/GMICE combinations: Boore et al.(1997) and Wald et al. (1999c) (BJF97 & Wald99); and Chiou and Youngs (2008) and Atkinson and Kaka (2007) (CY08 & AK07). Models that use a R_{JB} distance metric have been converted to R_{rup} for the M_W 5.5 scenario assuming a *point source* earthquake with a focal depth of 7 km. For the M_W 6.5 and 7.5 scenarios, we assume a vertically dipping, surface rupturing earthquake, in which case $R_{JB} = R_{rup}$..... 20

Figure 3.3 Residuals for macroseismic intensity prediction equations (IPEs) against global stable continental region (SCR) intensity data. Residuals are binned in 10-kilometer windows and the median residual is plotted. The standard deviation of the residuals is indicated. Vertical dashed lines indicate the maximum distance of usage as recommended by each of the authors 21

Figure 3.4 See above for figure caption..... 23

Figure 3.5 Residuals for macroseismic intensity prediction equations (IPEs) against global subduction zone (SZ) intensity data. Residuals are binned in 10-kilometer windows and the median residual is plotted. The standard deviation of the residuals is indicated. Vertical dashed lines indicate the maximum distance of usage as recommended by each of the authors 24

Figure 4.1 Functional forms of PGA and PGV to intensity relationships derived from various regions. The functions are plotted in thick lines for PGM and intensity ranges constrained by their respective datasets. Thin, dashed lines show the GMICEs when extrapolated beyond the datasets from which they were derived. The estimated intensities are in better agreement at larger values of PGM than at smaller values. It is clear that extrapolating GMICEs beyond the ranges constrained by data is not recommended 26

Figure 4.2 Magnitude and distance distribution of aggregate GMICE dataset. See Figure 12 for symbol legend 28

Figure 4.3 The PGM-intensity datasets collected as part of GMICE-related efforts of this study. Intensity as a function of (a) PGA and (b) PGV are shown in the first row. The second row shows intensity as a function of the mean ground motion level 29

LIST OF TABLES

Page

Table 3.1 Summary of the number of conventional macroseismic intensity assignments and DYFI? data used as constraints for estimating intensity in the ShakeMap Atlas, categorized by tectonic environment 12

Table 3.2 Summary of Intensity Prediction Equations (IPEs) Considered 13

Table 3.3 Total uncertainty in intensity units 14

Table 4.1 GMICE datasets collected 34

Table 4.2 Preferred relationships for the prediction of macroseismic intensities. Recommendations for preferred GMPEs are based on the study of Allen and Wald (2009) for usage in Global ShakeMap 35

1 Introduction

Macroseismic intensity data continue to play an important role in the seismological, engineering, and loss modelling communities. Indeed, the advent of the ShakeMap system (Wald et al., 1999a) and related systems like the Prompt Assessment of Global Earthquakes for Response (PAGER, Earle et al., 2009; Wald et al., 2008) have increased the visibility of macroseismic intensity not only in these arenas, but also in the view of the public, the media and educational realms, as well as earthquake response and planning communities. Critically, macroseismic observations can provide valuable constraints for reconstructing shaking distributions for historical events; often they are abundant whereas strong-motion recordings are sparse for such events.

The value of adding historic macroseismic data as constraints for ShakeMaps in the process of developing earthquake loss-models is documented in the ShakeMap Atlas (Allen et al., 2008) and the resulting exposure and loss catalogue (Allen et al., 2009). In addition to the PAGER system, many other proprietary and published impact assessment tools also call for intensity-based hazard inputs for estimating earthquake impacts (e.g., Eguchi et al., 1997; Erdik et al., 2008; Lantada et al., 2010; Musson, 2000; Wyss, 2008) as does the Global Earthquake Model currently under development (GEM Foundation, Crowley et al., 2010).

Beyond loss estimation, citizen-science contributions to macroseismic data collection online via systems like the USGS "Did You Feel It?" have shown the benefit of communicating earthquake hazards via macroseismic intensity (Wald et al., 1999b). While engineers and scientists are accustomed to working with peak ground motion values, from an educational and outreach perspective, GEM will most likely need to use macroseismic intensity to adequately communicate with many potential non-technical audiences. This further motivates the expression of ground motion hazards in terms of intensity values.

One primary advantage in the use of macroseismic data is that earthquake damage functions derived from physical properties of structures using analytical approaches and experimental data – like those from loss methodologies such as HAZUS (National Institute of Building Sciences, 2003) and DBELA (Crowley et al., 2004) – are not uniformly available for all global structure types. Further, the lack of ground motion recordings at the vast majority of the world's structural failures during past earthquakes necessitates the use of macroseismic observations for forward progress for many loss models. This includes so-called analytical models, which too must rely on observations or mappings (empirical, or expert-informed constraints) for computing losses to a portfolio of structures and casualty rates – none of which can be fully constrained in strictly analytic sense. At the very least, one would like to best estimate the ground motion values that occurred at such damage sites. This often involves back-engineering ground motions (including spectral values) from macroseismic intensities.

The essential problem at hand is an age-old quandary: what we require most for loss model calibration are high-quality strong-motion recordings (including frequency-varying spectral values) in the vicinity of well quantified, varying levels of damage to a wide range of structure types. Few such data exist. Rather, we must make use of the (admittedly circular) approach of inferring ground motions by assigning intensities to damage, and using intensities to ascribe shaking values near to damaged structures. If sufficient independent observational constraints from a variety of damaged structures used for assigning intensities point to similar shaking levels at a location, then their use for loss calibration is both logical and beneficial.

In addition, recent rapidly increasing data sets now exist for which strong motion recordings and macroseismic data are nearly collocated. With many such observations, shaking levels and intensity values can be successfully related, with quantifiable uncertainty. Such relations can then radically increase the potential for constraining shaking levels —not only

in the form of intensity, but also peak ground motions and spectral accelerations— in the vicinity of past earthquake damage and losses [e.g., ShakeMap Atlas (Allen et al., 2008), PAGER's Expo-Cat (Allen et al., 2009), and the Cambridge University Earthquake Damage Database (Spence et al., 2009)].

In Section 2, we describe how ShakeMap, particularly the new Version 3.5 of the software, uses (often abundant) macroseismic data in its native form and takes advantage of the relative uncertainties of all input data and shaking estimates to best constrain shaking intensity and peak and spectral values. We also summarize several ongoing efforts related to determining best practices for using macroseismic intensity data that are in progress by the authors as we draft this report. These efforts include revision of the ShakeMap software package that treats intensity in its native form (Worden et al., 2010), revision of the ShakeMap Atlas (from Version 1 to 2), and automated selection of the most appropriate ground-motion prediction equation (GMPE) and intensity prediction equation (IPE) for an earthquake based on whatever earthquake source information (e.g., location, depth, mechanism, tectonic regime) are available (Garcia et al., 2010).

Standardized, direct use of intensity data requires review of current state-of-the-art practices. The currently available peer-reviewed studies allowing for direct intensity prediction (IPEs), ground motion to intensity conversion equations (GMICEs), and intensity to ground motion conversion equations (IGMCEs) depend heavily on the data and shaking/loss pairings selected as well as the regression approaches employed. The authors concede that in comparison to GMPEs, for example, Next Generation Attenuation relations (Power et al., 2008), IPEs, GMICEs, and IGMCEs have not received the same level of rigor in their development, or scrutiny in their use. Hence, in Sections 3 and 4, we further examine the specific IPEs and GMICEs used, their data and derivations, and the conditions of their use. Our initial analysis shows that there are some notable differences among IPEs and GMICEs that on first examination appear to be regionally related. However, we consider other factors, particularly the ranges of magnitudes and intensities that may affect the regional dependencies. These complexities require an informed use for particular applications. Section 5 is brief, reporting on the few available IGMCEs. The lack of published IGMCEs needs to be remedied.

Finally, as the overall goal of this project is to provide guidance on how to best constrain or predict shaking (including intensities) on a regional and global scale, we have collected and examined datasets that associate intensity and ground motion data, and compared these against available relations (both IPEs and GMICEs). In Section 6, we summarize the overall strategy and provide guidance in their usage. We also provide recommendations for further refinements in the form of continued research and development efforts. As we use numerous acronyms throughout the document, we provide a Glossary at the end of the document.

2 Shakemap Related Issues

ShakeMap was originally designed as a tool to provide a "data-driven" estimate of ground shaking for California, and so it was designed to directly incorporate real-time strong-motion data to calibrate the shaking as interpolated across a spatial grid. Once the shaking distribution is estimated, for both those ShakeMaps constrained by strong-motion data and those without, the maps are converted to shaking "instrumental" intensity through the use of peak ground motion to intensity conversion equations (e.g., Atkinson and Kaka, 2007; Tselentis and Danciu, 2008; Wald et al., 1999c).

With the expanded use of ShakeMap for loss estimation, particularly with intensity as the input metric for both empirical (direct) and semi-empirical (indirect) loss models within the PAGER system (Wald et al., 2009) and as the hazard associated with new consequences databases (e.g., Cambridge University Earthquake Damage Database and PAGER's Expo-Cat), constraints for intensity maps from observed macroseismic intensities from past events become more important for producing a ShakeMap consistent with historic damage observations. In addition, ShakeMaps are now being produced globally for regions with less-abundant, or no real-time strong-motion data; these maps are almost always predominantly predictive, relying on GMPEs. However, these maps, too, allow for direct constraints from macroseismic data, though now in the form of near-real time observations contributed from the USGS "Did You Feel It?" system.

As discussed below, a substantial redesign of the ShakeMap system was required to treat macroseismic data in a more consistent fashion. In addition, for loss-estimation purposes, shaking uncertainties are desired as a function of spatial distribution, and the direct inclusion of intensity observations complicates the computation of such uncertainties. We not only have to account for the uncertainties in the application of GMPEs, IPEs, and GMICEs for peak ground motion and intensity estimation, but also for the uncertainties in the distance-dependent influence of available ground motion and intensity observations to surrounding locations, as well as intensity constraints provided by the conversion between observed instrumental ground-motion recordings and intensity.

The revision of the ShakeMap approach affects the maps that comprise the ShakeMap Atlas, and the next version of the Atlas will benefit from these modifications. In addition, the Atlas update will benefit from work done by Garcia et al (2010), which allows for an automated and more consistent selection of appropriate GMPEs in differing tectonic environments.

Finally, with regards to combining macroseismic and ground motion data, there are potential complications and dependencies when combining various sets of equations that allow conversion and prediction of ground motions and intensities. Indeed, Allen and Wald (2009) demonstrated that the combination of several GMPEs and GMICEs should not be assumed to be reliable for aggregated global ground-motion data (both instrumental and macroseismic) over all magnitude and distance ranges. Consequently, the combined epistemic uncertainty of these models required for evaluating shaking intensity may be significant, particularly when we wish to consider all global ground-shaking scenarios for Global ShakeMap (GSM), PAGER, and GEM applications.

2.1 Shakemap's New Approach for Incorporating Peak Motions and Macroseismic Data

The USGS has recently (late 2009) released Version 3.5 of ShakeMap, which among other changes, allows for more rigorous use and treatment of macroseismic data and their uncertainties (Worden et al., 2010). This fundamentally changes the approach taken to now explicitly include macroseismic data (e.g., historic, European Macroseismic Intensity, EMS; Modified Mercalli Intensity, MMI; or "Did You Feel It?", and others) in their native form.

Worden et al. (2010) describe a weighted-average approach for incorporating various types of data, specifically, observed peak ground motions and intensities, and estimates of these quantities from GMPEs, IPEs, and GMPE/GMICE combinations, into the ShakeMap ground motion and intensity mapping framework. Their approach allows for the possible combination of all of the following data sources and as well as estimates of: 1) nearby observations (ground motion measurements and reported intensities), 2) converted observations from intensity to ground motion (or vice-versa), and 3) estimated peak ground motions and intensities from prediction equations (or numerical estimates). Critically, each of these constraints can and must include at least an approximate estimate of its uncertainties, including those due to site-to-observation distance and potentially those associated with estimates when the fault geometry/distance are yet unknown. The ground motion and intensity estimates at each grid point are a weighted combination of these various data and estimates.

A compelling case for the benefit of uncertainty-weighted data and estimate constraints is provided by Worden et al. (2010) by using estimated amplitudes at locations of ground-motion observations (not used) and comparing predictions to the observations —a form of cross validation. In cases where no data are available, the ShakeMap prediction is identical with the GMPE prediction. With the addition of bias correction, that is, removing the inter-event term based on fitting the observed ground motions, the biased ShakeMap estimates represent a substantial improvement over the unbiased GMPE estimates (see Figure 2.1). Further, in locations where there are one or more nearby observations, the ShakeMap estimates are a substantial improvement over the biased GMPE by a considerable margin (Figure 2.1). In addition, although converting MMI to PGM introduces considerable uncertainty into the data mix, Worden et al. (2010) confirmed that including intensity data is an improvement over empirical predictions alone, a fundamental premise of the new ShakeMap methodology. Converting PGM data to intensity shows a marked inferiority to the native intensity approach, indicating that using native intensity data is a logical addition to the ShakeMap repertoire. This suggests that using observed intensity data may be beneficial even in regions where instrumental observations are abundant, if one goal is to produce the *most accurate intensity map* in addition to producing well-constrained peak-ground motion maps.

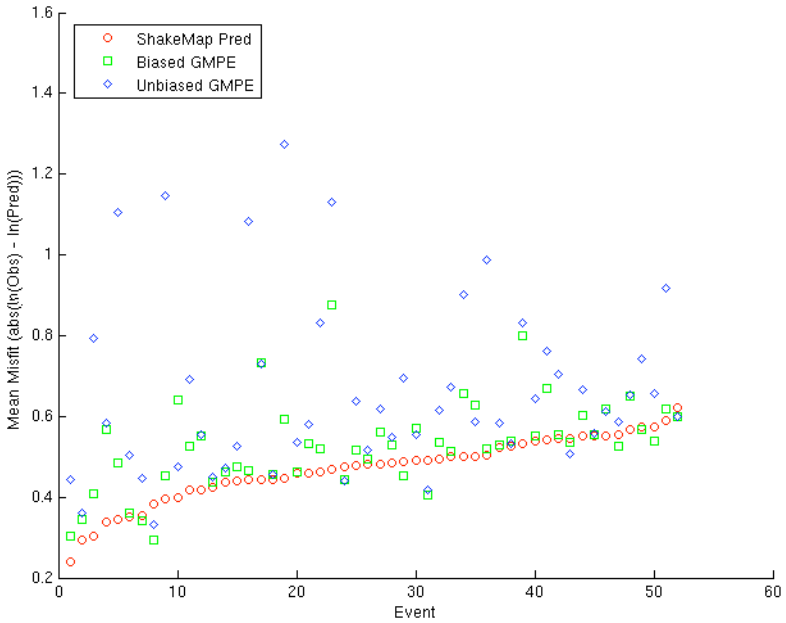

Figure 2.1 Mean PGV error for events with at least ten predictions, sorted by increasing mean error of ShakeMap predictions. From Worden et al. (2010).

This data combination adds additional functionality to the ShakeMap methodology, allowing utilization of near-real time and historical intensity data in their native form, in addition to less abundant ground motion data. Rigorous incorporation of the former data facilitate comparison of estimated ground motion maps and shaking values with loss and damage data, a combination that is fundamental for loss-model development and calibration. In addition, a natural by-product of the new ShakeMap (V3.5) interpolation and mapping process is a grid of total uncertainty at each point on the map, which becomes vital for comprehensive inventory loss calculations (e.g., Crowley et al., 2010). Unfortunately, many challenges remain with regard to rigorous quantification of the spatial distribution of shaking uncertainty. In particular, there are no clear guidelines for setting uncertainties on macroseismic assignments (whether historic or from DYFI?) and there are few robust functions that quantify the site-to-site variability of ground motion as a function of distance, amplitude and frequency.

2.2 Shakemap Atlas

The improved incorporation of ground motion and intensity data, and the uncertainty calculations that are now part of the ShakeMap (V3.5) package will be propagated into a revision of the ShakeMap Atlas (Allen et al., 2008). Version 2.0 of the Atlas will be produced using ShakeMap Version 3.5, thus all the aforementioned improvements in incorporating varied observations, conversions, and predictions will be included. In addition, the revised ShakeMap Atlas will also have other important improvements based on new data and studies performed since Atlas Version 1.0, including additional event-specific data sets (faults, macroseismic data, ground motion data), more recent events (through 2008), a wider suite of available GMPEs, and now a suite of default IPEs and GMICEs, as described later. In addition, we have recently developed a new, automated selection process to choose the appropriate GMPE for each event. Automating GMPE selection is relevant for the Atlas, given that thousands of events are included, as well as for probabilistic seismic hazard assessment (PSHA) applications.

Although some global regionalization efforts have been undertaken (e.g., Douglas et al., 2009) to help select GMPEs for seismic hazard purposes, they are primarily focused on determining the most appropriate GMPE (or weights for multiple GMPEs) that should be employed in a particular tectonic region. It is more difficult to select the appropriate GMPE (and specific coefficients) within a complex tectonic environment that includes, potentially, selecting among Stable Continental Region (SCR), Active Crustal Region (ACR), and Subduction Zone (SZ) equations.

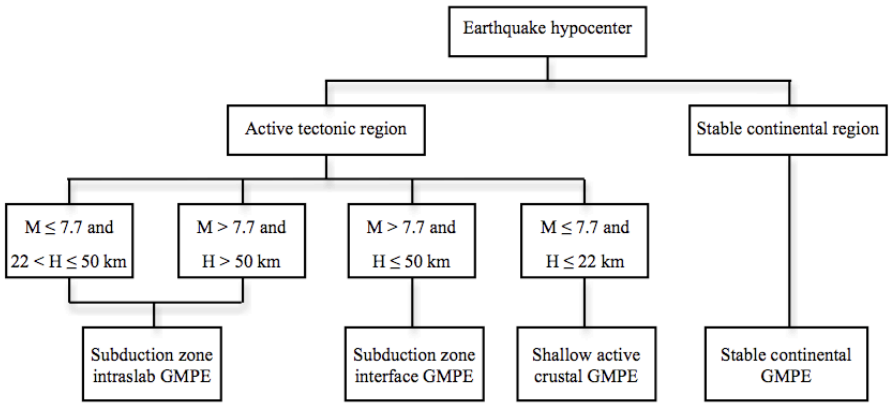

Figure 2.2 Logic tree currently in use for Global ShakeMap defining default tectonic environment from earthquake location and magnitude (from Allen et al., 2008).

Previously, GMPE assignments for Atlas and real-time events in GSM were done using a rather simple matrix of depth, magnitude and tectonic region (active tectonic or stable continent), distinguishing between, for example, crustal and

subduction zone GMPEs, and whether a subduction zone event was an interface or intraslab event (Figure 2.2). Garcia et al (2010) found numerous inconsistencies in the GMPEs used within specific events in the Atlas, since the selection of GMPEs and their variable source terms using simple automated approaches can be fraught with uncertainty in complex tectonic environments. Garcia et al (2010) thus proposed a new earthquake discrimination procedure to determine, in near-real time, the type of earthquake among different tectonic regimes and the appropriate corresponding GMPE to be used. The scheme was developed to assess the selection of GMPEs in GSM operations as part of an ongoing effort to improve the current performance of the system, since automated GMPE selection with the simple matrix in Figure 2.2 sometimes mischaracterizes events. The selection algorithm was validated against a large database of historical and recent earthquakes in the ShakeMap Atlas and was observed to reliably select appropriate GMPEs for earthquakes even within heterogeneous tectonic environments. Consequently, it is suitable both for real-time applications (GSM) and risk analyses for earthquakes anywhere on the globe.

In essence, Garcia et al (2010) approach the GMPE selection problem using all relevant data and information about the source and the region that are available at the point in time the decision is made. In real-time applications (for GSM, tectonic summaries, determining tectonic origin) some parameters used are not yet available (e.g., the faulting mechanism), so default parameters or alternative decision-making criteria must be supplied. For unknown source mechanisms, a default fault mechanism is determined at any location around the globe based on a composite mechanism derived from the global CMT and USGS-CMT catalogues (H. Benz, written communication, 2010). For catalog or randomly supplied events (e.g., from a probabilistic event set), most of these parameters are or can be pre-assigned; if not, the Garcia et al (2010) approach can be employed.

In all cases, the type of earthquake and the tectonic regime under consideration are crucial prerequisites needed to make a reasonable GMPE selection. The details of the strategy are provided in detail by Garcia et al (2010) and are only summarized briefly here. In short, first the epicentral location is used to select the Flinn-Engdahl Geographical Region (FEGR) (Flinn and Engdahl, 1965; Young et al., 1996). Next, the tectonic regime (ACR, SCR, or SZ) and seismological category (Figure 2.3) are assigned from the FEGR. The combination of hypocentral depth and mechanism are subsequently used to assign the GMPE (see Figure 2.3). For subduction zones, a final level of complexity is required since one needs to differentiate among four types of subduction-zone earthquakes: outer-rise, interface, intraslab, and upper-plate events, since they employ different GMPEs (or coefficients). Except for perhaps interface earthquakes, inside each group considerable differences in depth and focal mechanism can be found in a particular subduction zone. This is especially true for upper-plate seismicity, which includes forearc, volcanic-arc, and backarc events, each of them with different source and propagation characteristics.

Given this complexity, Garcia et al. (2010) take advantage of the procedure proposed by Hayes and Wald (2009) and Hayes et al. (2009) that maps out the depth of the subduction interface for many subduction zones worldwide. From the trench location, the first discriminant determines whether the earthquake is an outer-trench event or an inner-trench event. If inside the trench, the slab geometry constrained by Hayes et al. (2009) is used to determine both the source origin and the GMPE with appropriate assignment of coefficients.

The output of the algorithm is the definition of the tectonic region, the source mechanism, and the event's depth relative to the plate interface, if constrained. From these output parameters, the appropriate GPME and even any event-specific GMPE flags (coefficients for mechanism and interface or intraslab) are supplied. Critically, the strategy and algorithm provided by Garcia et al (2010) are intended to accommodate future improvements in GMPE and IPE development. For example, despite the fact we can identify outer-rise earthquakes with this approach, there are no suitable GMPEs for such a propagation path and source. If there is future progress in developing such equations, the default GMPE assigned for these cases will be replaced with a more appropriate GMPE.

As seen in Figure 2.4, this is not an academic exercise; ground motion estimates vary by more than a factor of two among different GMPEs and coefficients for the same source geometry. In theory, once one selects the most appropriate GMPE for a specific earthquake (or multiple, weighted GMPEs), one has reduced the epistemic uncertainty associated with

ground-motion predictions. This is also true for the prediction of macroseismic intensity through the use of both IPEs and GMICEs. However, in practice there is potential for favorable or unfavorable coupling between particular GMPEs and the GMICEs, as described next.

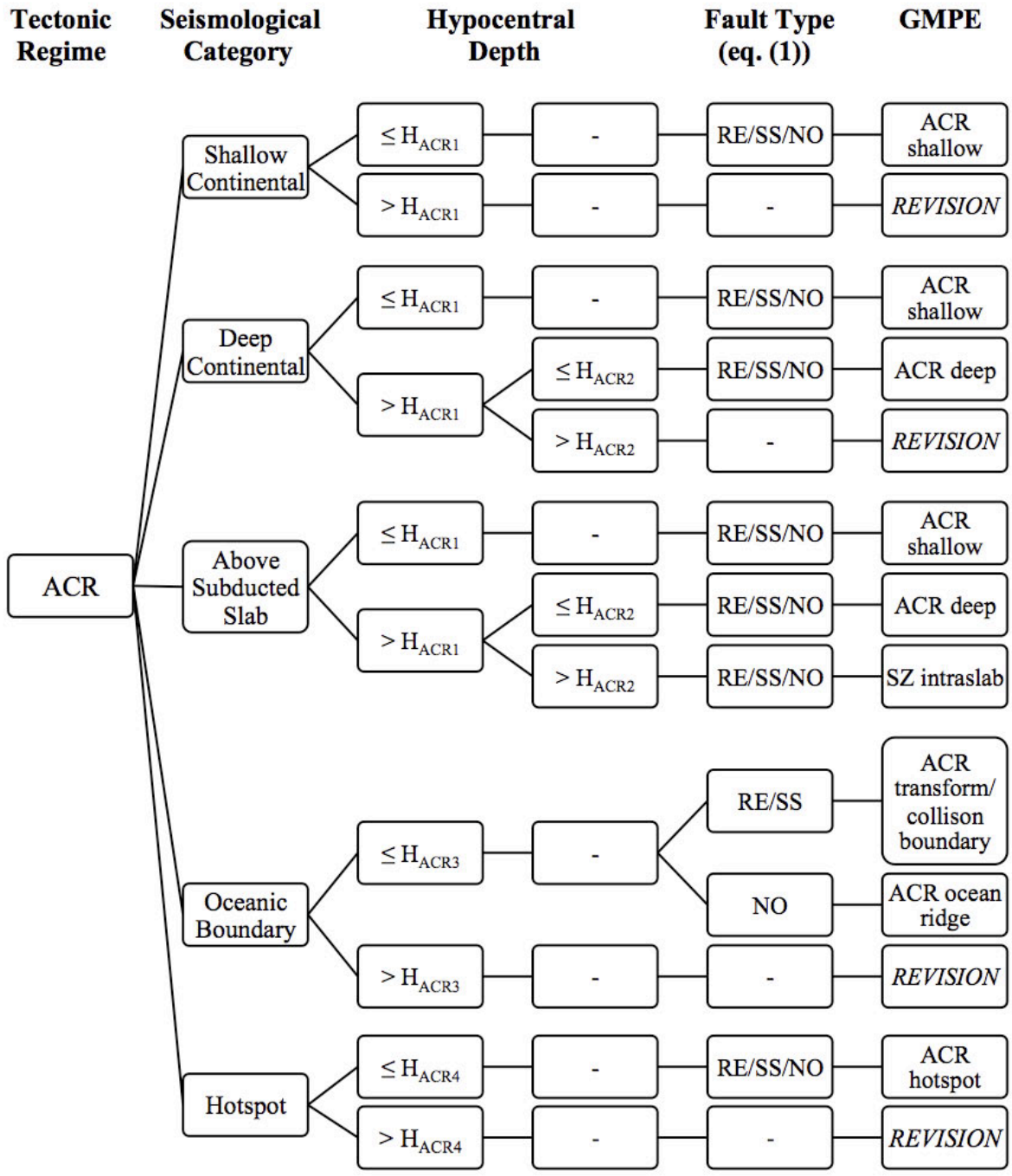

Figure 2.3 Flowchart of the earthquake/GMPE determination scheme for Active Crustal Regions (ACRs). Similarly complex logic is required to assign GMPEs for SCR and SZ regimes. From Garcia et al. (2010).

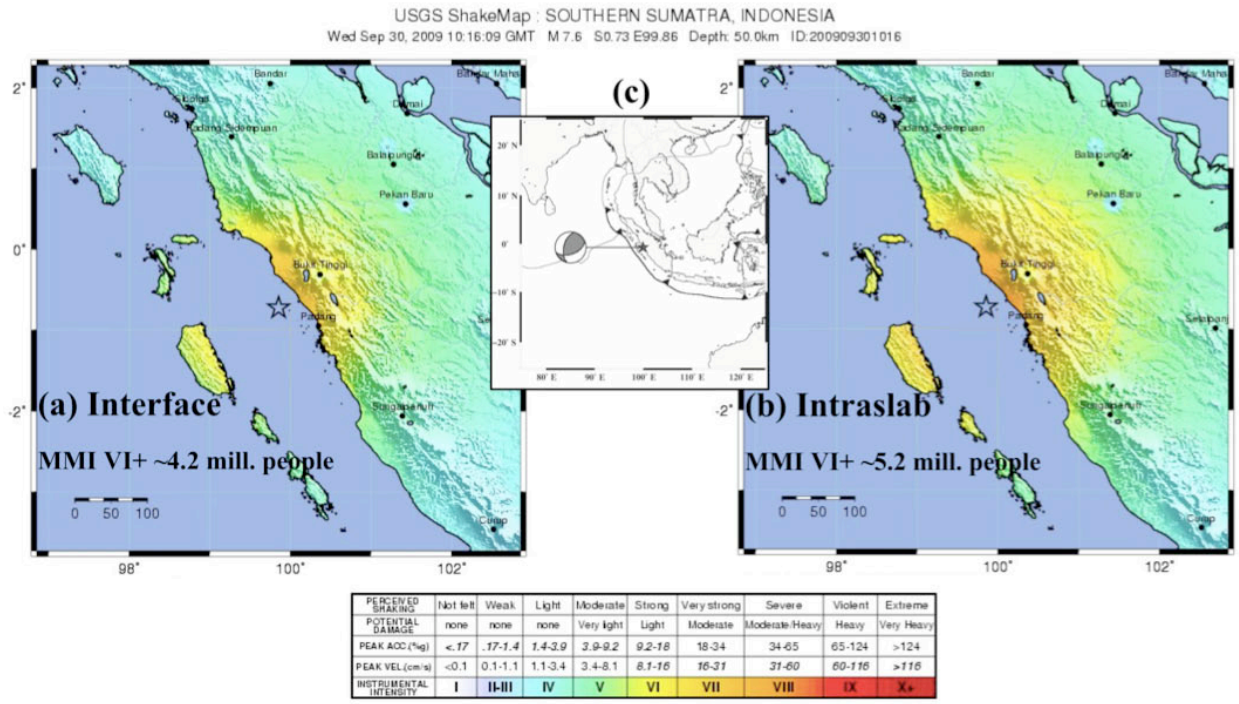

Figure 2.4 ShakeMaps produced using the National Earthquake Information Center (NEIC) preliminary location of the Padang (Indonesia) earthquake of September 30, 2009 (moment magnitude M_W 7.6; depth H = 50 km) using the subduction-zone GMPE by Youngs et al. (1997) for: (a) interface earthquakes; and (b) intraslab earthquakes. (c) Location map showing the focal mechanism obtained at NEIC from W-phase inversion 19 minutes after the origin time. In (a) and (b) population exposure at MMI VI and above, estimated from the PAGER system, is indicated (in millions of persons). Refined locations in the following days set the depth at 81 km, revealing the event was an intraslab earthquake (from Garcia et al., 2010).

2.3 Dependency between GMPEs and Conversion Equations

Allen and Wald (2009) evaluated several modern macroseismic intensity prediction equations against a global set of macroseismic observations for different tectonic settings (Allen et al., 2008). Although a few of the models appeared to capture some of the characteristics of average global intensity attenuation, no one model was observed to be desirable when tested against the global macroseismic database for active crust, subduction zone, or stable continent tectonic settings, respectively (Allen and Wald, 2009).

Allen and Wald (2009) also demonstrated a clear dependence between GMPEs and GMICEs. For example, they tested the use of the Wald et al. (1999c) GMICE combined with two Californian GMPEs; Boore et al. (1997) and Chiou and Youngs (2008). Peak ground-motion values were evaluated for each magnitude and distance pair, consistent with active crustal intensity observations compiled for the ShakeMap Atlas. Seismic site corrections were applied to each model based on V_{S30} estimates from topographic slope (Wald and Allen, 2007) for each intensity observation. Once the peak ground-motion values were evaluated for each model, the Wald et al. (1999c) GMICE was applied to provide an estimate of macroseismic intensity. Intensity residuals were subsequently calculated and median residuals, binned at 10-km increments, were compared for both GMPE-GMICE combinations.

When used with Chiou and Youngs (2008) GMPE, the Wald et al. (1999c) relations perform relatively well in the near-source region (approximately R_{rup} 10–20 km). However, the combination of these relations systematically underestimates macroseismic intensity at larger distances, with a median residual of 1.2 intensity units (Fig. 2.5a).

To examine the discrepancies between the predicted and observed intensities from the combination of the Chiou and Youngs (2008) GMPE and Wald et al. (1999c) GMICE, Allen and Wald (2009) recalculated the residuals using the Boore

et al. (1997) GMPE with Wald et al. (1999c) GMICE. The latter combination was the standard configuration for ShakeMap instrumental intensity prediction when GSM was first initiated in 2004 until the release of V3.5 in late 2009. Allen and Wald (2009) observed that the Boore et al. (1997) GMPE / Wald et al. (1999c) GMICE combination results in a much improved mapping of observed to predicted residuals, with a median residual near zero (Fig. 2.5b). However, Allen and Wald (2009) recognized that the Boore et al. (1997) GMPE tends to overestimate peak-ground motions, while the Wald et al. (1999c) GMICE underestimates macroseismic intensity at larger distances relative to the global instrumental and intensity database gathered for the Atlas. In summary, net result of the overestimation of ground-motion at larger distances from the Boore et al. (1997) GMPE and the underestimation of intensity from the Wald et al. (1999c) relations combines to provide relatively robust estimates of the overall shaking intensity. However, if one wishes to know both reliable peak ground-motion values and intensities consistent with global observations, the combination of the Boore et al. (1997) GMPE and the Wald et al. (1999c) GMICE could lead to erroneous analytical estimates of earthquake impact. This notable dependency between two relations warrants concern in that the best available GMPE and GMICE models may not necessarily work well in concert.

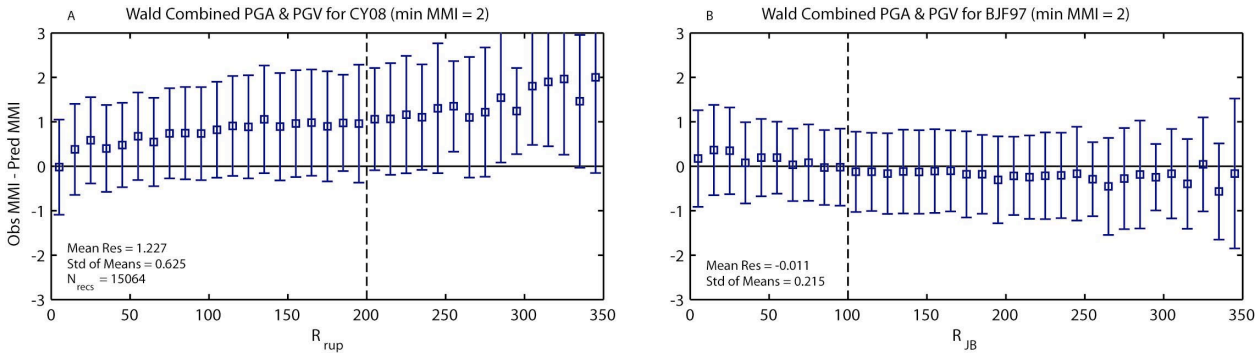

Figure 2.5 Residuals for the peak ground-motion-to-intensity conversions for global active crustal regions using the Wald et al. (1999c) GMICE relations. (a) Indicates the median intensity residuals using the Chiou and Youngs (2008) GMPE as the predictor of peak ground motions. (b) Indicates the median intensity residuals using the Boore et al. (1997) GMPE as the predictor of peak ground motions. Predicted instrumental ground motions are calculated using the aforementioned GMPEs and converted to intensity. The intensity residual is subsequently calculated. Residuals are binned in 10-kilometer windows and the median residual is plotted. The standard deviation of the residuals is indicated and vertical dashed lines indicate the maximum distance of usage of the GMPEs.

3 Intensity Prediction Equations (IPEs)

Intensity prediction equations (IPEs) have not received the attention of their more quantitative GMPE counterparts in the past. However, the usage of equations which directly predict macroseismic intensities, rather than from conversions from peak ground motions, has practical utility since direct estimation of intensity negates the need to account for the combined uncertainties in ground-motion estimates from GMPEs and GMICEs.

Traditionally, the attenuation of intensity with distance was defined in terms of epicentral intensity, I_0. The limitation with this approach is that the prediction equations need to be tied to subsequent equations which predict I_0 in order to be used in a predictive sense. Furthermore, many of the early IPEs are calibrated to surface-wave magnitude, M_S, or local magnitude, M_L. IPEs tied to M_S are less problematic than other magnitude scales – particularly at large magnitudes – since the commonly accepted M_W scale was originally calibrated against M_S (Hanks and Kanamori, 1979). If no clear magnitude scaling term is provided for equations which use I_0, then IPEs cannot be used in the forward sense without some assumption of epicentral intensity. Thus, we do not further consider IPEs based on I_0. Modern IPEs are typically tied to moment magnitude explicitly in their functional form.

IPEs often rely on different distance metrics as a predictor variable. For example, some models use epicentral distance, R_{epi}, (e.g., Bakun and Wentworth, 1997), whilst others use closest distance to rupture, R_{rup}, or some variant that considers extended fault sources, such as Joyner-Boore distance, R_{JB}, which represents the closest distance to the surface projection of the causative fault (Joyner and Boore, 1993). For small-magnitude earthquakes, where an earthquake can be approximated by a point source, the difference between point- and extended-source distance metrics can be minimal. However, at larger magnitudes where source finiteness can be significant, IPEs which use point-source distance metrics are not likely to be applicable. In our evaluation, we do include those IPEs which use point-source distance metrics, though we do not consider them to be preferred candidates for globally applicable IPEs (with exception for cases where fault dimensions are not yet ascertained).

The treatment of site effects using many IPEs is generally quite poor relative to their more quantitative GMPE counterparts. Several authors have identified marked intensity amplification effects for sites located on soft near-surface sediments (e.g., Borcherdt, 1970). Site-condition intensity amplification factors have previously been provided in other studies (e.g., Edwards et al., 2004; Eguchi et al., 1997); however, there is little quantitative information as to how these factors were derived. Sørensen et al. (2008) identifies an anisotropic correction term for the Vrancea, Romania, region. However, this correction term is strongly dependent on spatial location and cannot be used generally. Overall, little quantitative evidence can be identified by the authors to demonstrate intensity amplification effects and provide site-condition dependent macroseismic correction factors.

In their upcoming manuscript, Allen and Wald (2010) find only modest evidence of site-dependent amplification for sites with low V_{S30}. However, given uncertainties in constraining V_{S30} from topographic data (Wald and Allen, 2007) and the qualitative nature of intensity assignments, it is difficult to draw any statistically significant conclusions. Furthermore, the median V_{S30} for their complete active crustal dataset was determined to be 425 m/s. This suggests that the median IPEs presented herein are potentially applicable for sites about the CD boundary – a softer default site condition than that of common instrumental ground-motion prediction equations. The question as to how to modify IPEs to accommodate site amplification remains worthy of further study.

The main criterion in evaluating IPEs in the subsequent analyses is that they are scaled to moment magnitude rather than the epicentral intensity, I_0. Each of these equations is subsequently tested against observed macroseismic intensities from

global active crustal, subduction zone, and stable continental regions. In performing these comparisons, we do not consider the magnitude or distance ranges specified by the authors of a particular macroseismic intensity prediction model. In contrast, we include earthquake data of magnitude and distance ranges that are of interest to GSM and GEM operations.

3.1 Macroseismic Intensity Data

The bulk of the data used in the present study were gathered in the development of the ShakeMap Atlas V1 (Allen et al., 2008), which presently consists of over 5,600 ShakeMaps from earthquakes since 1973. Many of the events in the ShakeMap Atlas were not captured by strong-motion instruments, but were nonetheless well-documented with macroseismic observations. Data presented here were also employed by Allen and Wald (2009) to evaluate global IPEs and have since then been augmented with additional intensity data. Appendix I through III indicate the specific events which have been collated for active crustal, stable continental, and subduction zone regions, respectively.

For macroseismic intensity, the USGS uses Modified Mercalli Intensity (MMI) assignments consistent with the approach of Dewey et al. (1995). Specifically, intensity XI and XII are no longer assigned, and intensity X is available but has not been applied for several decades. Where intensity assignments are made with Medvedev-Sponheuer-Karnik (MSK–64), European macroseismic (EMS–98), or other intensity scales, we assume equivalency, and herein we make no attempt to justify this assumption. For more information about the comparison of macroseismic intensity scales, see Trifunac and Brady (1975) and Musson et al. (2009).

In addition to traditional intensity assignments conducted by experts (via post-disaster field surveys, from engineering and other reports, or from postal questionnaires), Allen et al. (2008) also employ the "USGS Did You Feel It?" (DYFI?) system to augment the intensity dataset from recent earthquakes. DYFI? data have been shown to be consistent with USGS MMI assignments over the entire range of intensities (Dewey et al., 2002), with minor differences at the lowest intensities. Not only is information from DYFI? valuable for areas that experience significant levels of shaking, it is also effective in constraining moderate ground-motions at larger distances (or for smaller earthquakes) that are not damaging. Such data explicitly constrain the fact that ground-motions were *not* damaging, whereas traditional macroseismic data-collection approaches often fail to collect or document such observations, focusing on higher intensity data and events with such data. The DYFI? data are invaluable constraints for many recent Atlas events, both in the U.S. (post-1999) and globally (post-2003), particularly for areas with few seismic instruments.

Macroseismic data is typically available in four forms in the studies analyzed here, and they are of variable quality depending on the accuracy of the reported location of the assigned intensity value. Some data are provided as tabulated latitude-and-longitude intensity assignments, while others may provide city or town names, which can usually be found and geocoded. The lowest level of accuracy comes from digitizing locations from an isoseismal map, and assigning ordinal intensity values based on location with respect to isoseismal lines. In the ShakeMap Atlas, Allen et al. (2008) assumed the following quality ranking, from highest to lowest, when considering these data:

1. Assigned intensities, tabulated with latitude and longitude site locations,
2. Assigned intensities with site locations digitized from historic or modern maps,
3. DYFI? intensities,
4. Intensities with site locations (typically local town or cities identified on a map) and intensity values digitized with respect to isoseismal contours.

Earthquakes in the Atlas were classified as belonging to active crustal, subduction zone, or stable continental regions using the logic outlined in Figure 2.2, as described in Allen et al. (2008), which considers magnitude, focal depth, and tectonic setting (i.e., Johnston et al., 1994). Table 1 summarizes the availability of intensity data (macroseismic and DYFI? intensities) in these various tectonic regions. We expect that the new classification schema proposed by Garcia et al.

(2010) will yield improved mapping of tectonic setting to ShakeMap Atlas V2 earthquakes. However, the present analyses do not yet take advantage of these advances.

Table 3.1 Summary of the number of conventional macroseismic intensity assignments and DYFI? data used as constraints for estimating intensity in the ShakeMap Atlas, categorized by tectonic environment

Tectonic Setting	Assigned Intensity Data	Number of Assigned Intensity Events	DYFI? Data	Number of DYFI? Events
Active crust	17,163	115	2,169	87
Subduction zone	3,546	47	1,073	83
Stable continent	17,314	30	1,188	14
Total	38,023	192	4,430	184

3.2 IPE Candidate Models

Table 3.2 provides a summary of the IPEs considered herein. Their functional forms are outlined below and the definitions of parameters used are indicated in Table 3.2. The candidate models were developed for a wide-range of geographic regions and are customised for particular magnitude and distance ranges. In our overall strategy for evaluating the candidate IPEs, we test each model equally based on the usage requirements of GSM and GEM. Consequently, we include all models for evaluating IPEs for active crust, subduction zone and stable continental regions, respectively.

Table 3.2 Summary of Intensity Prediction Equations (IPEs) Considered

Reference	Magnitude range	Distance range (km)	Intensity range used	Distance metric	Intensity type	Region
Bakun and Wentworth (1997)	$4.4 \le M_W \le 6.9$	< 500	3 – 9	R_{epi}	MMI	California, USA
Chandler and Lam (2002)	$3.3 \le M_W \le 8.0$	< 300	4 – 10	R_{epi}	MMI	South China
Bakun et al. (2003)	$3.7 \le M_W \le 7.3$	< 1200	3 – 7	R_{epi}	MMI	Eastern North America
Dowrick and Rhoades (2005)	$4.6 \le M_W \le 8.2$	< ~500	3 – 11	R_{rup}	MMI	New Zealand – Main Region
Dowrick and Rhoades (2005)	$5.2 \le M_W \le 7.3$	< ~500	3 – 11	R_{rup}	MMI	New Zealand – Deep Region
Bakun (2006)	$4.6 \le M_W \le 7.3$	< 500	3 – 8	R_{epi}	MMI	Basin and Range, USA
Bakun and Scotti (2006)	$4.9 \le M_W \le 6.0$	< 150	3 – 7	R_{epi}	MSK	French SCR
Bakun and Scotti (2006)	$4.9 \le M_W \le 6.0$	< 150	3 – 7	R_{epi}	MSK	Southern France
Atkinson and Wald (2007)	$2.3 \le M_W \le 7.8$	2 – 500	2.0 – 10[†]	R_{rup}	MMI	California, USA
Atkinson and Wald (2007)	$2.0 \le M_W \le 7.8$	6 – 1000	2.0 – 11+[†]	R_{rup}	MMI	Eastern North America
Pasolini et al. (2008)	$4.4 \le M_W \le 7.4$	1 – 200	4 – 11	R_{epi}	MCS	Italy
Sørensen et al. (2009a)	$6.3 \le M_W \le 7.0$	0 – 660	3 – 11	R_{JB}	MCS	Campania, Italy
Sørensen et al. (2009b)	$5.9 \le M_W \le 7.4$	0 – 335	5 – 10	R_{JB}	EMS-98	Marmara Sea, Turkey
Allen and Wald (2010)	$4.9 \le M_W \le 7.9$	< 300	3 – 10	R_{rup}	Mixed	Global active crust

[†] Estimated from Figure 2.4 of Atkinson and Wald (2007).

Table 3.3 Total uncertainty in intensity units

Parameter	Definition
h	Earthquake focal depth
I_x	Macroseismic intensity measure of type x, where x is EMS, MCS, MMI or MSK
M_W	Moment magnitude
R_{epi}	Epicentral distance (km)
R_{hyp}	Hypocentral distance (km)
R_{JB}	Joyner-Boore distance (km)
R_{rup}	Closest distance to rupture (km)
σ	Total uncertainty in intensity units

Bakun and Wentworth (1997): California, USA

$$I_{MMI} = 3.67 + 1.17 M_W - 3.19 \log\left(R_{epi}\right) \tag{3.1}$$

Chandler and Lam (2002): South China

$$I_{MMI} = -0.8919 + 1.4798 M_W - 0.1311 \ln\left[\left(R_{epi} + R_0\right)/R_0\right] - 0.0364 R_{epi}$$

$$\text{for } R_{epi} \le 45\,\text{km}$$

$$I_{MMI} = -0.8919 + 1.4798 M_W - 0.1311 \ln\left[\left(R_{epi} + R_0\right)/R_0\right] - 0.0364 R_{epi} + 0.0193\left(R_{epi} - 45\right)$$

$$\text{for } 45 < R_{epi} \le 75\,\text{km}$$

$$I_{MMI} = -0.8919 + 1.4798 M_W - 0.1311 \ln\left[\left(R_{epi} + R_0\right)/R_0\right] - 0.0364 R_{epi} + 0.0193\left(R_{epi} - 45\right) + 0.0085\left(R_{epi} - 75\right) \tag{3.2}$$

$$\text{for } R_{epi} > 75\,\text{km}$$

where:

$$R_0 = \frac{1}{2} \times 10^{(0.74 M_W - 3.55)}$$

$$\sigma \approx 0.7$$

Bakun et al (2003): Eastern North America

$$I_{MMI} = 1.41 + 1.68 M_W - 0.00345 R_{epi} - 2.08 \log\left(R_{epi}\right) \tag{3.3}$$

Dowrick and Rhoades (2005): New Zealand – Main Region

$$I_{MMI} = 4.40 + 1.26 M_W - 3.67 \log\left(r^3 + d^3\right)^{1/3} + 0.012h + 0.409\delta_c$$

where:

$$\delta_c = \begin{cases} 1 & \text{for crustal events} \\ 0 & \text{for all other events} \end{cases}$$

$$d = 11.78$$

$$r \approx R_{rup}$$

$$\sigma = 0.43$$

(3.4)

Dowrick and Rhoades (2005): New Zealand – Deep Region

$$I_{MMI} = 3.76 + 1.48 M_W - 3.50 \log r + 0.0031h$$

where:

$$r \approx R_{rup}$$

$$\sigma = 0.42$$

(3.5)

Bakun (2006): Basin & Range, USA

$$I_{MMI} = 0.44 + 1.70 M_W - 0.0048\Delta_h - 2.73 \log\left(\Delta_h\right)$$

where:

$$\Delta_h = \sqrt{R_{epi}^2 + h^2}$$

$$h = 10$$

$$\sigma = 0.58$$

(3.6)

Bakun and Scotti (2006): French SCR

$$I_{MSK} = 4.48 + 1.27 M_W - 3.37 \log\left(\sqrt{R_{epi}^{\ 2} + h^2}\right)$$

(3.7)

Bakun and Scotti (2006): Southern France

$$I_{MSK} = 4.66 + 1.27 M_W - 3.83 \log\left(\sqrt{R_{epi}^{\ 2} + h^2}\right)$$

(3.8)

Atkinson and Wald (2007): California, USA

$$I_{MMI} = 12.27 + 2.270\left(M_W - 6\right) + 0.1304\left(M_W - 6\right)^2 - 1.30\log R$$
$$- 0.0007070R + 1.95B - 0.577M_W \log R$$

where:

$$R = \sqrt{R_{rup}{}^2 + h^2}$$

$$h = 14.0$$

$$B = \begin{cases} 0 & \text{for} \quad R \le 30.0 \\ \log\left(R/30.0\right) & \text{for} \quad R > 30.0 \end{cases}$$

$$\sigma \approx 0.4$$

(3.9)

Atkinson and Wald (2007): Eastern North America

$$I_{MMI} = 11.72 + 2.36\left(M_W - 6\right) + 0.1155\left(M_W - 6\right)^2 - 0.44\log R$$
$$- 0.002044R + 2.31B - 0.479M_W \log R$$

where:

$$R = \sqrt{R_{rup}{}^2 + h^2}$$

$$h = 17.0$$

$$B = \begin{cases} 0 & \text{for} \quad R \le 80.0 \\ \log\left(R/80.0\right) & \text{for} \quad R > 80.0 \end{cases}$$

$$\sigma \approx 0.4$$

(3.10)

Pasolini et al. (2008): Italy

$$I_{MCS} = I_E - 0.0086\left(\sqrt{R_{epi}{}^2 + h^2} - h\right) - 1.037\left[\ln\left(\sqrt{R_{epi}{}^2 + h^2}\right) - \ln\left(h\right)\right]$$

where:

$$I_E = 2.460M_W - 5.862$$

$$h = 3.91$$

$$\sigma = 0.69$$

(3.11)

Sørensen et al (2009): Campania, Italy

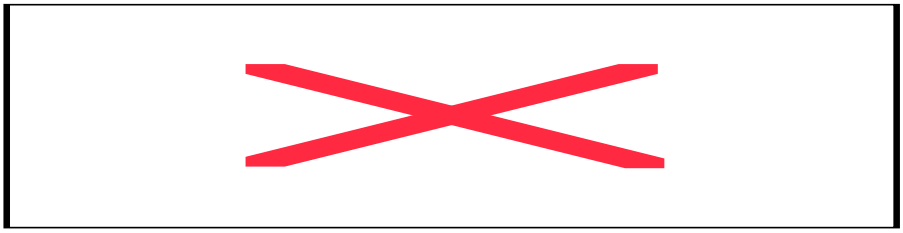

(3.12)

Sørensen et al (2009): Marmara Sea Region, Turkey

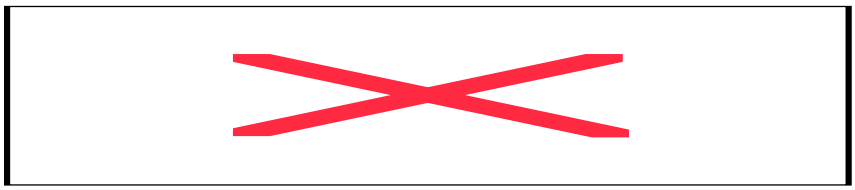

(3.13)

Allen and Wald (2010): Global Active Crust

$$I = 3.15 + 1.03M - 1.11\ln\sqrt{R_{rup}^2 + \left[1 + 0.72\,\mathrm{e}^{(M-5)}\right]^2}$$
$$\sigma(R_{rup}) = 0.73, \quad \text{for} \quad R_{rup} = 100 \text{ km} \tag{3.14}$$

3.2.1 Tectonically Active Regions

Figure 3.1 indicates median residuals, binned with distance, for each of the candidate MMI intensity prediction models. Over 17,000 macroseismic intensity observations from active crustal regions around the world were used to evaluate the models. Of the candidate models, we observe that the Allen and Wald (2010) intensity prediction model yields the lowest average residuals over the magnitude and distance range examined (Fig. 3.1N). These results, however, should be tempered by the knowledge that the Allen and Wald (2010) IPE was developed using the same dataset used to evaluate all other candidate models tested herein. Consequently, this may not be seen as a fair comparison for the other candidate models developed for specific regions and magnitude and distance ranges. That acknowledged, the Allen and Wald (2010) IPE was developed with arguably a more comprehensive macroseismic intensity dataset of moderate-to-large magnitude earthquake data than any of the regional models. It has been suggested that differences in ground-motion observed between regions may be a consequence of limitations in ground-motion datasets over incomplete magnitude and distance ranges (Bommer et al., 2007; Douglas, 2007).

Excluding the Allen and Wald (2010) IPE, the Bakun and Wentworth (1997) prediction model (Fig. 3.1A), developed for California earthquakes, yields the lowest average residuals over the distance range examined. However, this model tends to overestimate intensity at small epicentral distances (R_{epi} < 20 km) because the intensity level does not saturate at near-source distances.

The Atkinson and Wald (2007) IPE for California (Fig. 3.1I) appears to underestimate observed intensities by one-half to a full-intensity unit for much of the distance range considered. However, the Atkinson and Wald (2007) IPE, on average, appears to perform well at distance ranges less than 30 km. Other relations examined herein do not appear to be applicable for use in GSM for active tectonic regions based on the comparison against our global macroseismic intensity dataset. Appendix IV indicates the performance of each of the candidate IPEs for different magnitude ranges against the evaluation dataset. In general, the Allen and Wald (2010) IPE performs the most consistently across the full magnitude range.

Finally, we compare several common intensity prediction methods (Fig. 3.2). We include both direct IPEs and intensities predicted through a combination of GMPEs and GMICEs. The two GMPE and GMICE combinations are the Boore et al. (1997) GMPE and Wald et al. (1999c) GMICE (BJF97-Wald99 combination) and the Chiou and Youngs (2008) GMPE and Atkinson and Kaka (2007) GMICE (CY08-AK07). The former combination has been used widely in USGS ShakeMap operations since 1999, while the latter combination was found by Allen and Wald (2009) to provide the lowest average residuals against global macroseismic intensity data. Both of the GMPE-GMICE combinations are calculated based on a common site-condition of V_{S30} 425 m/s.

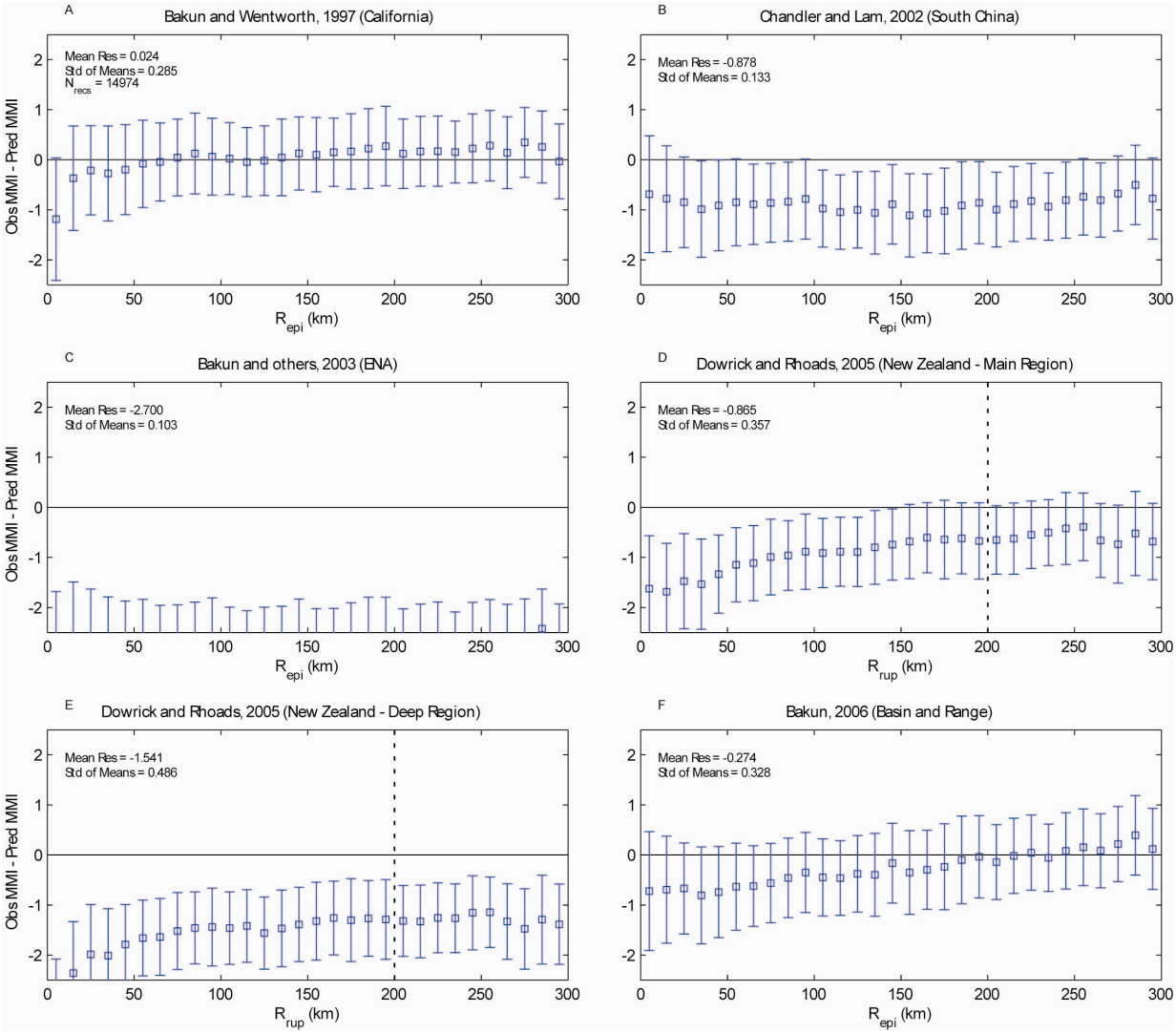

Figure 3.1 Residuals for macroseismic intensity prediction equations (IPEs) against global active crust intensity data. Residuals are binned in 10-kilometer windows and the median residual is plotted. The standard deviation of the residuals is indicated. Vertical dashed lines indicate the maximum distance of usage as recommended by each of the authors

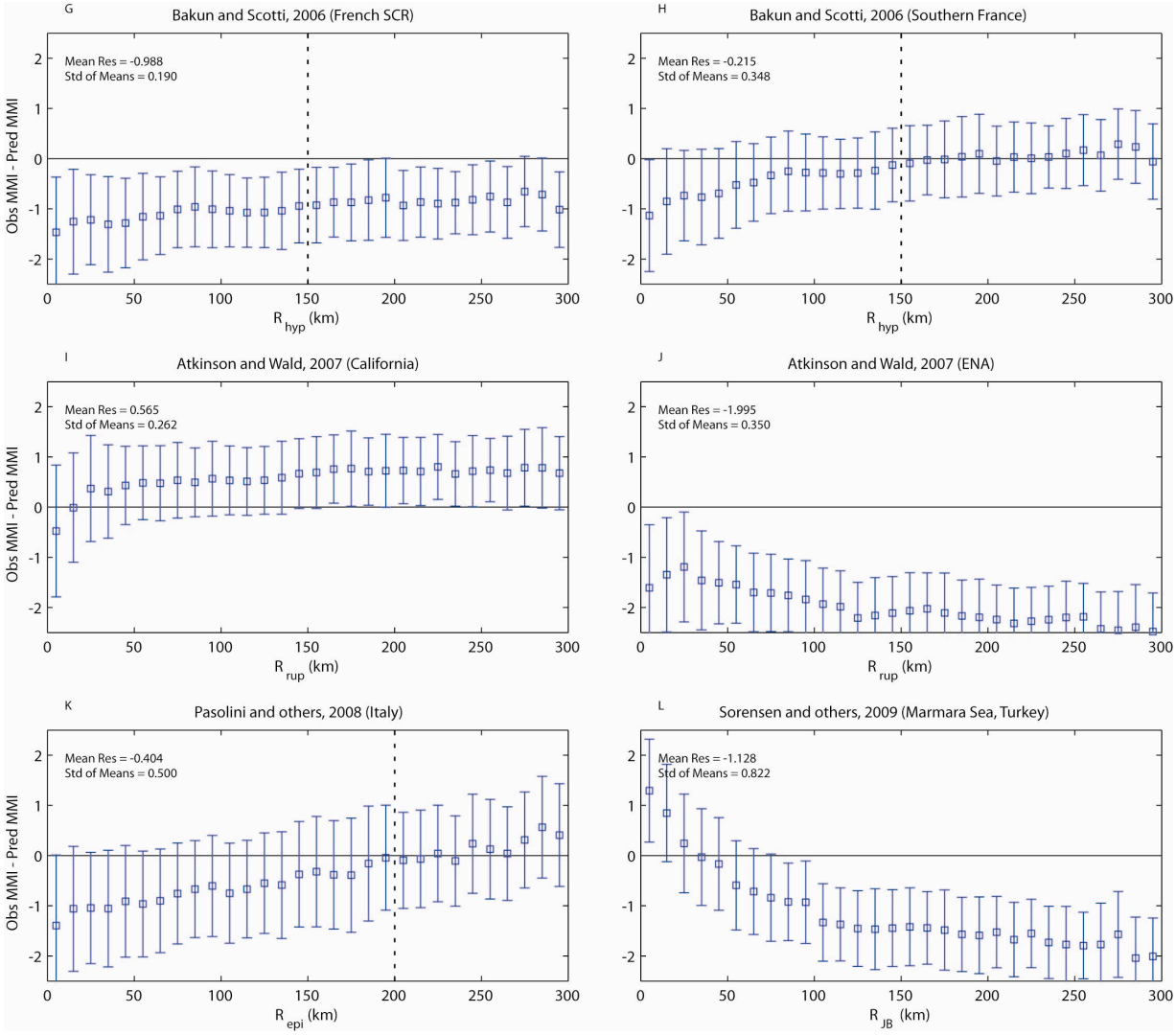

Figure 3.1 continued

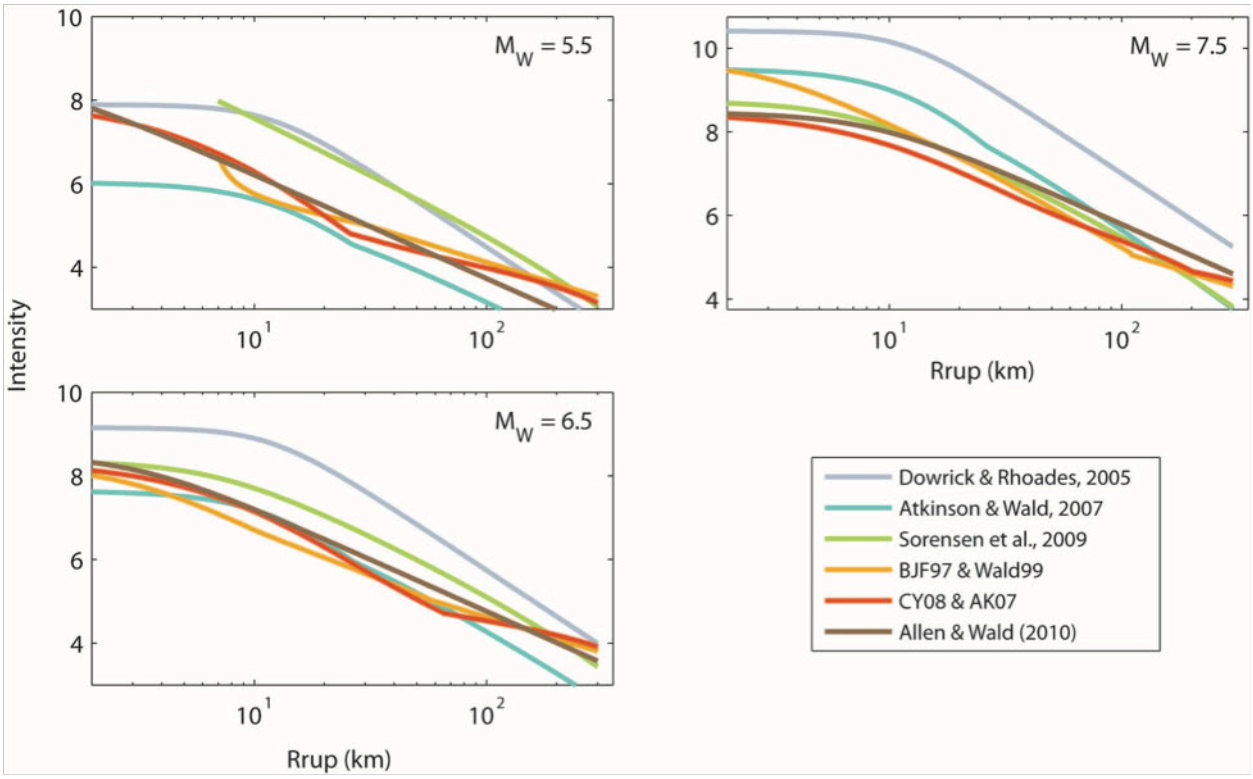

Figure 3.2 Comparison of several common intensity prediction methods for shallow active crustal regions (ACRs) assuming a uniform site condition with V_{S30} of 425 m/s at magnitudes of M_W 5.5, 6.5 and 7.5. Four of the techniques apply direct IPEs: Dowrick and Rhoades (2005); Atkinson and Wald (2007); Sørensen et al. (2009b); and Allen and Wald (2010). The other two models use GMPE/GMICE combinations: Boore et al.(1997) and Wald et al. (1999c) (BJF97 & Wald99); and Chiou and Youngs (2008) and Atkinson and Kaka (2007) (CY08 & AK07). Models that use a R_{JB} distance metric have been converted to R_{rup} for the M_W 5.5 scenario assuming a *point source* earthquake with a focal depth of 7 km. For the M_W 6.5 and 7.5 scenarios, we assume a vertically dipping, surface rupturing earthquake, in which case $R_{JB} = R_{rup}$.

3.2.2 Stable Continental Regions

Over 17,000 macroseismic observations from stable continental regions around the world were used to evaluate the candidate macroseismic intensity prediction equations (Fig. 3.3). None of the candidate IPE models were determined to be particularly adequate for global SCRs. Of the candidate models, the Chandler and Lam (2002) equation for Southern China (Fig. 3.3B) and the Bakun (2006) equation for the Basin and Range (Fig. 3.3F) appear to provide the lowest median residuals for near-source (approximately R_{epi} < 50 km) intensity observations in stable continental regions. However, both of these models do not perform very well beyond this distance range, underestimating ground shaking for combined stable continent observations. Moreover, when examining the magnitude dependence of the two aforementioned equations, it becomes clear that these two models are generally only applicable for small to moderate-magnitude earthquakes (approximately $4.5 \leq M_W \leq 5.5$) where abundant SCR data are available (Appendix V).

The Bakun et al. (2003) (Fig. 3.3C) and Atkinson and Wald (2007) (Fig. 3.3J) models have been developed specifically for the eastern North American SCR. The Atkinson and Wald (2007) IPE does an excellent job at predicting DYFI? data for moderated-sized events in the central and eastern US, even to the extent of reproducing the flattening of attenuation in the distance range from 70 to 150 km due to Moho bounces that are clear in the observations; however, the range of intensities is limited in such a comparison. In general, since the Bakun et al. (2003) and Atkinson and Wald (2007) models appear to overestimate intensities for the combined global SCR dataset, it is difficult to recommend one or more IPEs from the candidate models for use in global SCRs.

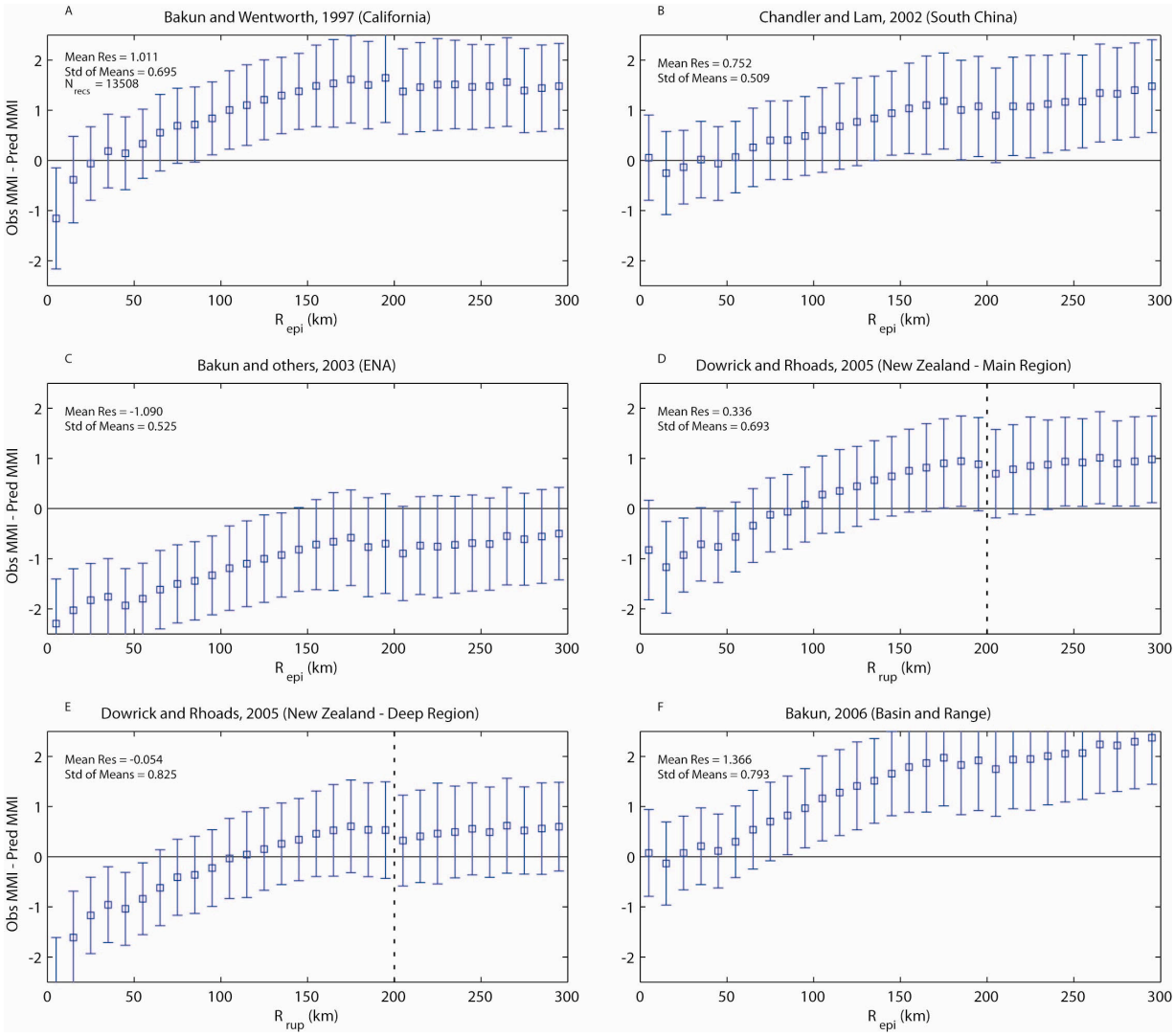

Figure 3.3 Residuals for macroseismic intensity prediction equations (IPEs) against global stable continental region (SCR) intensity data. Residuals are binned in 10-kilometer windows and the median residual is plotted. The standard deviation of the residuals is indicated. Vertical dashed lines indicate the maximum distance of usage as recommended by each of the authors

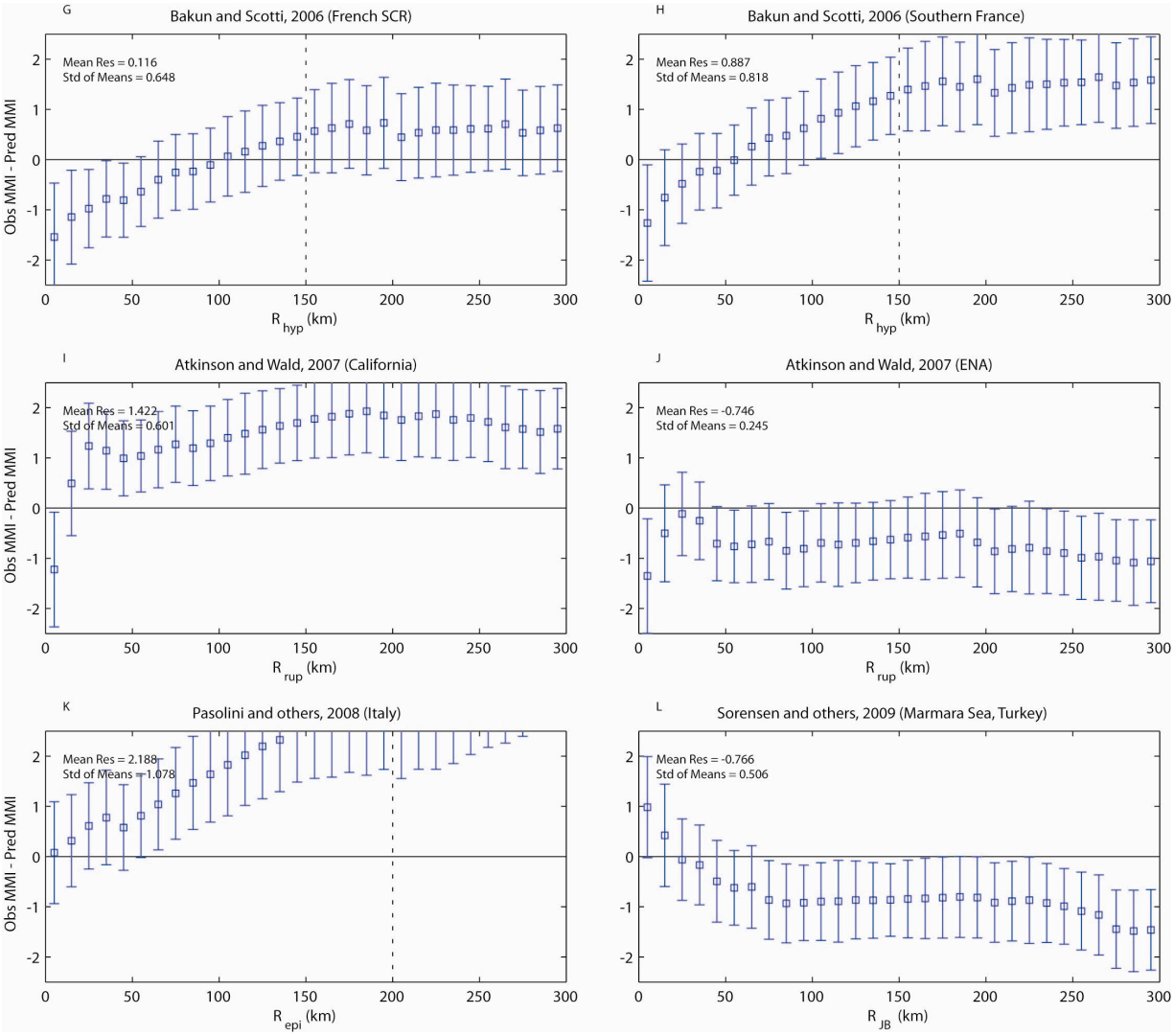

Figure 3.3 continued

3.2.3 Subduction zones

In our literature survey, we did not find any modern macroseismic intensity prediction equations for subduction zones that were specifically scaled to moment magnitude M_W. Consequently, we test the same set of macroseismic intensity prediction equations as presented in Table 1. A relatively modest number of over 3,500 macroseismic intensity observations from global subduction-zone earthquakes were used in this analysis (Fig. 3.4). Of the 14 candidate intensity-prediction equations, we observe that the Bakun and Scotti (2006) model developed for southern France generally provides the lowest median residuals for subduction-zone earthquakes (Fig. 3.4H). This raises some questions as to the physical meaning of this result, given that we could argue that the southern France region could not be considered an active subduction-zone, particularly given that the calibration events are from moderate-magnitude shallow crustal earthquakes. Consequently, despite its good performance relative to the other candidate models, we cannot recommend the Bakun and Scotti (2006) IPE for global subduction zone regions.

The Bakun and Wentworth (1997) model overestimates intensity at epicentral distances less than approximately 50 km, but yields consistently low median residuals at larger epicentral distances (Fig. 9A). It is interesting to note that the Bakun and Wentworth (1997) relation provides low residuals at larger distances (approximately R_{epi} > 50 km) for both active crustal (Fig. 2.5A) and subduction-zone (Fig. 3.3A) earthquakes. This suggests that average global attenuation properties

in the crust surrounding shallow active tectonic and subduction zones are similar at intermediate epicentral distances from the earthquake source. It is likely that at distances greater than approximately 50 km, high-frequency surface waves (*Lg*) dominate observed ground motions (e.g., Herrmann and Kijko, 1983), and these are the seismic waves that are perceptible to humans (Frankel, 1994; Trifunac and Brady, 1975) and that dominate macroseismic earthquake effects. The observation that the Bakun and Wentworth (1997) prediction model overestimates subduction-zone intensity data at shorter epicentral distances may be a consequence of more emergent ground motions at longer periods than typically observed from shallow active crustal earthquakes, thus resulting in lower intensities at the epicentral area of subduction zone earthquakes.

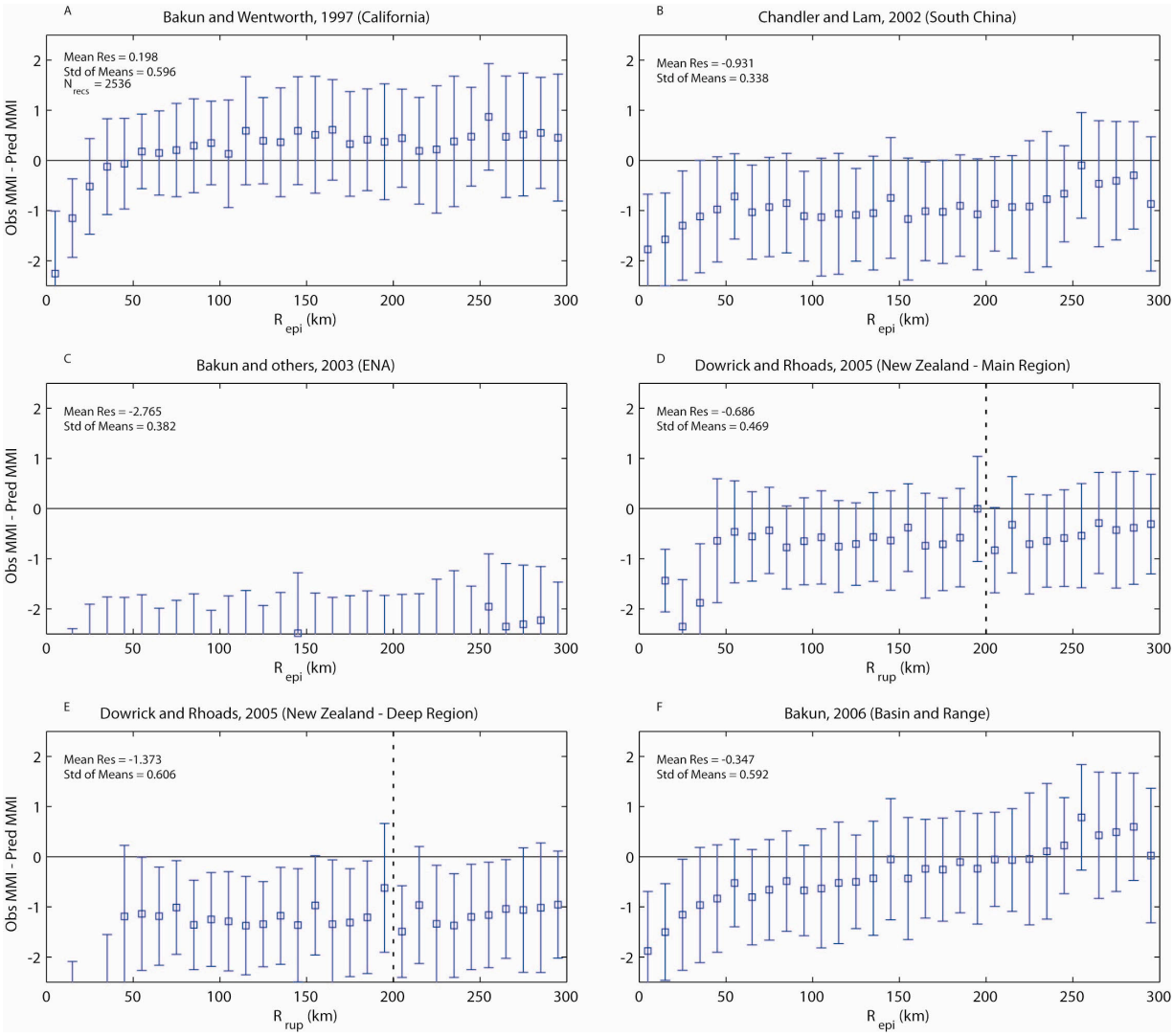

Figure 3.4 See above for figure caption

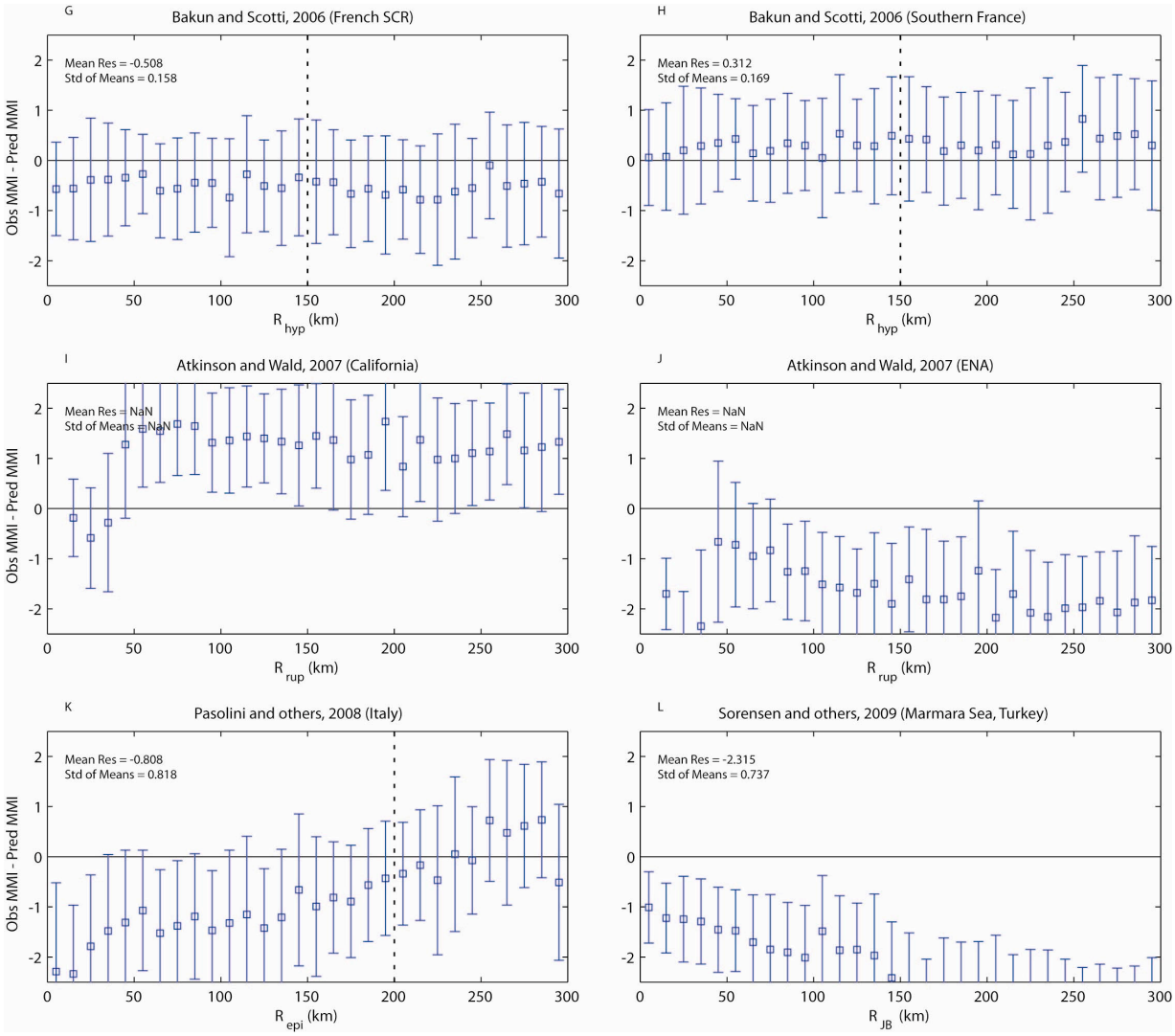

Figure 3.5 Residuals for macroseismic intensity prediction equations (IPEs) against global subduction zone (SZ) intensity data. Residuals are binned in 10-kilometer windows and the median residual is plotted. The standard deviation of the residuals is indicated. Vertical dashed lines indicate the maximum distance of usage as recommended by each of the authors

4 Ground Motion to Intensity Conversion Equations (GMICEs)

For GMICEs, a very significant limitation of the current collection is that they (mostly) consider only ground motion to intensity estimates; that is, intensity is the dependent variable in the regression. Normally then, one should only use these relations for computing the intensity given a ground motion, and not to estimate peak motions from intensity data. In practice, these relations are often used for both purposes. Likewise, GMICE development is also very limited and heterogeneous in both data and approach. We address these limitations in detail.

Allen and Wald (2009) evaluated the performance of several GMICEs (Atkinson and Kaka, 2007; Tselentis and Danciu, 2008; Wald et al., 1999c) relative to global data. Of these GMICEs, the Wald et al. (1999c) relation specifies a standard deviation of approximately one MMI unit, while the Atkinson and Kaka (2007) equation specifies a standard deviation of 0.8 intensity units. Instrumental ground-motion prediction equations (GMPEs) also possess uncertainties, which in general are a factor of roughly 2 in ground-motion. [Note: from Wald et al. (1999c), one intensity unit is approximately a factor of two in ground motion,] Consequently, in ShakeMap intensity estimation, where GMPEs are used to estimate PGA and PGV, and GMICEs are used to convert PGA and PGV into intensity, the uncertainty on the ShakeMap intensity estimates has to account for both GMPE and GMICE uncertainties (Eqn 4.1). ShakeMap V3.5 has the capability of outputting maps of intensity uncertainties, but it will not be configured to produce these as part of the standard suite of ShakeMap products until uncertainties for actual macroseismic data (including assignment subjectivity) can be ascertained, and the uncertainty of scaling the influence of available intensity observations to surrounding locations is better characterized.

$$\sigma_I = \sqrt{\sigma_{GMPE}^2 + \sigma_{GMICE}^2} \tag{4.1}$$

While use of GMPE-GMICE combinations to estimate intensity may have larger uncertainties than use of IPEs, the advantage of the GMPE-GMICE approach is that GMPE models have, until recently, been significantly more sophisticated than IPEs. The typical IPE has 2-3 predictor variables (Section 3.2), while NGA-type GMPEs have upwards of 10 predictor variables. In addition, for risk-related analyses, it may be of interest to compare empirical, intensity-based loss estimates with analytical, PGM-based approaches using a common GMPE. There is also some comfort in having a functional form that relates PGM and MMI estimates when using the GMPE-GMICE combination; having a GMPE and IPE from different studies can lead to a disconnect of ground motion and intensity estimates, so the GMICE provides a bridge between them.

We collected published studies on regionally derived GMICE that made available the underlying peak ground motion (PGM) – intensity datasets, with the goal of assembling an aggregate dataset for deriving a GMICE valid for global active crustal regions. We chose to start with active crustal regions, since there are few available studies on GMICE for subduction and stable continental regions. Figure 4.1 shows the functional forms of selected modern regional GMICE. These relationships are derived from datasets of paired PGM and intensity observations, with strong motion stations and intensity observations typically within 2-3 km of each other. At discrete intensity levels (for instance, every 0.5 or 1 intensity units), a mean ground motion value is obtained, and a linear or bi-linear relationship predicting intensity as a function of peak ground motion is derived. The variations in relationships between PGM and intensity shown in Figure 4.1 are typically used as evidence of regional variability in GMICEs. However, there are numerous other sources of variation, which include: macroseismic assignment subjectivity, macroseismic availability bias, differences among macroseismic scales, aleatory uncertainty due to incomplete datasets, and true regional differences. Atkinson and Kaka (2007) point out that accounting for magnitude and distance dependence removes the regional variation in PGM to intensity relationships. Our GMICE-related efforts in this study involved collecting published datasets of paired PGM-intensity observations, which are primarily from active crustal regions, and assembling a consistent set of metadata in preparation for deriving a new

GMICE (with magnitude and distance dependence) based on the assembled dataset. Table 4 lists characteristics of the GMICE datasets we are including in our aggregate dataset. In some cases, datasets from more recent studies include those from earlier investigations. For instance, the Faenza and Michelini (2010) dataset includes the earlier Faccioli and Cauzzi (2006) dataset. The Atkinson and Kaka (2007) dataset includes data from the earlier Atkinson and Sonley (2000) investigation. While the Gerstenberger et al. (2010) relationships are shown in Figure 4.1, the underlying dataset is not yet available (and not shown in Figure 4.1 or Table 4.2) due to some unresolved issues in pairing PGM and intensity at lower intensity levels.

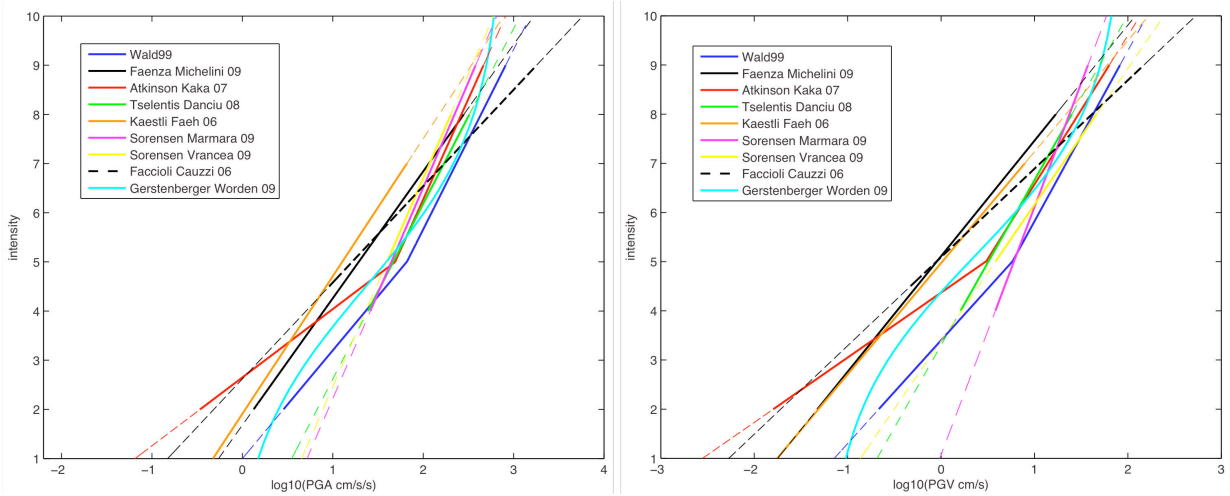

Figure 4.1 Functional forms of PGA and PGV to intensity relationships derived from various regions. The functions are plotted in thick lines for PGM and intensity ranges constrained by their respective datasets. Thin, dashed lines show the GMICEs when extrapolated beyond the datasets from which they were derived. The estimated intensities are in better agreement at larger values of PGM than at smaller values. It is clear that extrapolating GMICEs beyond the ranges constrained by data is not recommended

4.1 GMICE Functional Forms and Datasets

In the following section, we document some of the details of selected modern GMICE studies. Figure 4.2 shows the magnitude and distance ranges covered by these various datasets. It is worth noting that all studies differ from each other in details such as definition of peak ground motion, how to assign ground motion-intensity pairs, distance measures (if available), or the type of metadata supplied. These differences, along with the use of different intensity scales, and different magnitude and distance ranges spanned by the input datasets, all contribute to the scatter in the data, as shown in Figure 4.3, as well as to the differences in derived functional forms, as shown in Figure 4.1.

Macroseismic intensity and peak ground motion pairing

GMICE studies require a pairing of peak ground motion and macroseismic intensity. The various GMICE datasets we collected all have slightly different ways of pairing ground motions. For instance, Faenza and Michelini (2010) allow a strong motion station to form a pair with all intensity observations within a 3 km radius, while Wald et al. (1999c) pair a strong motion station with the closest macroseismic observation within a 2- or 3-km radius (we obtained both versions of the Wald et al. (1999c) dataset). For any new GMICE relationship that would be derived from the aggregate dataset we have assembled, the influence of the different pairing approaches employed by the contributing datasets would remain a source of variability. The ShakeMap Atlas dataset (listed as Allen et al. (2008) in Table 4.1), or the dataset of Gerstenberger et al. (2010), which includes more than 200,000 DYFI? and traditional MMI intensity observations from California, are potential datasets that could be used to explore and quantify the effects of different PGM-intensity pairing approaches. That said, the Atlas dataset may potentially be biased to larger median ground motions at lower intensity

levels since it does not consider small data from smaller earthquakes, which have abundant ground-motion intensity pairs, as demonstrated by Gerstenberger et al. (2010).

Considerations for using an aggregate dataset

For assembling an aggregate dataset that can be used to investigate regional variability in GMICEs, and possibly develop a new relationship for tectonically active regions, we focused on the datasets of Wald et al. (1999c) from California (W99), Kaestli and Faeh (2006) from Switzerland, Italy, and France (KF06), Atkinson and Kaka (2007) from California and the central and eastern US (AK07), Tselentis and Danciu (2008) from Greece (TD08), and Faenza and Michelini (2010) from Italy (FM10). In addition, we use PGM-intensity pairs from the ShakeMap Atlas (Allen et al., 2008) dataset. At this stage, we limit the aggregate dataset to include studies where the intensity data are assigned intensities based on felt reports and observed damage. We do not include studies, such as Sørensen et al (2007), wherein the intensity assignments to strong motion stations are based on readings from isoseismal contours. It is foreseen that any future aggregate analysis using both assigned and isoseismal-based intensity data points will have to weigh these two different types of intensities differently, with additional uncertainty given to the latter. In addition, while some studies, such as AK07 and TD08 include investigations of the depedence of intensity selected response spectral periods, we focus primarily on PGA and PGV, since these studies all indicate that PGV has the best correlation with intensity at higher intensity levels, and since PGA and PGV are the ground motion parameters common to the selected datasets.

In total, the aggregate dataset spans a magnitude range of $2 \leq M \leq 8.1$, with strong motion stations up to distances of 707 km from the source. The magnitude and distance distribution of the assembled dataset, which consists of 4029 strong motion station to intensity pairs (without accounting for possible overlap between the various datasets), is shown in Figure 4.2. Accounting for the overlap between the various datasets, which is a necessary step before using the aggregate dataset in deriving new GMICE and IGMCE, will result in a slight reduction in the total number of ground motion to intensity pairs. The Atlas, W99, and FM10 datasets define PGM as the larger of the horizontal components (maxEnv, or maximum envelope, definition of peak ground motion). The KF06, AK07, and TD08 studies treat each of the horizontal channels independently. Because GMICE relationships usually work with log(PGM) (since log(PGM) data are normally distributed), treating the horizontal channels independently is equivalent to defining PGM as the geometric mean of 2 horizontal channels (GM, or geometric mean, definition of peak ground motion). The FK06 and TD08 studies have the necessary metadata (event IDs along with station and channel names) to use the maxEnv definition of PGM. Due to corruption of the archived data files, it is not possible to match channels for a given station recording of a given event to determine the maxEnv definition with the AK07 dataset (Atkinson, pers. comm.). Transforming the data to a common PGM definition will require use of a conversion (Beyer and Bommer, 2006; Watson-Lamprey and Boore, 2007) between the maxEnv and GM definitions of PGM, which have some degree of uncertainty involved.

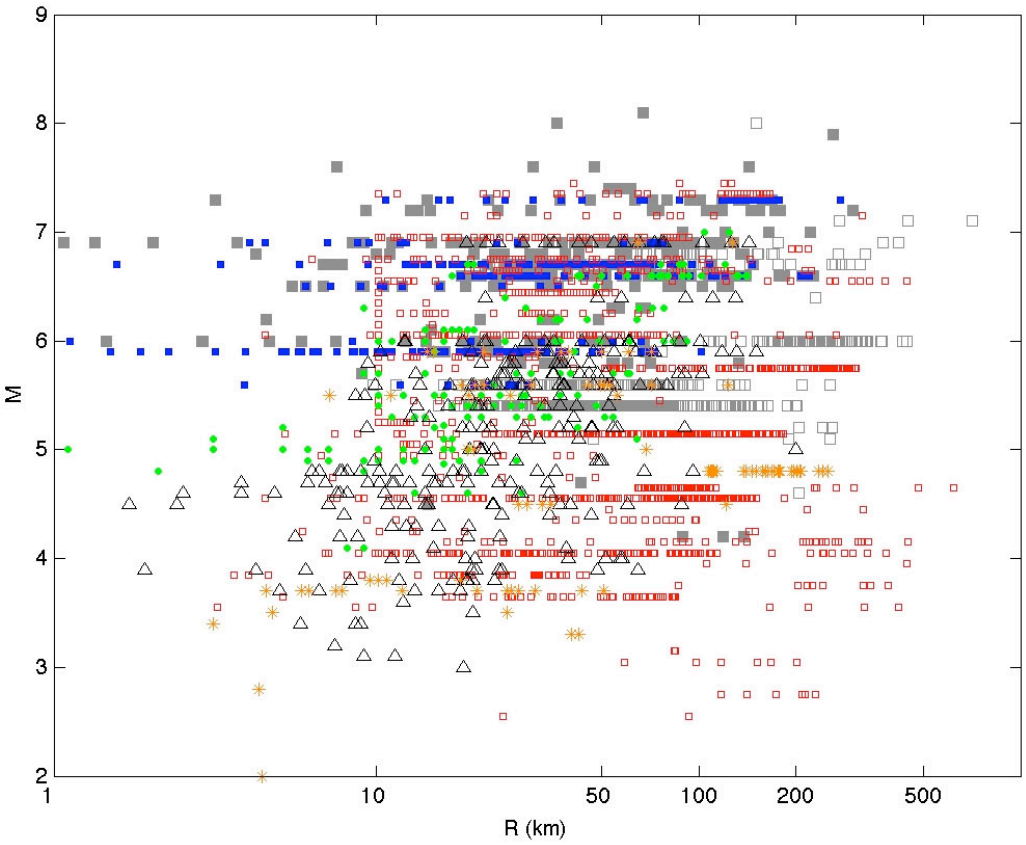

Figure 4.2 Magnitude and distance distribution of aggregate GMICE dataset. See Figure 4.3 for symbol legend

In using an aggregate dataset assembled from published studies (as opposed to starting from the raw waveform and macroseismic databases ourselves), we introduce additional sources of variability (aside from those already mentioned above), since conversion relationships will have to be used to have consistent definitions of PGM and distance measures (the distance measures in Figure 4.2 are a mix of epicentral, hypocentral, rupture, and Joyner-Boore distances). In addition, with use of the aggregate dataset, we are unable to quantify the effect of different approaches to pairing ground motions to intensity assignments. This would remain another source of variability.

It is worth noting that in a number of these GMICE studies, which attempt to estimate intensity as a function of PGM, the regression is set-up with the mean ground motion level as the predictor variable, and intensity as the dependent variable. This is not the standard set up for a regression analysis, since traditional regression analyses assume that there are no errors in the independent variable (in this case, PGM), and that the errors are on the dependent variable (in this case, intensity). Because GMICEs are generally not invertible, the assembled GMICE dataset can (and should) also be used to derive a corresponding IGMCE (intensity to ground motion conversion equation). This can be done via orthogonal distance regressions that specifically derive invertible conversion equations (Faenza and Michelini 2010), or by performing separate regressions in the two directions (Gerstenberger et al., 2010).

Allen and Wald (2009) evaluated the performance of various GMICEs relative to the ShakeMap Atlas dataset, which included fault geometry for larger events. In real-time operations, the initial ShakeMaps typically use a point source, which, for large events with finite rupture dimensions, will have large uncertainties in the distance calculations. It is an open question whether GMICEs with or without distance-dependence terms perform better for these initial point-source ShakeMaps for finite rupture events. For completeness, future GMICE studies should provide equations converting

ground motion to intensity (GMICE) and intensity to ground motion (IGMCE) with and without magnitude and distance dependence.

Though the discussion on site-conditions and amplifications in the previous was focussed on the IPE perspective, an advantage of the GMICE approach, in a purely predictive sense, is that amplifications are explicitly captured through the use of a GMPE. Consequently, GMICEs do not require any knowledge of site-condition or amplification factors.

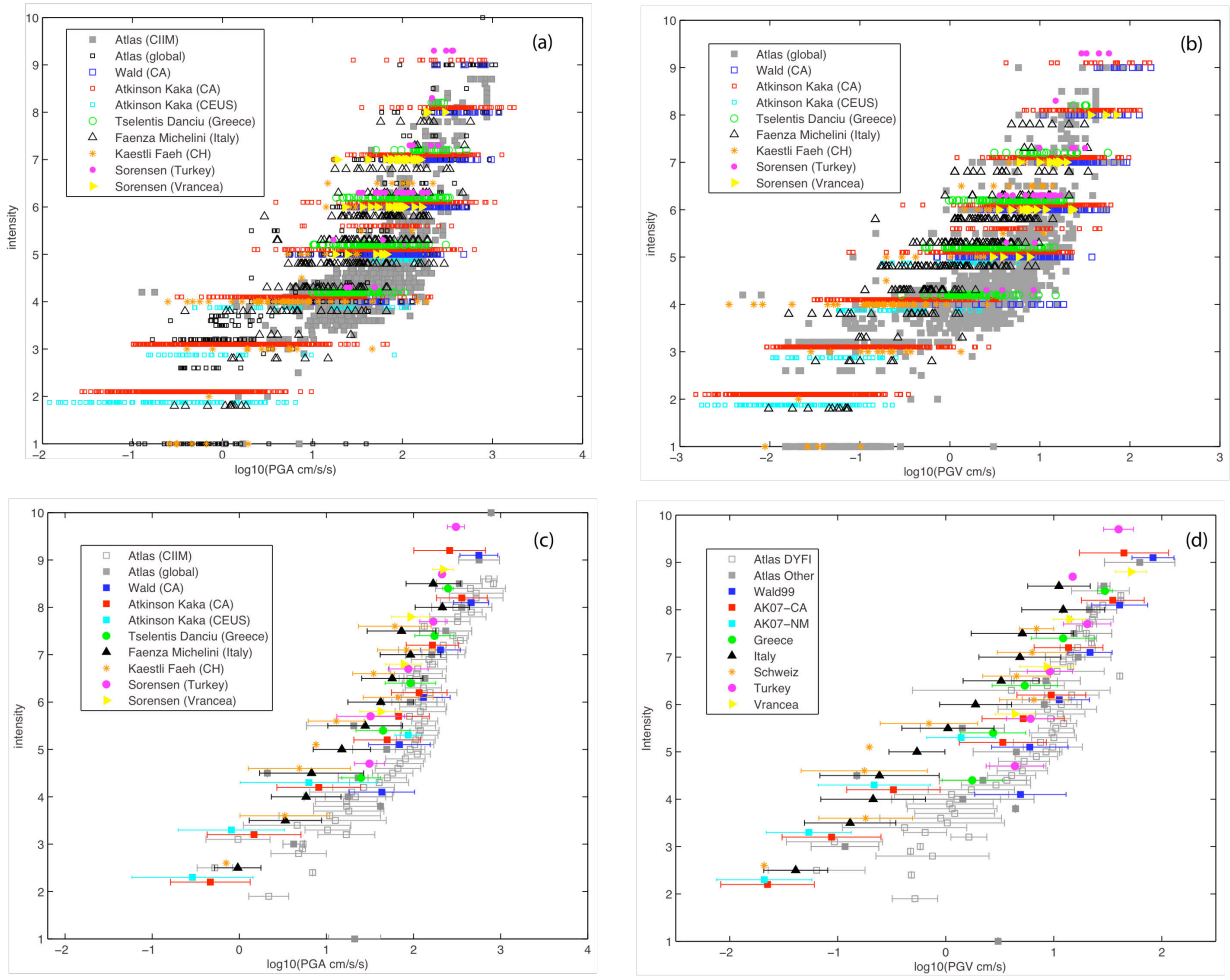

Figure 4.3 The PGM-intensity datasets collected as part of GMICE-related efforts of this study. Intensity as a function of (a) PGA and (b) PGV are shown in the first row. The second row shows intensity as a function of the mean ground motion level

In the following sections, we list the functional forms of selected modern GMICE from active crustal, subduction zone, and stable continental regions. Note that not all of the studies listed here contribute to our aggregate PGM-intensity dataset. When a particular GMICE study investigates intensity as a function of more than one ground motion parameter (for instance, PGA, PGV, and response spectra at various periods), we write the equations using the notation of the originating authors without filling in the values of the regression coefficients or uncertainty σ (as each ground motion parameter has its own set of coefficients and corresponding uncertainty). It should be emphasized that GMICE (and IGMCE) have uncertainties that must be accounted for when characterizing the uncertainty of the predicted intensities or ground motions.

4.1.1 Active Crustal Regions

Wald et al. (1999c): California, USA

Bi-linear relationships predicting MMI as a function of PGA and PGV

Dataset:

- PGM and intensity data from 8 California earthquakes with 5.8 ≤ M ≤ 7.3, and 5 ≤ I_{MMI} ≤ 9
- PGM defined as the larger of two horizontal components
- Geometric mean and σ of PGM data at given intensity level
- Modified Mercalli intensity scale with integer assignments
- 342 PGM-intensity pairsAssociation of PGM with intensity:
- The nearest intensity observation within 3 km of a strong motion station constitutes a PGM-intensity pair. If there are no MMI observations within 3 km of the station, then the station will not contribute to the PGM-MMI dataset. Each strong motion station is paired with 1 intensity observation.

Functional form**:**

Kaestli and Faeh (2006): Switzerland, Italy, and France

$$\begin{aligned} I_{MMI} &= 3.66\log_{10}(PGA) - 1.66 \quad (\sigma = 1.08) \text{ for } I_{MM} < 5 \\ I_{MMI} &= 3.47\log_{10}(PGV) + 2.35 \quad (\sigma = 0.98) \text{ for } I_{MM} \geq 5 \end{aligned} \tag{4.2}$$

Linear relationship between PGM and intensity

Dataset:

- PGM and intensity data from 157 Central European earthquakes with 2 ≤ M ≤ 6.9, and 1 ≤ I ≤ 7
- Each horizontal time history is treated separately
- PGA, PGV, PGD, Arias and Housner intensities
- 268 PGM-intensity pairs
- MCS intensities for Italy, MSK intensities for France, and EMS98 intensities for Switzerland

Associating PGM with intensity:

- The nearest intensity value within 2 km of a strong motion station is assigned to the station. Only the nearest intensity value is used, in the case that there are multiple intensity observations within 2 km of the station.

Functional form:

$$I = a + b\log_{10} PGM \tag{4.3}$$

Atkinson and Kaka (2007): Central and Eastern United States and California

Bilinear relationship predicting MMI intensity as a function of PGM

Dataset:

- PGM and intensity data from 29 CUS and 48 California earthquakes with 2.5 ≤ M ≤ 7.4, and 2 ≤ I_{MMI} ≤ 9
- Each horizontal time history treated separately
- PGA, PGV, PSA at 0.3, 1.0, and 3.2 Hz
- Includes the Atkinson and Sonley (2000) California strong motion dataset
- Fault or hypocentral distance
- Modified Mercalli scale with real number assignments
- 2608 PGM-intensity pairs

Association of PGM with intensity:

- A CIIM (Community Internet Intensity Map) value is assigned at each strong motion station based on general proximity to one or more CIIM observations.

- Uncertainty of 1 intensity unit on intensity assignment at strong motion station

Functional form:

$$
\begin{aligned}
&I_{MMI} = c_1 + c_2 \log_{10} PGM + c_5 + c_6 M + c_7 \log_{10} D \quad \text{for } \log_{10} PGM \le \log_{10} PGM(I5) \\
&I_{MMI} = c_3 + c_4 \log_{10} PGM + c_5 + c_6 M + c_7 \log_{10} D \quad \text{for } \log_{10} PGM \ge \log_{10} PGM(I5) \\
&where: \\
&M = \text{magnitude} \\
&D = \text{fault or hypocentral distance (km)} \\
&PGM(I5) = \text{peak ground motion value at intensity 5}
\end{aligned}
\tag{4.4}
$$

Tselentis and Danciu (2008): Greece

PGM to intensity conversion with magnitude and distance dependence

Dataset:

- PGM and intensity data from 89 Greek earthquakes with 4 ≤ M ≤ 6.9, and 4 ≤ I_{MMI} ≤ 8
- Each horizontal time history is treated separately
- PGA, PGV, Arias intensity, and CAV (Cumulative Average Velocity)
- 310 PGM-intensity pairs
- Vs30 at station available

Association of PGM with intensity:

- The nearest available MMI value (within uncertainty of 1 intensity unit) is assigned to the strong motion station location. If more than 1 MMI value was observed near the station at equal distance, the average was used.

Functional form:

$$
\begin{aligned}
&I_{MMI} = a + b \log_{10} PGM + mM + r \log_{10} R + sS \\
&\sigma_{I_{MMI}} = 1 \\
&where \\
&M = \text{magnitude} \\
&R = \text{epicentral distance (km)} \\
&S = \text{site condition dummy variable (0 for rock, 1 for soft soil)}
\end{aligned}
\tag{4.5}
$$

Allen et al. (2008): ShakeMap Atlas (global active crust)

The ShakeMap Atlas was a source of PGM-intensity pairs, but does not have an associated GMICE.

Dataset:

- PGM and intensity data from 63 global earthquakes, with 4.2 ≤ M ≤ 8.1 and 1 ≤ I_{MMI} ≤ 10 (note: not all ShakeMap Atlas events contributed PGM-intensity pairs, due to the constraint that the intensity observation must be within 3 km of the recording station)
- PGM is defined as the larger of two horizontal components
- DYFI and CIIM reported in 0.1 intensity increments
- PGA and PGV
- 1827 PGM-intensity pairs

Association of PGM with intensity:

- The closest intensity observation within 3 km to a station constitutes a pair.

Faenza and Michelini (2010): Italy

Orthogonal Distance Regression (ODR) on PGA and PGV with I_{MCS}

Dataset:

- PGM and intensity data from 66 Italian earthquakes with $3.9 \leq M_w \leq 7.9$, and $2 \leq I_{MCS} \leq 8$
- ITACA strong motion database (http://itaca.mi.ingv.it)
- DBMI intensity database (http://emidius.mi.ingv.it/DMI04/)
- Mercalli-Cancani-Sieberg (MCS) scale with assignments at 0.5 increments
- PGM is defined as the larger of two horizontal components
- Geometric mean and σ of PGM data at each intensity level (at 0.5 intervals)
- 266 intensity-PGM pairs

Association of PGM with intensity:

- All locations reporting intensities within 3 km of ground motion recording are considered pairs. Thus, a single strong motion station can be paired with multiple intensity observations.
- Uncertainty of 0.5 intensity units on intensity assignment to strong motion station

Functional form:

$$I_{MCS} = a + b \log_{10} PGM \tag{4.6}$$

Gerstenberger et al. (2010): California, USA, extended range

Logistic functions for PGM = f(I_{MMI}) and MMI = f(PGM) relationship

Dataset:

- PGM and intensity data from 1,213 M > 3 California events with 174,206 ground motion recordings
- 179,033 geocoded CIIM reports (no values between MMI 1, 2, and 2.5)
- Pre-CIIM intensity (retrospective) reports and MMI from historical events
- CIIM reported in 0.1 intensity increments
- PGA, PGV, SA0.3, SA1.0, SA3.0 sec

Association of PGM with intensity:

- Pairing all MMI and ground motion recordings within 2 km
- 35,130 MMI-PGM pairs for California
- 4,000 PGM amplitudes associated with multiple MMIs

Functional form:

$$I_{MMI} = \frac{MMI_{\min} + MMI_{\max} \cdot 10^{a+b \cdot PGM}}{1 + 10^{a+b \cdot PGM}}$$
$$where \tag{4.7}$$
$$MMI_{\min} = \text{minimum } I_{MMI} \text{ possible } (=1)$$
$$MMI_{\max} = \text{maximum } I_{MMI} \text{ possible } (=10.5)$$

4.1.2 Stable Continental Regions

Kaka and Atkinson (2004): eastern North America

Linear relationship between PGM and intensity accounting for magnitude- and distance-dependence

Dataset:

- PGM and intensity data from 18 ENA events with $3.6 \leq M \leq 7.3$, and $2 \leq I_{MMI} \leq 10$
- PGV and 5% damped PSA at 1, 5, and 10 Hz
- For historical events, PGV and PSA are estimated using the Atkinson and Boore (1995) GMPE

Association of PGM with intensity:

- An MMI is assigned at each strong motion station based on general proximity to one or more MMI observations.
- Uncertainty of 1 intensity unit on intensity assignment at strong motion station

Functional form:

$$I_{MMI} = (c_1 - c_3) + c_2 \log_{10} PGM - c_R \log_{10} D$$
$$where \qquad (4.8)$$
$$D = \text{distance (km)}$$

4.1.3 Stable Continental Regions

Kaka and Atkinson (2004): eastern North America

Linear relationship between PGM and intensity accounting for magnitude- and distance-dependence

Dataset:

- PGM and intensity data from 18 ENA events with $3.6 \leq M \leq 7.3$, and $2 \leq I_{MMI} \leq 10$
- PGV and 5% damped PSA at 1, 5, and 10 Hz
- For historical events, PGV and PSA are estimated using the Atkinson and Boore (1995) GMPE

Association of PGM with intensity:

- An MMI is assigned at each strong motion station based on general proximity to one or more MMI observations.
- Uncertainty of 1 intensity unit on intensity assignment at strong motion station

Functional form:

$$I_{MMI} = (c_1 - c_3) + c_2 \log_{10} PGM - c_R \log_{10} D$$
$$where \qquad (4.8)$$
$$D = \text{distance (km)}$$

4.1.4 Subduction Zones

Sørensen et al. (2007): Vrancea, Romania

Linear relationship between PGM and intensity

Dataset:

- PGM and intensity data from 4 Vrancea earthquakes, with 6.4 ≤ M ≤ 7.4, and 5 ≤ I_{EMS-98} ≤ 8
- 46 PGA-intensity pairs, 30 PGV-intensity pairs
- Integer intensity assignments

Association of PGM with intensity:

- Macroseismic intensity maps were digitized and intensity values assigned to locations of strong motion stations.

Functional form:

$$I_{EMS-98} = a + b \log_{10} PGM \tag{4.9}$$

Table 4.1 GMICE datasets collected

Reference	Magnitude range	Distance range (km)	PGM Definition	Intensity range used	Distance metric	Intensity type	No. of pairs	Region
Wald et al. (1999c)	5.6 ≤ M ≤ 7.3	< 276	Larger of 2 horizontal comps	4 - 9	R_{rup}, R_{JB}	MMI	342	California, USA
Kaestli and Faeh (2006)	2.0 ≤ M ≤ 6.9	< 253	Independent horizontal comps	1 - 7	R_{epi}	mixed	268	Switzerland
Atkinson and Kaka (2007)	2.5 ≤ M ≤ 7.4	< 618	Independent horizontal comps	2 – 9	R_{rup}, R_{hyp}	mixed	2608	California and Central Eastern USA
Tselentis and Danciu (2008)	4.0 ≤ M ≤ 6.9	< 141	Independent horizontal comps	4 – 8	R_{epi}	MMI	310	Greece
Allen et al. (2008)	4.1 ≤ M≤ 8.1	< 707	Larger of 2 horizontal comps	1 - 10	R_{rup}	mixed	1827	Global active crust
Faenza and Michelini (2010)	3.0 ≤ M ≤ 6.9	< 200	Larger of 2 horizontal comps	2 - 8	R_{epi}	MCS	266	Italy
Aggregate dataset (this study)	2.0 ≤ M ≤ 8.1	< 707	Larger of 2 horizontal comps	1 - 10	R_{rup}	mixed	4029	Global active crust

Table 4.2 Preferred relationships for the prediction of macroseismic intensities. Recommendations for preferred GMPEs are based on the study of Allen and Wald (2009) for usage in Global ShakeMap

Region	GMPE	IPE	GMICE
ACR	Chiou and Youngs (2008)	Allen and Wald (2010)	Wald et al. (1999c)/ Atkinson and Kaka (2007)
SCR	Atkinson and Boore (2006) / Campbell (2003)	Atkinson and Wald (2007)†	Wald et al. (1999c) / Atkinson and Kaka (2007)
SZ	Youngs et al (1997)	Allen and Wald (2010)‡	Wald et al. (1999c)/ Atkinson and Kaka (2007)

† Not recommended for earthquakes larger than approximately M_W 6.0.

‡ IPE likely not to perform very well for large-magnitude (greater than approximately M_W 8.0) or intra-slab earthquakes. However, no other candidate model appeared to be applicable based on tectonic regime and data used to develop the model.

5 Intensity to Ground Motion Conversion Equations (IGMCEs)

Since the advent of the ShakeMap system (Wald et al., 1999a), numerous studies have addressed the question of estimating intensity from PGM. Conversion equations in this direction (GMICEs) are a necessary step in the ShakeMap process of estimating intensity from the available peak ground motion observations. Conversion equations in the other direction, that is, intensity to ground motion conversion equations (IGMCEs) are usually necessary with historical earthquake studies, where intensity data are available, and it is of interest to estimate peak ground motion. Additionally, these conversions are also of interest when DYFI or CIIM data are used as inputs into ShakeMap (as has now been facilitated with Version 3.5). While it is common practice to simply invert a GMICE to get an IGMCE, it is not necessarily correct, as one standard GMICE, for instance, Wald *et al*. (1999c) is not invertible. The Faenza and Michelini (2010) relationship is an exception, since it is based on an orthogonal distance regression, and is thus designed to be both a GMICE and an IGMCE. However, this relationship may not be assumed to be universally applicable, in part since there are few high intensity data and most events are in a limited, moderate magnitude range. In general, the same dataset can be used to derive both a GMICE and an IGMCE (e.g., Gerstenberger et al., 2010). However, separate regressions (or an orthogonal distance regression) for the two directions have to be performed and this leads to a non-unique result.

Faenza and Michelini (2010): Italy

See Section 4.1 for description of dataset and association of intensity with PGM

Functional form:

$$\log_{10} PGM = \frac{I_{MCS} - a}{b} \tag{5.1}$$

Gerstenberger et al. (2010): Southern California, USA, extended range

See Section 4.1 for description of dataset and association of intensity with PGM

Functional form:

$$\log_{10} PGM = \frac{\log_{10} PGM_{\min} + \log_{10} PGM_{\max} \cdot 10^{(a+bI_{MMI})}}{1 + 10^{(a+bI_{MMI})}}$$
$$where \tag{5.2}$$
$$\log_{10} PGM_{\min} = \text{minimum considered PGM}$$
$$\log_{10} PGM_{\max} = \text{maximum considered PGM}$$

Murphy and O'Brien (1977): global

Dataset:

- 1500 strong motion accelerograms from 900 Western US, 500 Japanese, and 60 Southern European earthquakes with $3.0 \le M \le 8.0$, $1 \le I_{MMI} \le 10$
- PGM defined as the largest of available (2 or 3) components

- US events with I_{MMI}, Japanese events with I_{JMA}, European events with I_{MS} (Mercalli-Sieberg) or I_{MSK} (Medvedev-Sponheuer-Karnik); Japanese and European intensities converted to I_{MMI}

Association of intensity with PGM:

- 10% of values have intensity observations at the recording site, 50% are based on observations in the immediate vicinity of the site, 20% assigned by previous investigators, 20% from published isoseismal maps

Functional form:

$$\log_{10} PGA = 0.25 I_{MMI} + 0.25$$
$$\log_{10} PGA = 0.14 I_{MMI} + 0.24 M - 0.68 \log_{10} R + \beta_k$$
$$where: \quad (5.3)$$
$$R = \text{epicentral distance}$$
$$\beta_k = \text{regional constant (=0.60 for western US; =0.69 for Japan, =0.88 for southern Europe)}$$

Trifunac and Brady (1975): western United States

Linear relationship between PGM and intensity

Dataset:

- 57 western United States earthquakes with 187 strong motion records, with $3.0 \leq M \leq 7.7$, and $3 \leq I_{MMI} \leq 9$
- PGA, PGV, and PGD
- Modified Mercalli scale

Association of intensity with PGM:

- No details specified

Functional form:

$$\log_{10} PGM = a + b I_{MMI} \quad (5.4)$$

6 Summary and recommendations

Ongoing developments, including projects within GEM, are improving databases of earthquake consequences. These datasets are critical for improved loss-model (including fragility function) development and calibrations, yet the best loss data are not necessarily (and are mostly not) associated with recorded ground motions where the consequences occurred. This necessitates documentation of the "best practices" for estimating the shaking hazard associated with observed shaking-related losses. The results of this study provide the basic framework for constraining ground motion and intensity values for historic earthquakes as well as for real-time ShakeMaps applications globally.

Much of this report has focused on identifying methods to generate more accurate real-time ShakeMaps in response to global events, including those where often little is known about the earthquake source or its impact. Consequently, the evaluation of various prediction methods has focused on identifying models that are appropriate on a global scale, with little acknowledgement of local or regionally-specific attenuation effects. Such effects continue to be difficult to ascertain due to the heterogeneity and reduction in data quantity as the geographic scale is reduced.

A reference repository of IPEs and GMICEs for regions around the globe has been provided. Along with these references, we have also systematically collected global intensity ground motion data and associated intensity value pairs provided by many of the authors referenced above. This data repository is a non-archival database; additional time and resources beyond the scope of this work would be necessary to deliver an archival quality database. We recommend that GEM adopt these data and continue to build this into a comprehensive database for future analyses.

One might infer that Table 5, our summary of preferred relations for predicting macroseismic intensity, could constitute an extremely concise summary of this report. Indeed, this constitutes the current status of GMPE/GMICE selection for ShakeMap 3.5 operations. Unfortunately, such an inference would miss many of the ongoing subtle concerns about the use of macroseismic intensity in ShakeMap, hazard analyses and communication, loss-calibration, and loss estimation. The authors believe that this first pass at analyses of the approaches to best practices in the use of macroseismic data shows not only the complications and uncertainties in its use, but also how some of the strategies enumerated below may reduce these uncertainties and, hopefully, simplify the use of macroseismic intensity in these arenas.

Much of the state-of-the-art and most of the strategies outlined in this report would have significantly improved prospects if macroseismic data, ground motion data, and analyses of both data sets in concert were more systematic. We strongly recommend that GEM-sponsored activities in the areas of GMPEs and macroseismic intensity have increased levels of coordination to ensure compatible and consistent ground motion and intensity strategies/solutions. For instance, the future development of a set of consistent and compatible GMPEs/IPEs/GMICEs/IGCMEs, would require the availability of, or the capability to generate, an NGA-type strong motion database, with macroseismic intensity as one of the parameters tabulated (along with PGM). This would afford macroseismic intensity studies equal footing with GMPE studies in terms of metadata available (with all the types of predictor variables that GMPE studies collect), and allow for derivation of IPEs, GMICEs, and IGMCEs that have an additional level of consistency with the GMPEs. The tabulated intensities should have weights or quality factors assigned, depending on whether they are assigned intensities, DYFI?, or from isoseismal maps. As an initial step, a first version of such a joint dataset could be generated by going through the NGA dataset (Power et al., 2008) and assigning an intensity and corresponding intensity quality factor to each of the records, and subsequently deriving a set of IPEs, GMICEs and IGMCEs from that dataset. However, we wish to make clear that treating intensity as simply another ground motion parameters is a gross over-simplification. The subtleties inherent in working with macroseismic intensity data (for instance, the use of ordinal and continuous intensity assignments, the distance

dependence in pair generation, the details of how to assign intensities to strong motion station locations, the use of various intensity scales throughout the world, etc), mean that, while there shared themes, macroseismic intensity is essentially a different beast from ground motion data. The subsequent and more ambitious endeavour would be to provide tools to select user-defined spatial intersections of the ground motion and intensity databases, allowing for the generation of the necessary joint datasets, while respecting the inherently different natures of the underlying data.

To enable and facilitate the research and development efforts in the area of macroseismic intensity required to meet GEM's need for global model components, we recommend that GEM form an Intensity Consortia, independent, but strongly coordinated, with GEM GMPE efforts, with the following tasks:

1. Coordinate with GEM GMPE Consortia to ensure compatible ground motion and intensity strategies and solutions.
2. Develop a living database of macroseismic data, which will include at minimum, the observed value, metric (MMI, EMS-98, etc), uncertainty rating, location, text description, reference. Work with the IASPEI Macroseismic Working Group to develop XML standard for macroseismic data exchange among historical and internet-based data sources. Ensure compatibility of macroseismic database with NGA strong motion database.
3. Coordinate with GEM GMPE Consortia to provide tools to select user-defined spatial intersections of the Ground Motion and Intensity databases. Assign intensities and associated uncertainty to the NGA database.
4. Develop and provide global GMPE/GMICE selector tool
5. Research on IPE and GMICE/IGMCE transportability, regionalization
6. Continue analyses of macroseismic (including DYFI?) data to derive or assign uncertainties i) for individual macroseismic observations, ii) as a function of distance to a macroseismic observation. Implement these coefficients in ShakeMap and produce such output as an uncertainty grid for intensity (in addition to PGM);
7. GMICE and IGMCE regressions, with uncertainties, for PGM to intensity, and vice versa
8. Development of new IPEs for at least subduction (SZ) and stable continental (SCR) tectonic regimes; Selection of and refinements to validated active crustal region (ACR) IPEs. Develop site condition amplification factors for IPEs, if these can be constrained.
9. Enhance tools for Vs30 determination on a global scale. Develop coefficients for higher-resolution topography and calibration regionally based on new/existing Vs30 datasets. Aggregate Vs30 datasets.
10. Compilation of calibration events. Assign intensity/ground motion pairs at sites for selected events. Generate ShakeMaps using various combinations of GMPE/IPE/GMICE/IGMCE. Examine the relative merits of IPEs and the combination of GMPEs/GMICEs in intensity prediction relative to calibration events.

REFERENCES

Document References

Allen T. I., Wald D. J., Hotovec A. J., Lin K., Earle P. S., and Marano K. D. [2008] "An Atlas of ShakeMaps for selected global earthquakes", U.S. Geological Survey Open-File Report 2008-1236 47, Golden, USA.

Allen T. I. and Wald D. J. [2009] "Evaluation of ground-motion modeling techniques for use in Global ShakeMap: a critique of instrumental ground-motion prediction equations, peak ground motion to macroseismic intensity conversions, and macroseismic intensity predictions in different tectonic settings", U.S. Geological Survey Open-File Report 2009-1047 114, Golden, USA.

Allen T. I., Wald D. J., Earle P. S., Marano K. D., Hotovec A. J., Lin K. and Hearne M. [2009] "An Atlas of ShakeMaps and population exposure catalog for earthquake loss modeling", *Bull. Earthq. Eng.* **7,** 701-718, DOI: 10.1007/s10518-009-9120-y.

Allen T. I., and Wald D. J. [2010] "Prediction of macroseismic intensities for global active crustal earthquakes", *J. Seismol.* in prep.

Atkinson G. M. and Boore D.M [1995] "Ground-motion relations for eastern North America", *Bull. Seism. Soc. Am.* **85,** 17-30.

Atkinson G. M., Sonley E. [2000]. Relationships between Modified Mercalli Intensity and response spectra, *Bull. Seism. Soc. Am.* **90,** 537-544.

Atkinson, G. M. and Boore D. M. [2006] "Earthquake ground-motion predictions for eastern North America", *Bull. Seism. Soc. Am.* **96,** 2181-2205.

Atkinson G. M. and Kaka S. I. [2007] "Relationships between felt intensity and instrumental ground motion", *Bull. Seism. Soc. Am.* **97,** 497–510.

Atkinson G. M. and Wald D.J. [2007] "Did You Feel It?" intensity data: A surprisingly good measure of earthquake ground motion, *Seism. Res. Lett.* **78,** 362-368.

Bakun W. H. and Wentworth C. M. [1997] "Estimating earthquake location and magnitude from seismic intensity data", *Bull. Seism. Soc. Am.* **87,** 1502-1521.

Bakun W. H., Johnston A. C. and Hopper M. G. [2003] "Estimating locations and magnitudes of earthquakes in eastern North America from Modified Mercalli Intensities", *Bull. Seism. Soc. Am.* **93,** 190–202.

Bakun W. H. [2006] "MMI attenuation and historical earthquakes in the Basin and Range Province of western North America", *Bull. Seism. Soc. Am.* **96,** 2206–2220.

Bakun W. H. and Scotti O. [2006] "Regional intensity attenuation models for France and the estimation of magnitude and location of historical earthquakes", *Geophys. J. Int.* **164,** 596–610.

Beyer K., and Bommer J. J. [2006] "Relationships between median values and between aleatory variabilities for different definitions of the horizontal component of motion", *Bull. Seism. Soc. Am.* **96,** 1512–1522.

Bommer, J. J., Stafford P. J., Alarcón J. E. and Akkar S. [2007] "The influence of magnitude range on empirical ground-motion prediction", *Bull. Seism. Soc. Am.* **97,** 2152–2170.

Boore D. M., Joyner W. B. and Fumal T. E. [1997] "Equations for estimating horizontal response spectra and peak acceleration from Western North American earthquakes: A summary of recent work", *Seism. Res. Lett.* **68,** 128-153.

Borcherdt R. D. [1970] "Effects of local geology on ground motion near San Francisco Bay," *Bull. Seism. Soc. Am.* **60,** 29-61.

Campbell K. W. [2003] "Prediction of strong ground motion using the hybrid empirical method and its use in the development of ground-motion (attenuation) relations in eastern North America", *Bull. Seism. Soc. Am.* **93,** 1012–1033.

Chandler A. M. and Lam N. T. K. [2002] "Intensity attenuation relationship for the South China region and comparison with the component attenuation model", *J. Asian Earth Sci.* **20,** 775-790.

Chiou, B. S.-J. and Youngs R. R. [2008] "An NGA model for the average horizontal component of peak ground motion and response spectra", *Earthq. Spectra* **24,** 173–215.

Crowley H., Pinho R. and Bommer J. J. [2004] "A probabilistic displacement-based vulnerability assessment procedure for earthquake loss estimation", *Bull. Earthq. Eng.* **2,** 173–219.

Crowley H., Cerisara A., Jaiswal K., Keller K., Luco K., Pagani M., Porter K., Silva V., Wald D., Wyss B. [2010] GEM1 Seismic Risk Report: Part 2, GEM Technical Report 2010 - 5., GEM Foundation, Pavia, Italy.

Dewey J. W., Reagor B. G., Dengler L. and Moley K. [1995] "Intensity distribution and isoseismal maps for the Northridge, California, earthquake of January 17, 1994", U.S. Geological Survey Open-File Report 95-92 35.

Dewey, J. W., Hopper M. G., Wald D. J., Quitoriano V. and Adams E. R. [2002] "Intensity distribution and isoseismal maps for the Nisqually, Washington, earthquake of 28 February 2001", U.S. Geological Survey Open-File Report 02-0346, U.S. Geological Survey Open-File Report 02-0346 57.

Douglas J. [2007] "On the regional dependence of earthquake response spectra", *ISET J. Earthq. Tech.* **44,** Paper No. 477, 71–99.

Douglas J., Faccioli E., Cotton F. and Cauzzi C. [2010] "Selection of ground-motion prediction equations for GEM1", GEM Technical Report 2010-E1, GEM Foundation, Pavia, Italy.

Dowrick D. J., and Rhoades D. A. [2005] "Revised models for attenuation of modified mercalli intensity in New Zealand earthquakes", *NZ Soc. Earthq. Eng.* **38,** 185-214.

Earle P. S., Wald D. J., Jaiswal K. S., Allen T. I., Hearne M. G., Marano K. D., Hotovec A. J. and Fee J. M. [2009] "Prompt Assessment of Global Earthquakes for Response (PAGER): A system for rapidly determining the impact of earthquakes worldwide", U.S. Geological Survey Open-File Report 2009–1131. Golden 15.

Edwards M. R., Robinson D., McAneney K. J. and Schneider J. [2004] "Vulnerability of residential structures in Australia", *13th World Conf. Earthq. Eng.*, Vancouver, Canada.

Eguchi R. T., Goltz J. D., Seligson H. A., Flores P. J., Blais N. C., Heaton T. H. and Bortugno E. [1997] "Real-time loss estimation as an emergency response decision support system: the early post-earthquake damage assessment tool (EPEDAT)", *Earthq. Spectra* **13,** 815-832.

Erdik, M., Cagnan Z., Zulfikar C., Sesetyan K., Demircioglu M. B., Durukal E. and Kariptas C. [2008] "Development of rapid earthquake loss assessment methodologies for Euro-Med region", 14th World Conf. Earthq. Eng. Beijing, China, Paper S04-004.

Faccioli E. and Cauzzi C. [2006] “Macroseismic intensities for seismic scenarios, estimated from instrumentally based correlations", First European Conference on Earthquake Engineering and Seismology. Geneva, Switzerland 10pp.

Faenza L., and Michelini A. [2010] “Regression analysis of MCS intensity and ground motion parameters in Italy and its application in ShakeMap”, *Geophys. J. Int.* **180,** 1138-1152.

Frankel A. [1994] “Implications of felt area-magnitude relations for earthquake scaling and the average frequency of perceptible ground motion”, *Bull. Seism. Soc. Am.* **84,** 462-465.

Garcia D., Wald D. J., Lin K. and Allen T. I. [2010] “An earthquake discrimination scheme to optimize Global ShakeMap performance for modern and historical earthquakes, in prep”.

Gerstenberger M. C., Worden C. B., Rhoades D. A. and Wald D.J. [2010] “Probabilistic relationships between peak ground motion and Modified Mercalli Intensity, in revision“.

Hanks T. C. and Kanamori H. [1979] “A moment magnitude scale“, *J. Geophys. Res.* **84,** 2348–2350.

Hayes G. P. and Wald D. J. [2009] “Developing framework to constrain the geometry of the seismic rupture plane on subduction interfaces *a priori* – a probabilistic approach”, *Geophys. J. Int.* **176,** 951–964.

Hayes G. P., Wald D. J. and Keranen K. [2009] ”Advancing techniques to constrain the geometry of the seismic rupture plane on subduction interfaces a priori: Higher-order functional fits”, *Geochem. Geophy. Geosy.* **10,** doi:10.1029/2009GC002633.

Herrmann R. B. and Kijko A. [1983] ”Modeling some empirical vertical component *Lg* relations”, *Bull. Seism. Soc. Am.* **73,** 157-171.

Johnston A. C., Coppersmith K. J., Kanter L. R. and Cornell C. A. [1994] “The earthquakes of stable continental regions, Volume 1-Assessment of large earthquake potential, Electric Power Research Institute”, Palo Alto, California, TR-102261-V1.

Joyner W. B. and Boore D. M. [1993] “Methods for regression analysis of strong-motion data“, *Bull. Seism. Soc. Am.* **83,** 469-487.

Kaestli P. and Faeh D. [2006] “Rapid estimation of macroseismic effects and ShakeMaps using macroseismic data, First European Conference on Earthquake Engineering and Seismology”, Geneva, Switzerland 10pp.

Lantada N., Irizarry J., Barbat A. H., Goula X., Roca X., Susagna T. and Pujades L. G. [2010] “Seismic hazard and risk scenarios for Barcelona, Spain, using the Risk-UE vulnerability index method”, *Bull. Earthq. Eng.* **8,** 201–229.

Murphy, J. R. andO'Brien L. J. [1977] “The correlation of peak ground acceleeration amplitude eith seismic intensity and other physical parameters”, *Bull. Seism. Soc. Am.* **67,** 877-915.

Musson R. M. W. [2000] “Intensity-based seismic risk assessment”, *Soil Dyn. Earthq. Eng.* **20,** 353-360.

Musson, R. M. W., Grünthal G. and Stucchi M. [2009] “The comparison of macroseismic intensity scales”, *J. Seismol.* DOI 10.1007/s10950-009-9172-0.

National Institute of Building Sciences [2003] “Multi-hazard loss estimation methodology, earthquake model, HAZUS-MH MR1: advanced engineering and building module, technical and user's manual”, FEMA. Federal Emergency Management Agency 119 pp.

Pasolini C., Albarello D., Gasperini P., D’Amico V and Lolli B. [2008] “The attenuation of seismic intensity in Italy, part II: modeling and validation”, *Bull. Seism. Soc. Am.* **98,** 692–708.

Power M., Chiou B., Abrahamson N., Bozorgnia Y., Shantz T. and Roblee C. [2008] “An overview of the NGA project”, *Earthq. Spectra* **24,** 3–21.

Sørensen M. B., Stromeyer D. and Grünthal G. [2007] “Deliverable 4.1: Generation of area-specific relationships between ground motion parameters (PGA, PGV) at certain sites, magnitude M and distance R to the causative fault and site intensities in terms of EMS-98”; Databank of intensity data points and related parameters, Seismic eArly warning For EuRope, GFZ Potsdam 19.

Sørensen M. B., Stromeyer D. and Grünthal G. [2008] “Estimation of macroseismic intensity – new attenuation and intensity vs. ground motion relations for different parts of Europe“, 14th World Conf. Earthq. Eng. Beijing, China, Paper 07-0024.

Sørensen M. B., Stromeyer D. and Grünthal G. [2009a] “Intensity attenuation in the Campania region, Southern Italy”, *J. Seismol.* DOI 10.1007/s10950-009-9162-2.

Sørensen M. B., Stromeyer D. and Grünthal G. [2009b] “Attenuation of macroseismic intensity: a new relation for the Marmara Sea region, northwest Turkey“, *Bull. Seism. Soc. Am.* **99,** 538–553.

Spence R. J. S., Coburn A. W. and Ruffle S. J. [2009] “Estimation of vulnerability functions based on a global earthquake damage database”, *Geophys. Res. Abs.* **11,** EGU2009-12387.

Trifunac M. D. and Brady A. G. [1975] “On the correlation od seismic intensity scales with the peaks of recorded strong ground motion”, *Bull. Seism. Soc. Am.* **65,** 139-162.

Tselentis G.-A. and Danciu L. [2008] “Empirical relationships between Modified Mercalli Intensity and engineering ground-motion parameters in Greece“, *Bull. Seism. Soc. Am.* **98,** 1863–1875.

Wald D. J., Quitoriano V., Heaton T. H, Kanamori H., Scrivner C. W. and Worden B. C. [1999a] “TriNet "ShakeMaps": Rapid generation of peak ground-motion and intensity maps for earthquakes in southern California“, *Earthq. Spectra* **15,** 537-556.

Wald D. J., Quitoriano V., Dengler L. and Dewey J. W. [1999b] “Utilization of the Internet for rapid community intensity maps“, *Seism. Res. Lett.* **70,** 680-697.

Wald D. J., Quitoriano V., Heaton T. H. and Kanamori H. [1999c] “Relationship between peak ground acceleration, peak ground velocity, and Modified Mercalli Intensity in California,” *Earthq. Spectra* **15,** 557-564.

Wald, D. J. and Allen T.I. [2007] “Topographic slope as a proxy for seismic site conditions and amplification”, *Bull. Seism. Soc. Am.* **97,** 1379-1395.

Wald, D. J., Earle P. S., Allen T. I., Jaiswal K., Porter K. and Hearne M. [2008] “Development of the U.S. Geological Survey’s PAGER system (Prompt Assessment of Global Earthquakes for Response)”, *14th World Conf. Earthq. Eng.*, Beijing, China.

Wald, D. J., Jaiswal K., Marano K., Earle P. and Allen T. I. [2009] “Advancements in casualty modeling facilitated by the USGS Prompt Assessment of Global Earthquakes for Response (PAGER) System”, *Second International Workshop on Disaster Casualties*, University of Cambridge, UK.

Watson-Lamprey J. A. and Boore D. M. [2007] “Beyond SaGMRotI: Conversion to SaArb, SaSN, and SaMaxRot,” *Bulletin of the Seismological Society of America* **97,** 1511-1524.

Worden C. B., Wald D. J. Allen T. I., Lin K, G. Cua and Garcia D. [2010] “Integration of macroseismic and strong-motion earthquake data in ShakeMap for real-time and historic earthquake analyses”, *Bull. Seism. Soc. Am.* in review.

Wyss, M. [2008] “Estimated human losses in future earthquakes in central Myanmar”, *Seism. Res. Lett.* **79,** 520-525.

Youngs R. R., Chiou S.-J., Silva W. J. and Humphrey J. R. [1997] “Strong ground motion attenuation relationships for subduction zone earthquakes“, *Seism. Res. Lett.* **68,** 58-73.

Website references

1. United States Geological Survey PAGER System
PAGER: Prompt Assessment of Global Earthquakes for Response.
[Available at http://earthquake.usgs.gov/pager/]

2. United States Geological Survey ShakeMap Atlas
ShakeMap Archive: The ShakeMap Atlas.
[Available at http://earthquake.usgs.gov/shakemap/]

3. Cambridge University Earthquake Damage Database
[Available at http://www.arct.cam.ac.uk/EQ/]

APPENDIX A Active Crustal Macroseismic Data

Individual earthquakes that comprise the active crustal macroseismic intensity database with 6 or more available observations. Many of the events where DYFI? data were collected are not indicated in the present list. Most maximum intensity values given to one decimal point are from the online DYFI? system. Note that not all macroseismic data gathered are Modified Mercalli Intensities (MMI). However, in this study we assume equivalence between the various intensity scales used around the world, with the exception of the Japanese intensity scale.

Event ID	Event name	Mag	Latitude	Longitude	No. recs.	Max Intensity	R_{rup} range (km)
196002292340	Agadir, Morocco	6.3	30.450	-9.620	33	9	7.4-263.7
196209011920	Buyin-Zara, Iran	6.6	35.630	49.870	184	9	0.1-54.1
196307260417	Skopje, Yugoslavia	6.1	42.008	21.455	15	9	6-130.1
196606280426	Parkfield, California	6.1	35.875	-120.487	175	7	1-319.9
196608191222	Varto, Turkey	6.8	39.161	41.580	390	8.5	0.1-74.6
196707300000	Caracas, Venezuela	6.6	10.555	-67.310	40	8	18.5-318.2
196804090229	Borrego Mountain, California	6.6	33.157	-116.194	252	8	0.9-312.2
196805231724	Inangahua, New Zealand	7.2	-41.760	171.960	108	10	9.1-318.4
196808311047	Dasht-e Bayaz, Iran	7.2	34.045	58.960	90	9	0.1-61.6
197009121430	Lytle Creek, California	5.4	34.270	-117.540	221	7	9.5-210.3
197102091400	San Fernando, California	6.6	34.400	-118.391	553	11	4.7-318.2
197212230629	Managua, Nicaragua	6.2	12.146	-86.269	56	8	0.5-107.1
197412281211	Pattan, Pakistan	6.2	35.023	72.900	45	8	14.6-47.6
197502041136	Haicheng, China	7.0	40.667	122.646	22	9	1.3-39.5
197508012020	Oroville, California	5.8	39.503	-121.392	319	8	12.2-288.5
197602040901	Guatemala	7.6	15.296	-89.145	54	8	6.3-150.1
197604090708	Ecuador	6.6	0.850	-79.564	45	8	18.3-298.9
197605062000	Friuli, Italy	6.5	46.262	13.300	704	9.5	10-307.3
197607271942	Tangshan, China	7.6	39.590	118.185	81	9	1.1-256.3
197609150315	Friuli, Italy	6.0	46.314	13.206	35	8.5	5.6-256.9
197610060912	Ecuador	5.7	-0.726	-78.732	69	8	5.4-207.6
197711230926	Caucete, Argentina	7.5	-31.729	-67.755	124	9	13.7-314.1
197712192334	Bob-Tangol, Iran	5.9	30.915	56.414	30	7.5	0.3-15.4

Event ID	Event name	Mag	Latitude	Longitude	No. recs.	Max Intensity	R_{rup} range (km)
197808132254	Santa Barbara, California	5.8	34.373	-119.652	58	7	14.7-230.1
197809161535	Tabas, Iran	7.3	33.242	57.382	178	9	1.6-56.5
197902282127	St. Elias, Alaska	7.5	60.661	-141.652	18	6	40.6-292
197904150619	Montenegro, Serbia	6.9	42.001	19.154	124	9	7-265.7
197908061705	Coyote Lake, California	5.7	37.069	-121.600	266	7	7.9-315.2
197910152316	Imperial Valley, California	6.5	32.814	-115.648	209	9	5-317.7
197911140221	Korizan, Iran	6.5	33.959	59.723	23	6	2.8-102.9
197911271710	Khuli-Buniabad, Iran	7.0	34.059	59.757	24	8	1.1-57.1
198001241900	Livermore, California	5.8	37.712	-121.728	281	7	15.2-297.3
198001270233	Livermore, California	5.8	37.737	-121.740	105	7	16.5-282.5
198005251633	Mammoth Lakes, California	6.2	37.525	-118.835	251	7	19.1-318.6
198005271450	Mammoth Lakes, California	5.9	37.417	-118.797	306	6	19.5-317.5
198006090328	Victoria, Mexico	6.3	32.268	-114.908	94	5	34.6-315.5
198010101225	El Asnam, Algeria	7.1	36.143	1.404	47	9	1.6-290.3
198011200329	BRAZIL	5.2	-4.411	-38.331	10	7	15.1-240.9
198011231834	Irpinia, Italy	6.9	40.788	15.310	1010	10	0.3-319.6
198011261735	COLOMBIA	5.2	8.028	-72.442	83	7	11.7-296.2
198102141727	Baiano, Italy	4.9	40.995	14.614	85	7.5	5.7-107.9
198102242053	Corinth, Greece	6.6	38.159	22.976	277	9	16.8-188.3
198102250235	Corinth, Greece (Aftershock)	6.3	38.097	23.170	178	9	6.9-173.3
198104261209	Westmoreland, California	5.9	33.125	-115.644	100	7	14-289.8
198106221753	Peru	5.8	-13.185	-74.463	8	7	17.6-76.6
198212130912	Dhamar, Yemen	6.2	14.675	44.223	8	8	0.6-14.1
198305022342	Coalinga, California	6.3	36.218	-120.305	398	8	10.3-319.9
198307220239	Coalinga, California	5.7	36.195	-120.338	199	6	9.3-307
198310281406	Borah Peak, Idaho	6.9	44.078	-113.800	186	7	6.8-316.6
198404242115	Morgan Hill, California	6.2	37.303	-121.707	418	8	4.7-310.2
198406241329	Godley River, New Zealand	6.1	-43.598	170.667	80	8	19.7-280.3
198607080920	North Palm Springs, California	6.0	33.969	-116.779	292	7	12.1-270.4
198703020142	Edgecumbe, New Zealand	6.5	-38.015	176.921	238	9	0.1-287.8

Event ID	Event name	Mag	Latitude	Longitude	No. recs.	Max Intensity	R_{rup} range (km)
198710011442	Whittier Narrows, California	5.9	34.061	-118.135	421	8	12-305.1
198711240154	Elmore Ranch, California	6.0	33.257	-115.756	126	6	13.2-275.8
198711241315	Superstition Hills, California	6.5	33.070	-115.952	209	7	14-299
198812070741	Spitak, Armenia	6.7	40.919	44.118	293	9	0.2-267.3
198910180004	Loma Prieta, California	6.9	37.110	-121.764	562	8	1.5-319.1
199002100327	Lake Tennyson, New Zealand	6.0	-42.322	172.865	104	8	17.7-231.2
199005130423	Weber, New Zealand	6.4	-40.292	176.157	172	8	21.4-318.5
199006202100	Manjil, Iran	7.4	37.001	49.216	10	9	3.5-61
199007160726	Luzon, Philippines	7.7	15.721	121.180	8	8	2.2-108.4
199012130024	Sicily, Italy	5.8	37.286	15.402	256	7.5	20.6-206.7
199110192123	Uttarkashi, India	6.8	30.730	78.775	13	9	4.1-138.5
199206281157	Landers, California	7.3	34.190	-116.520	295	9	0.1-318
199208190204	Suusamyr, Kyrgyzstan	7.2	42.111	73.588	41	9	3.5-103.4
199210121309	Cairo, Egypt	5.8	29.729	31.158	12	8	22.5-72.8
199210181511	Altrato, Colombia	7.1	7.093	-76.764	23	9	2.6-214.8
199307220457	Colombia	6.0	6.380	-71.206	10	8	23.2-257.9
199401171230	Northridge, California	6.7	34.164	-118.563	962	9	5.2-317.1
199408180113	Mascara, Algeria	5.9	35.480	-0.092	22	7	12.7-66.1
199501162046	Kobe, Japan	6.9	34.580	135.025	32	9	0.5-247.1
199505130847	Kozani-Grevena, Greece	6.6	40.151	21.713	548	8	16.5-308.4
199505271303	Neftegorsk, Russia	7.0	52.604	142.823	63	8	1.1-225.9
199511220415	Gulf of Akaba, Saudi Arabia	7.2	28.762	34.808	68	9	5.2-294.5
199602031114	Lijiang, China	6.6	27.271	100.262	19	9	1.9-107.4
199707091924	Cariaco, Venezuela	7.0	10.448	-63.533	82	8	0-118.2
199709260940	Umbria-Marche, Italy	6.0	43.078	12.781	877	9	1.2-246.2
199804121055	Bovec, Slovenia	5.6	46.271	13.653	28	8.5	7.8-39
199805220448	Aiquile, Bolivia	6.6	-17.783	-65.401	12	8	0.1-69.9
199806271355	Adana-Ceyhan, Turkey	6.3	36.903	35.325	9	8	15.3-30.3
199807090519	Faial Island, Portugal	6.1	38.621	-28.566	31	8	10.4-48.9
199901251819	Armenia, Colombia	6.1	4.440	-75.659	13	9	23.4-318.8

Event ID	Event name	Mag	Latitude	Longitude	No. recs.	Max Intensity	R_{rup} range (km)
199903281905	Chamoli, India	6.5	30.480	79.400	90	8	9-32.1
199908170001	Kocaeli, Turkey	7.6	40.773	30.003	14	9	1.8-186.7
199909071156	Athens, Greece	6.0	38.119	23.598	31	9	0.4-26
199910160946	Hector Mine, California	7.1	34.517	-116.450	144	7	1.3-319.3
200202030711	Ishakli, Turkey	6.5	38.527	31.227	12	7	5-65.1
200203251456	Nahrin, Afghanistan	6.1	36.050	69.210	57	7	10.9-25.6
200210311033	Molise, Italy	5.7	41.738	14.852	50	7	5.7-47.9
200211032212	Denali, Alaska	7.9	63.541	-147.731	47	8	13.6-313.6
200305211844	Boumerdes, Algeria	6.8	36.880	3.694	156	9	3.2-316.8
200312260156	Bam, Iran	6.6	28.950	58.268	24	10	0.4-184.3
200402240227	Al Hoceima, Morocco	6.4	35.184	-3.985	24	9	0.1-36.4
200409281715	Parkfield, California	6.0	35.761	-120.307	436	6.3	4.9-316.9
200510080350	Kashmir, Pakistan	7.6	34.465	73.584	62	9.1	2.8-318.8
200603310117	Chalan Chulan, Iran	6.1	33.500	48.780	11	8	20.1-59.4
200605262253	Yogyakarta, Indonesia	6.3	-7.955	110.430	17	8.8	9-253.4
200703250041	Noto Peninsula, Japan	6.7	37.220	136.690	17	6.2	64.2-317.5
200710310304	Milpitas, California	5.6	37.432	-121.776	433	6.2	9.9-247.6
200802090712	Baja California, Mexico	5.1	32.419	-115.292	72	5.6	34.1-261.7
200802211416	Wells, Nevada	6.0	41.153	-114.867	106	6.9	15-318.8
200805120628	Wenchuan, China	7.9	30.986	103.364	32	10	2.8-313.7
200807291842	Chino Hills, California	5.4	33.953	-117.761	675	6.4	15.1-313.5

APPENDIX B Stable Continental Region Macroseismic Data

B.1 Results

Individual earthquakes that comprise the stable continental region macroseismic intensity database with 6 or more available observations. Many of the events where DYFI? data were collected are not indicated in the present list. Most maximum intensity values given to one decimal point are from the online DYFI? system. Note that not all macroseismic data gathered are Modified Mercalli Intensities (MMI). However, in this study we assume equivalence between the various intensity scales used around the world, with the exception of the Japanese Meteorological Agency (JMA) intensity scale.

Event ID	Event name	Mag	Latitude	Longitude	No. recs.	Max Intensity	R_{rup} range (km)
196712102251	Koyna, India	6.3	17.390	73.774	11	8	4.8-64
196810140258	Meckering, Australia	6.5	-31.523	116.978	124	8	2.2-397.5
197003101715	Calingiri, Australia	5.5	-31.093	116.513	146	6	3.8-300.7
197303091909	Picton, Australia	5.5	-34.023	150.110	245	6.5	29.1-376.6
197404032305	Mt. Carmel, Illinois	4.7	38.592	-88.094	1314	6	11.4-399.4
197603250041	Lepanto, Arkansas	5.0	35.637	-90.327	701	6	15.4-398.9
197809030508	Swabian Jura, Germany	5.2	48.261	8.978	569	7.5	15.4-109.6
197906020947	Cadoux, Australia	6.1	-30.822	117.104	166	9	0.3-392.4
198007271852	Sharpsburg, Kentuky	5.0	38.205	-83.943	1138	7	16.6-396.2
198201091253	Miramichi, Canada	5.5	46.988	-66.618	226	6	86.9-398.9
198201210033	Faulkner County, Arkansas	4.7	35.170	-92.208	105	6	2.4-257.7
198206280957	Bad Marienberg, Germany	4.8	50.733	7.804	295	5.5	10.1-202.4
198310071018	Goodnow, New York	4.9	43.953	-74.342	2353	6	10.2-398.9
198311080049	Liege, Belgium	4.9	50.630	5.500	545	7	4.3-232.6
198801220035	Tennant Creek #1, Australia	6.2	-19.866	133.795	35	7	38.6-394.5
198801221204	Tennant Creek #3, Australia	6.6	-19.896	133.854	7	6	71.3-331.2
198811252346	Saguenay, Canada	5.8	48.061	-71.277	879	8	31.1-399.4
198905280255	Mt Olga, Australia	5.8	-25.139	130.755	14	7	30.8-275.9
198912272326	Newcastle, Australia	5.4	-32.952	151.610	118	8	10.6-348.8
199001170638	Meckering, Australia	4.2	-31.654	117.067	68	6	3.6-249.2
199204130120	Roermond, Netherlands	5.4	51.150	5.930	2730	7	15.3-399.4

Event ID	Event name	Mag	Latitude	Longitude	No. recs.	Max Intensity	R_{rup} range (km)
199309292225	Latur-Killari, India	6.2	18.060	76.478	45	8	14.2-37.3
199408061103	Ellalong, Australia	4.7	-32.917	151.292	208	7.5	1.9-327.1
199609250453	Thomson Reservoir, Australia	4.5	-37.863	146.422	83	6	12.7-207.7
199703050615	Burra, Australia	4.8	-33.768	138.931	203	6	20-292.1
199708100920	Collier Bay, Australia	6.2	-16.159	124.333	37	7	71.6-399.8
200008291205	Boolarra, Australia	4.2	-38.402	146.245	357	5	15.2-198.7
200101260316	Bhuj, India	7.6	23.402	70.287	98	9	15.2-263.7
200204201050	Au Sable Forks, New York	5.1	44.487	-73.718	1541	6.1	97.2-399.9
200302222041	Saint Die, France	5.0	48.317	6.626	1098	6	9.7-166
200804180937	Mt. Carmel, Illinois	5.2	38.450	-87.890	673	6.3	12.3-399.4
200804181514	Mt. Carmel, Illinois (Aftershock)	4.6	38.483	-87.891	39	4.4	53.4-245.5
200804210538	Mt. Carmel, Illinois (Aftershock)	4.0	38.483	-87.857	257	4.6	12.2-383.7

APPENDIX C Subduction Zone Macroseismic Data

Individual earthquakes that comprise the subduction zone macroseismic intensity database with 6 or more available observations. Many of the events where DYFI? data were collected are not indicated in the present list. Most maximum intensity values given to one decimal point are from the online DYFI? system. Note that not all macroseismic data gathered are Modified Mercalli Intensities (MMI). However, in this study we assume equivalence between the various intensity scales used around the world (with the exception of the JMA intensity scale).

Event ID	Event name	Mag	Latitude	Longitude	No. recs.	Max Intensity	R_{rup} range (km)
196005221911	Concepcion, Chile	9.5	-38.235	-73.047	21	11	12.5-92.9
196403280336	Prince William Sound, Alaska	9.2	61.017	-147.648	88	8	3.6-294.8
196504291528	Puget Sound, Washington	6.5	47.317	-122.333	472	8	65.8-299
196707291024	Bucaramanga, Colombia	5.9	6.788	-73.073	33	8	162.3-283.9
197005312023	Peru	7.9	-9.248	-78.841	71	9	66-300
197107090303	Valparaiso, Chile	6.6	-32.536	-71.154	17	9	72.7-298.9
197304242130	Colombia	6.6	4.908	-78.114	6	7	163.7-289.8
197307310541	Chile	5.5	-37.716	-73.425	8	5	60.1-121.9
197401050833	Peru	6.6	-12.351	-76.307	12	6	93.6-177.1
197406091416	Peru	5.7	-5.805	-81.010	7	5	84.9-259.9
197410031421	Lima, Peru	8.1	-12.254	-77.524	112	8	33.6-237.8
197608161611	Moro Gulf, Philippines	8.0	6.292	124.089	16	7	56.3-278.9
197701180541	Cape Campbell, New Zealand	6.1	-41.748	174.384	90	5	58.5-289.5
197703041921	Vrancea, Romania	7.5	45.776	26.702	701	8	80-298.8
197903141107	Petatlan, Mexico	7.5	17.759	-101.222	19	8	17-296.6
197912120759	Tumaco, Colombia	8.1	1.603	-79.363	35	9	36-300
198104180032	Peru	5.5	-13.116	-74.373	59	7	41.1-94.5
198110180431	Colombia	5.9	8.111	-72.499	135	8	41.3-256.2
198303311312	Popayan, Colombia	5.6	2.439	-76.659	7	7	30.3-40.6
198503032247	Valparaiso, Chile	7.9	-33.132	-71.708	27	7.5	36.9-232.1
199003251322	Nicoya Gulf, Costa Rica	7.3	9.941	-84.775	7	8	13.8-71
199204251806	Petrolia, California	7.2	40.337	-124.088	72	8	10.5-293.7
199406021817	East Java, Indonesia	7.8	-10.409	112.934	12	5	147.1-191.5

Event ID	Event name	Mag	Latitude	Longitude	No. recs.	Max Intensity	R_{rup} range (km)
200102281854	Nisqually, Washington	6.8	47.112	-122.603	463	8.1	50-299.9
200106232033	Arequipa, Peru	8.4	-16.385	-73.505	19	8	28.5-289.5
200301220206	Tecoman, Mexico	7.5	18.900	-104.063	69	7	28.9-214.6
200412260058	Banda Aceh, Sumatra, Indonesia	9.0	3.287	95.972	3	9.1	19.4-77
200503281609	Nias, Indonesia	8.6	2.069	97.097	8	9.1	40-282.1
200507230734	Honshu, Japan	5.9	35.520	139.970	11	5.7	73.4-93.4
200708152340	Pisco, Peru	8.0	-13.358	-76.522	41	8.9	30.9-284.3
200711141540	Tocopilla, Chile	7.7	-22.247	-69.890	14	7	30-235.3

APPENDIX D Magnitude Dependence of Selected Active Crustal IPEs

The transition of intensity residuals with magnitude for candidate IPEs for active crustal regions. The series of plots show the transition of the median residuals in 0.5 magnitude windows. The magnitude window is indicated on the top-left plot in each figure.

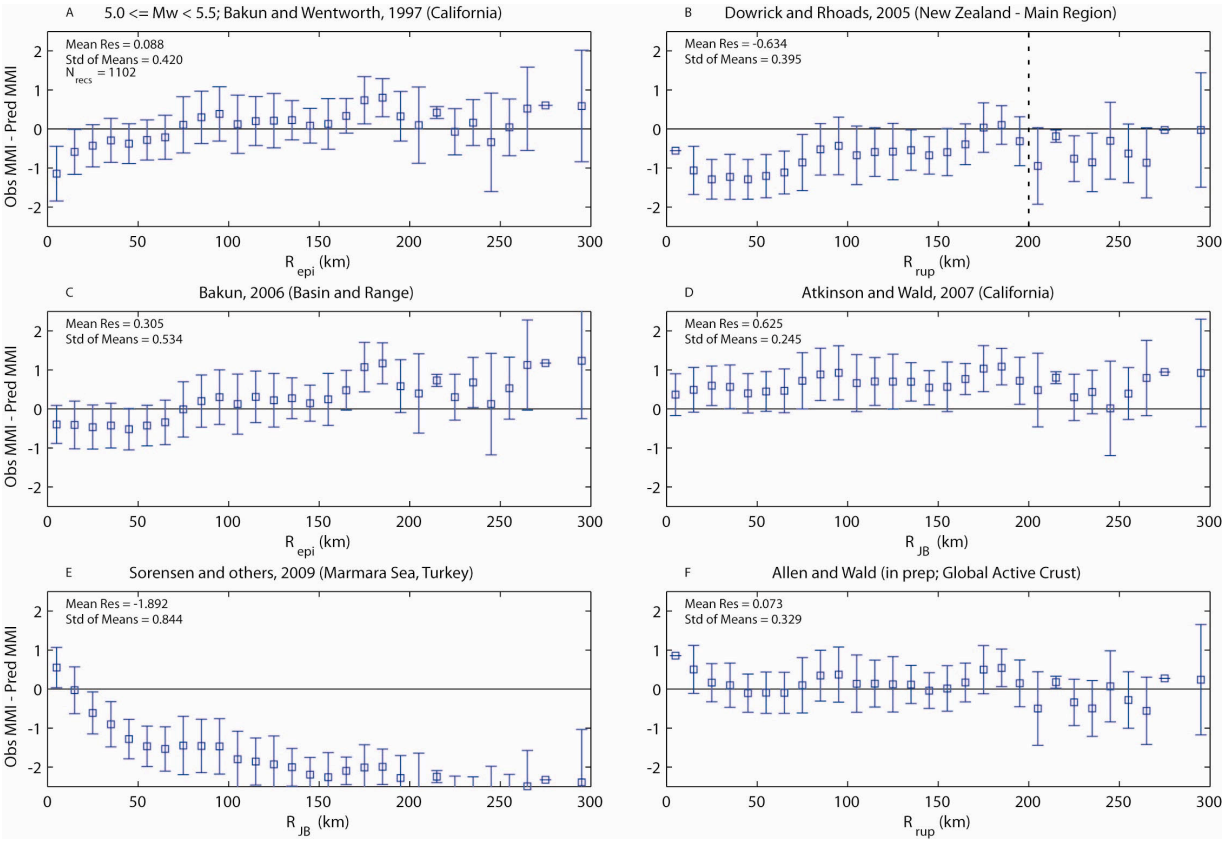

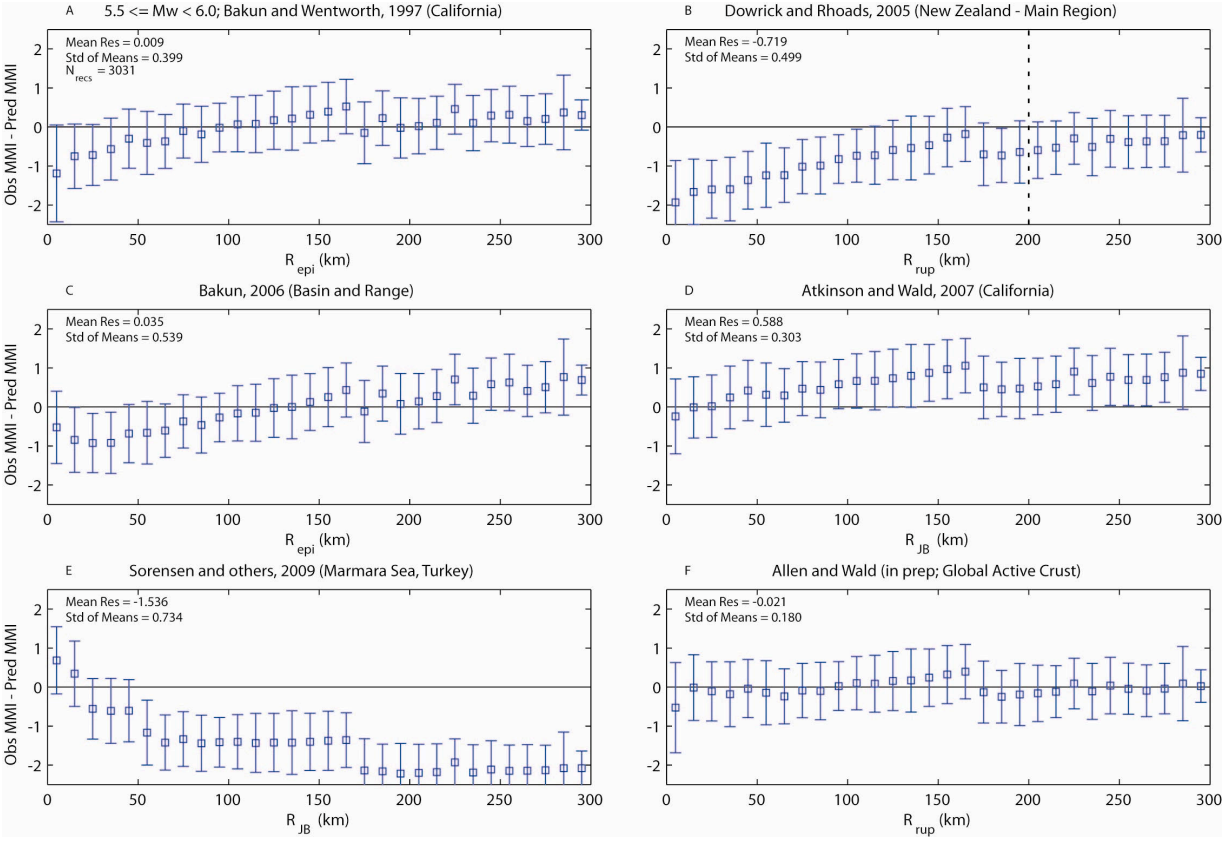
A
5.5 <= Mw < 6.0; Bakun and Wentworth, 1997 (California)
Mean Res = 0.009
Std of Means = 0.399
N recs = 3031
B
Dowrick and Rhoads, 2005 (New Zealand - Main Region)
Mean Res = -0.719
Std of Means = 0.499
C
Bakun, 2006 (Basin and Range)
Mean Res = 0.035
Std of Means = 0.539
D
Atkinson and Wald, 2007 (California)
Mean Res = 0.588
Std of Means = 0.303
E
Sorensen and others, 2009 (Marmara Sea, Turkey)
Mean Res = -1.536
Std of Means = 0.734
F
Allen and Wald (in prep; Global Active Crust)
Mean Res = -0.021
Std of Means = 0.180
Obs MMI - Pred MMI
R epi (km)
R rup (km)
R JB (km)

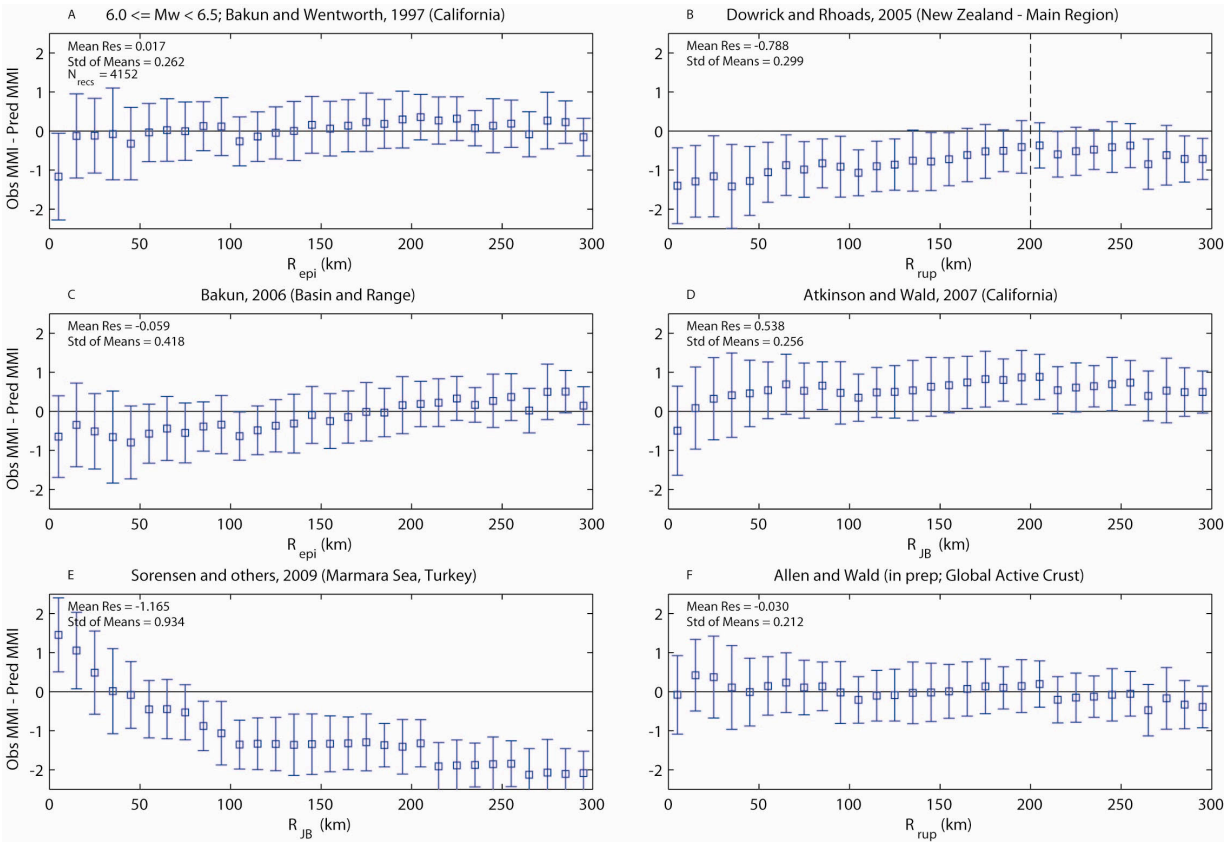
A
6.0 <= Mw < 6.5; Bakun and Wentworth, 1997 (California)
Mean Res = 0.017
Std of Means = 0.262
N recs = 4152
B
Dowrick and Rhoads, 2005 (New Zealand - Main Region)
Mean Res = -0.788
Std of Means = 0.299
C
Bakun, 2006 (Basin and Range)
Mean Res = -0.059
Std of Means = 0.418
D
Atkinson and Wald, 2007 (California)
Mean Res = 0.538
Std of Means = 0.256
E
Sorensen and others, 2009 (Marmara Sea, Turkey)
Mean Res = -1.165
Std of Means = 0.934
F
Allen and Wald (in prep; Global Active Crust)
Mean Res = -0.030
Std of Means = 0.212
Obs MMI - Pred MMI
R epi (km)
R rup (km)
R JB (km)

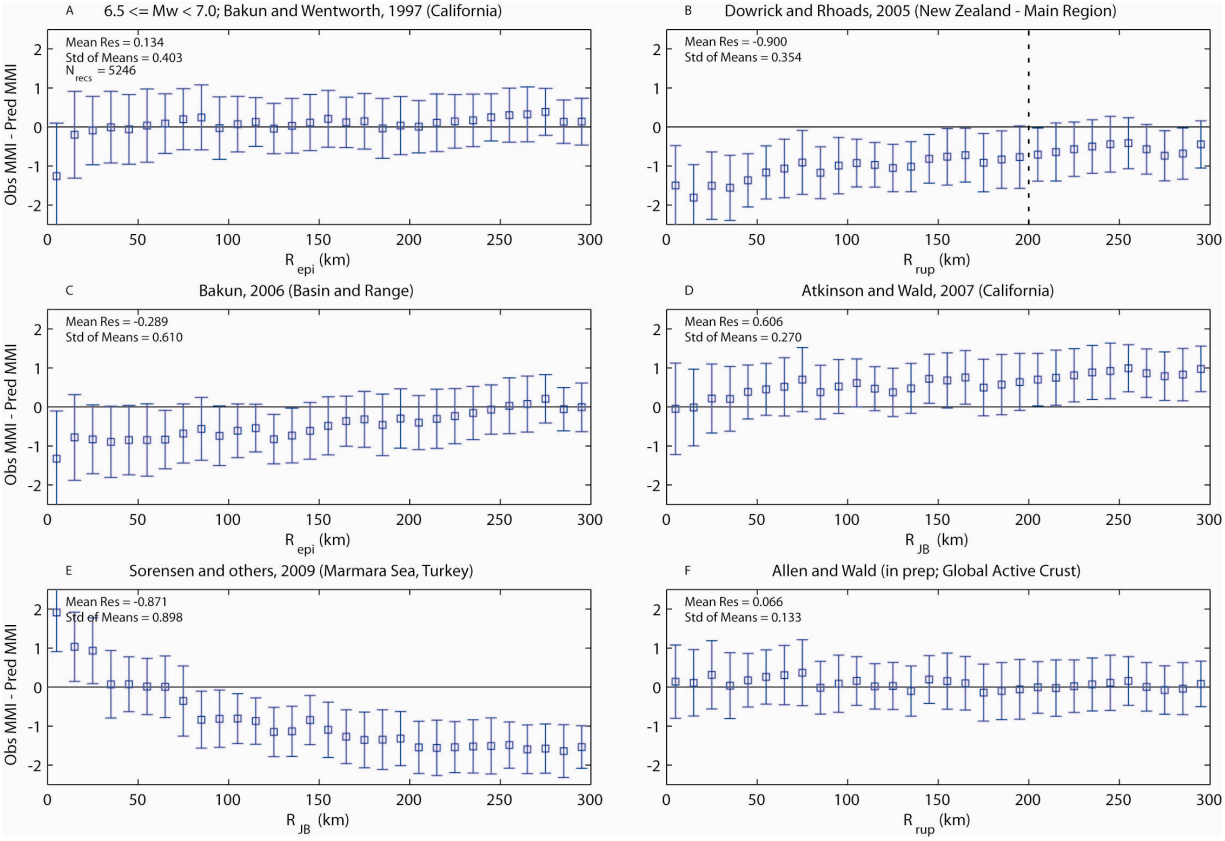
A
6.5 <= Mw < 7.0; Bakun and Wentworth, 1997 (California)
Mean Res = 0.134
Std of Means = 0.403
N recs = 5246
B
Dowrick and Rhoads, 2005 (New Zealand - Main Region)
Mean Res = -0.900
Std of Means = 0.354
C
Bakun, 2006 (Basin and Range)
Mean Res = -0.289
Std of Means = 0.610
D
Atkinson and Wald, 2007 (California)
Mean Res = 0.606
Std of Means = 0.270
E
Sorensen and others, 2009 (Marmara Sea, Turkey)
Mean Res = -0.871
Std of Means = 0.898
F
Allen and Wald (in prep; Global Active Crust)
Mean Res = 0.066
Std of Means = 0.133
Obs MMI - Pred MMI
R epi (km)
R JB (km)
R rup (km)

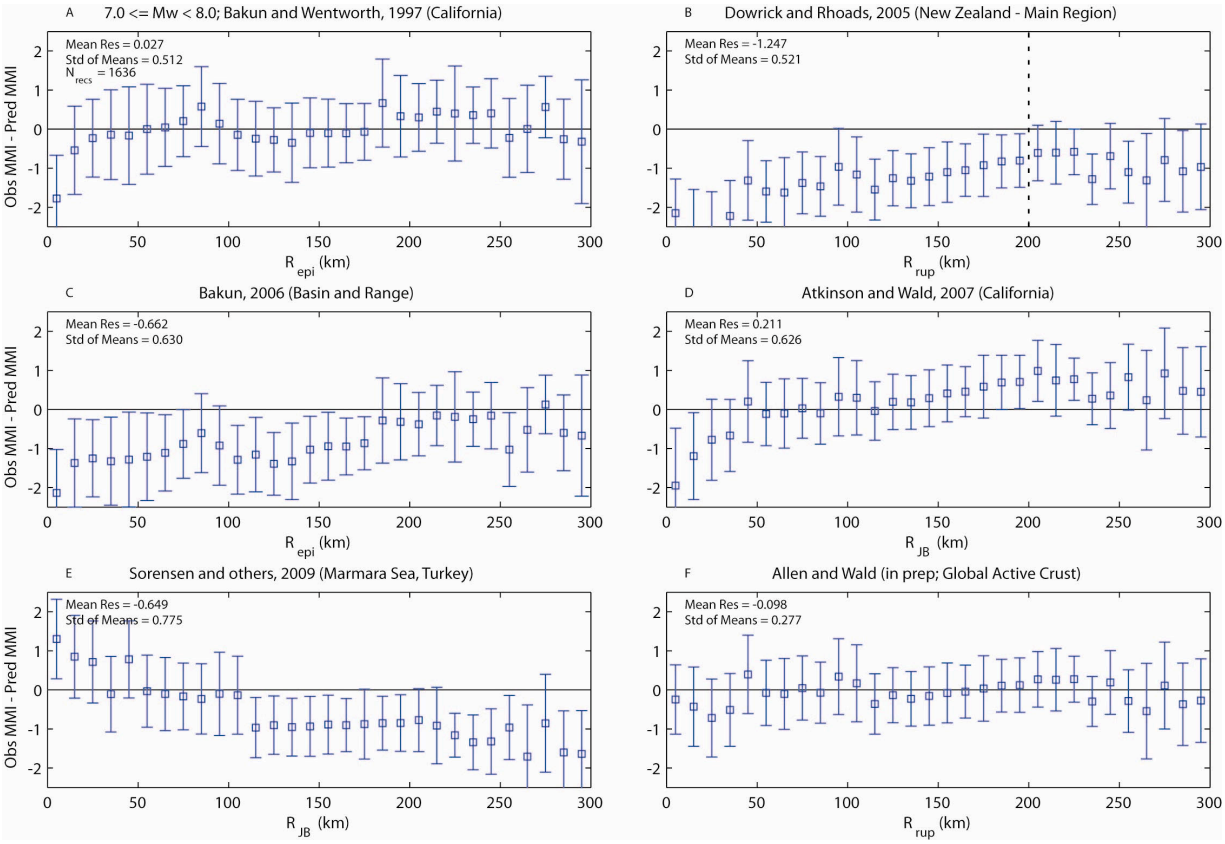
A
7.0 <= Mw < 8.0; Bakun and Wentworth, 1997 (California)
Mean Res = 0.027
Std of Means = 0.512
N recs = 1636
B
Dowrick and Rhoads, 2005 (New Zealand - Main Region)
Mean Res = -1.247
Std of Means = 0.521
C
Bakun, 2006 (Basin and Range)
Mean Res = -0.662
Std of Means = 0.630
D
Atkinson and Wald, 2007 (California)
Mean Res = 0.211
Std of Means = 0.626
E
Sorensen and others, 2009 (Marmara Sea, Turkey)
Mean Res = -0.649
Std of Means = 0.775
F
Allen and Wald (in prep; Global Active Crust)
Mean Res = -0.098
Std of Means = 0.277
Obs MMI - Pred MMI
R epi (km)
R JB (km)
R rup (km)

APPENDIX E Magnitude Dependence of Selected Stable Continental IPEs

The transition of intensity residuals with magnitude for candidate IPEs for stable continental regions. The series of plots show the transition of the median residuals in 0.5 magnitude windows. The magnitude window is indicated on the top-left plot in each figure.

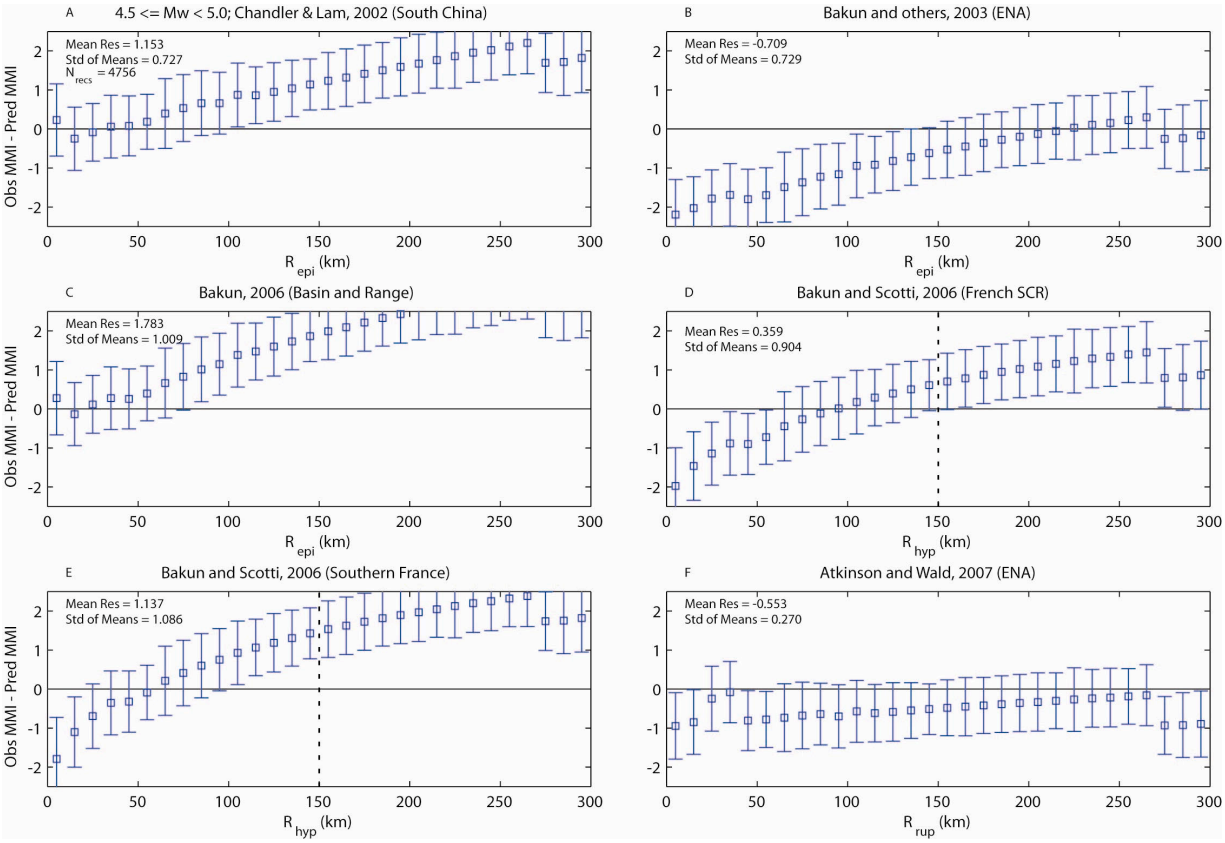

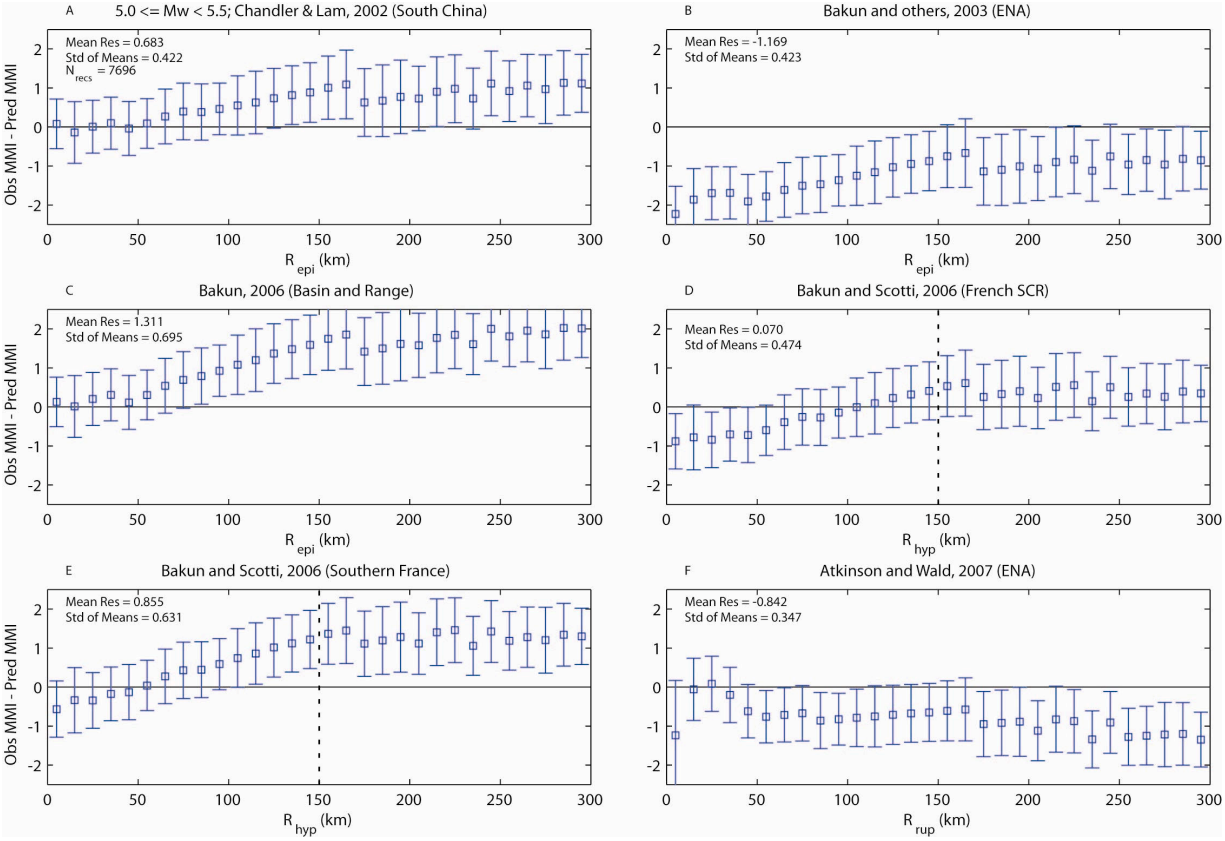
A
5.0 <= Mw < 5.5; Chandler & Lam, 2002 (South China)
Mean Res = 0.683
Std of Means = 0.422
N recs = 7696
B
Bakun and others, 2003 (ENA)
Mean Res = -1.169
Std of Means = 0.423
C
Bakun, 2006 (Basin and Range)
Mean Res = 1.311
Std of Means = 0.695
D
Bakun and Scotti, 2006 (French SCR)
Mean Res = 0.070
Std of Means = 0.474
E
Bakun and Scotti, 2006 (Southern France)
Mean Res = 0.855
Std of Means = 0.631
F
Atkinson and Wald, 2007 (ENA)
Mean Res = -0.842
Std of Means = 0.347
Obs MMI - Pred MMI
R epi (km)
R hyp (km)
R rup (km)

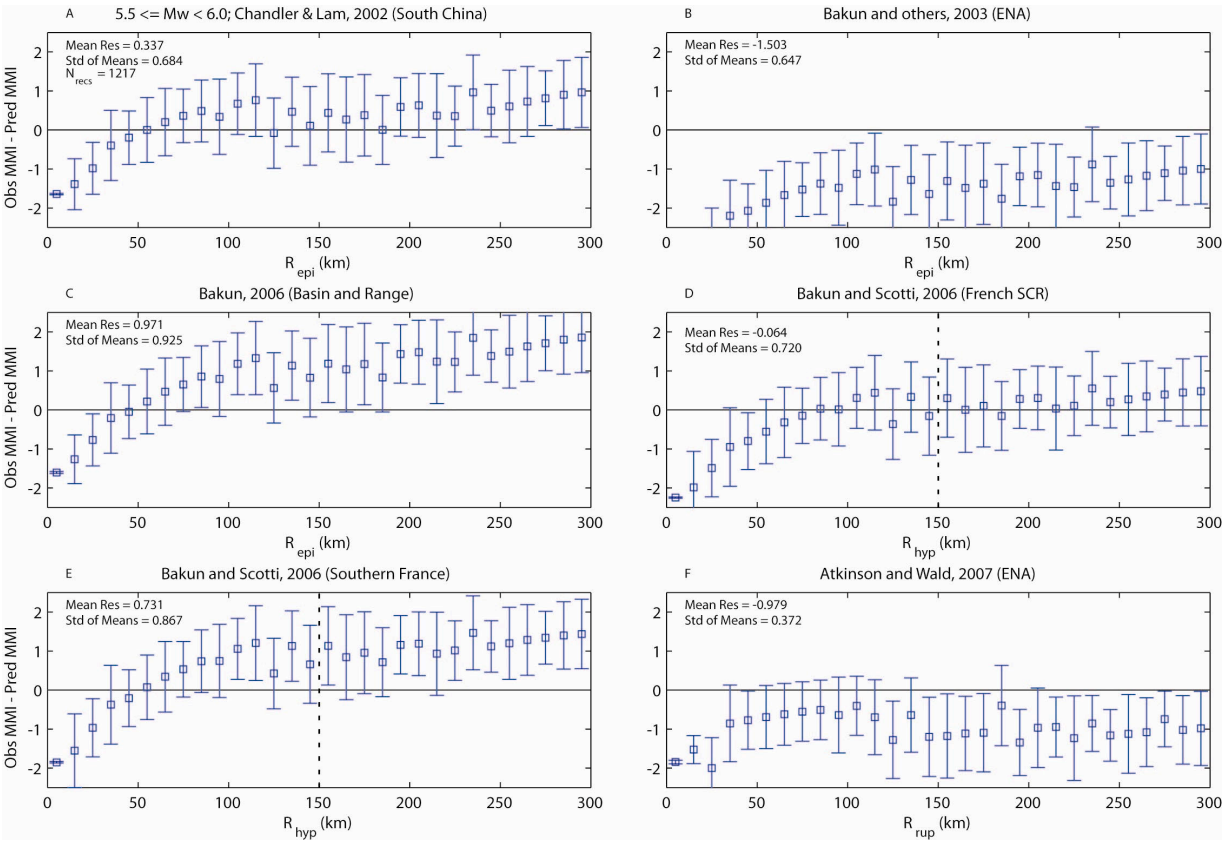
A
5.5 <= Mw < 6.0; Chandler & Lam, 2002 (South China)
Mean Res = 0.337
Std of Means = 0.684
N recs = 1217
B
Bakun and others, 2003 (ENA)
Mean Res = -1.503
Std of Means = 0.647
C
Bakun, 2006 (Basin and Range)
Mean Res = 0.971
Std of Means = 0.925
D
Bakun and Scotti, 2006 (French SCR)
Mean Res = -0.064
Std of Means = 0.720
E
Bakun and Scotti, 2006 (Southern France)
Mean Res = 0.731
Std of Means = 0.867
F
Atkinson and Wald, 2007 (ENA)
Mean Res = -0.979
Std of Means = 0.372
Obs MMI - Pred MMI
R epi (km)
R hyp (km)
R rup (km)

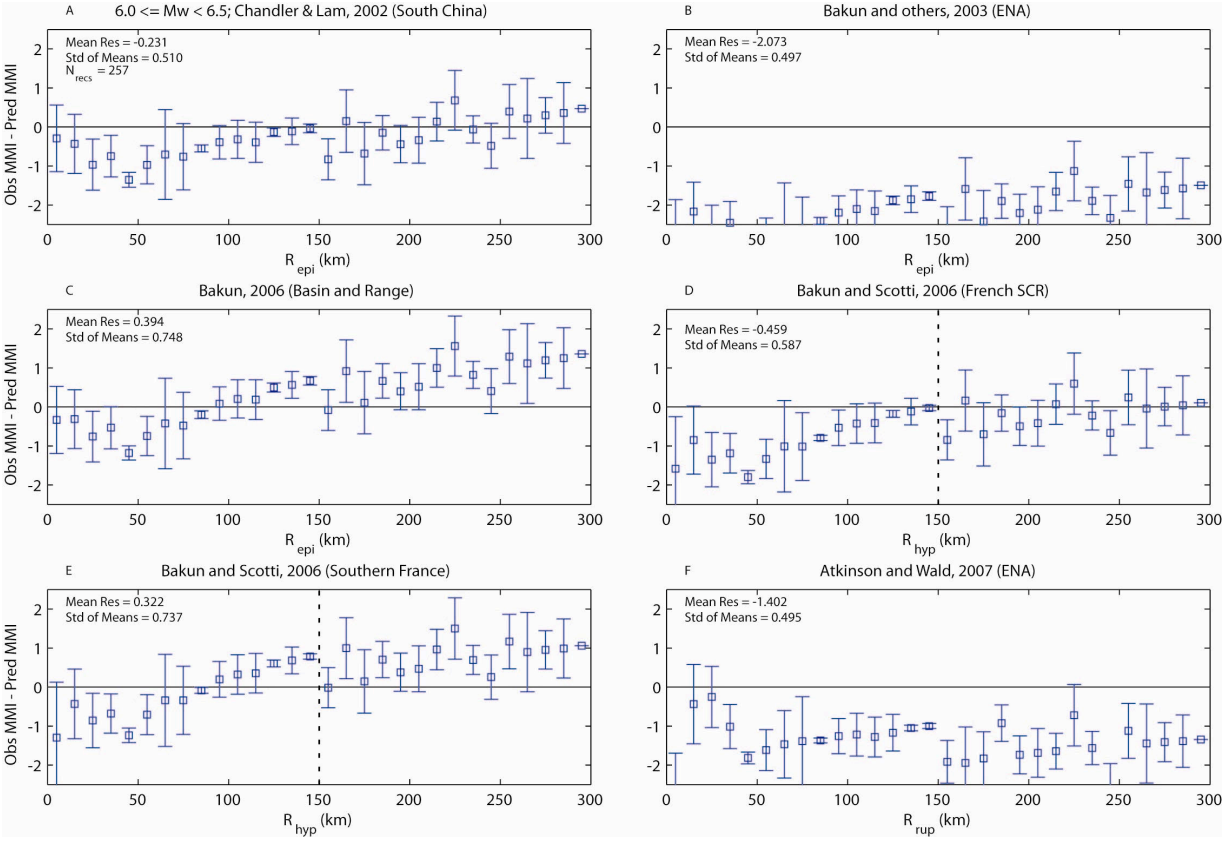
A
6.0 <= Mw < 6.5; Chandler & Lam, 2002 (South China)
Mean Res = -0.231
Std of Means = 0.510
N recs = 257
B
Bakun and others, 2003 (ENA)
Mean Res = -2.073
Std of Means = 0.497
C
Bakun, 2006 (Basin and Range)
Mean Res = 0.394
Std of Means = 0.748
D
Bakun and Scotti, 2006 (French SCR)
Mean Res = -0.459
Std of Means = 0.587
E
Bakun and Scotti, 2006 (Southern France)
Mean Res = 0.322
Std of Means = 0.737
F
Atkinson and Wald, 2007 (ENA)
Mean Res = -1.402
Std of Means = 0.495
Obs MMI - Pred MMI
R epi (km)
R hyp (km)
R rup (km)

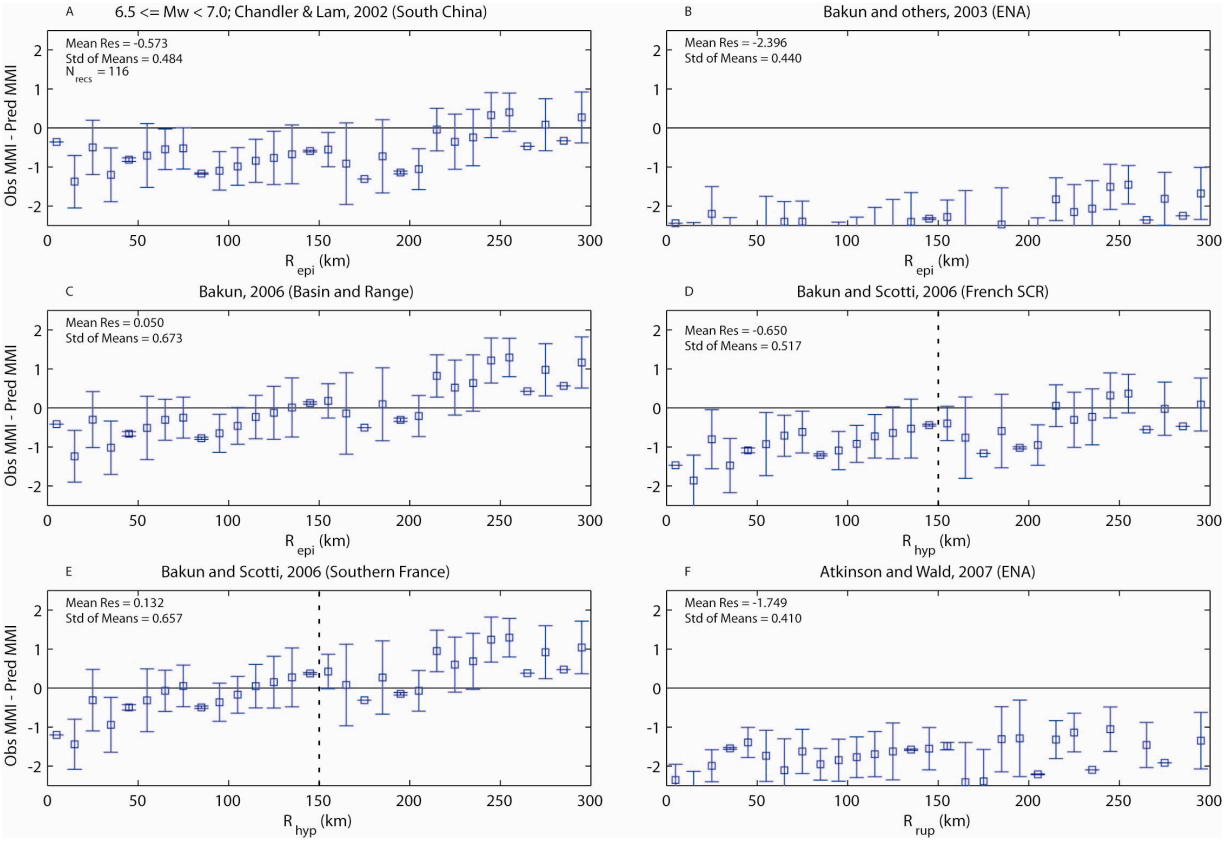
A
6.5 <= Mw < 7.0; Chandler & Lam, 2002 (South China)
Mean Res = -0.573
Std of Means = 0.484
N recs = 116
B
Bakun and others, 2003 (ENA)
Mean Res = -2.396
Std of Means = 0.440
C
Bakun, 2006 (Basin and Range)
Mean Res = 0.050
Std of Means = 0.673
D
Bakun and Scotti, 2006 (French SCR)
Mean Res = -0.650
Std of Means = 0.517
E
Bakun and Scotti, 2006 (Southern France)
Mean Res = 0.132
Std of Means = 0.657
F
Atkinson and Wald, 2007 (ENA)
Mean Res = -1.749
Std of Means = 0.410
Obs MMI - Pred MMI
R epi (km)
R hyp (km)
R rup (km)

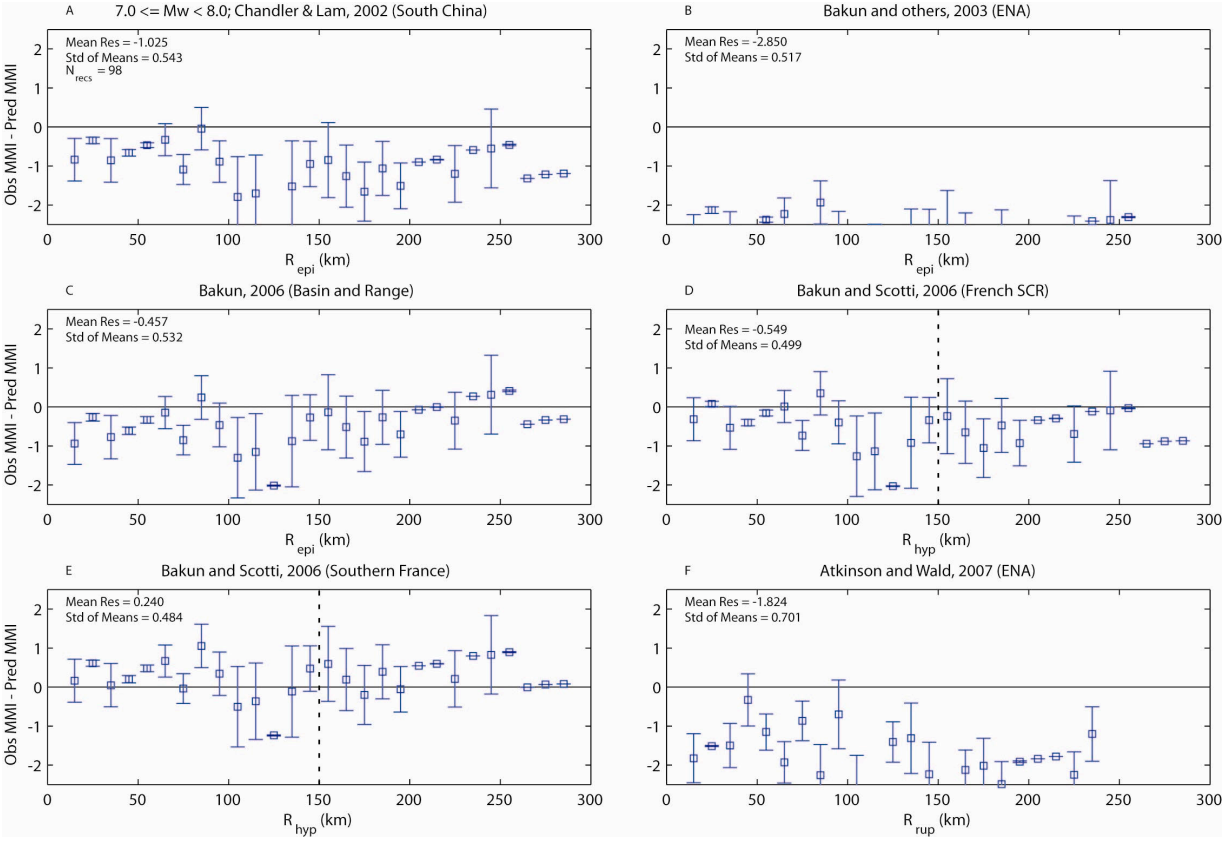
A
7.0 <= Mw < 8.0; Chandler & Lam, 2002 (South China)
Mean Res = -1.025
Std of Means = 0.543
N recs = 98
B
Bakun and others, 2003 (ENA)
Mean Res = -2.850
Std of Means = 0.517
C
Bakun, 2006 (Basin and Range)
Mean Res = -0.457
Std of Means = 0.532
D
Bakun and Scotti, 2006 (French SCR)
Mean Res = -0.549
Std of Means = 0.499
E
Bakun and Scotti, 2006 (Southern France)
Mean Res = 0.240
Std of Means = 0.484
F
Atkinson and Wald, 2007 (ENA)
Mean Res = -1.824
Std of Means = 0.701
Obs MMI - Pred MMI
R epi (km)
R hyp (km)
R rup (km)